NASA TECHNICAL NOTE

NASA TN D-7430

NASA TN D-7430

HEAT-TRANSFER AND PRESSURE DISTRIBUTIONS FOR LAMINAR SEPARATED FLOWS DOWNSTREAM OF REARWARD-FACING STEPS WITH AND WITHOUT MASS SUCTION

by Ronald D. Brown and Antoni K. Jakubowski

Langley Research Center
Hampton, Va. 23665

NATIONAL AERONAUTICS AND SPACE ADMINISTRATION • WASHINGTON, D. C. • AUGUST 1974

1. Report No.	2. Government Accession No.	3. Recipient's Catalog No.
NASA TN D-7430		

4. Title and Subtitle	5. Report Date
HEAT-TRANSFER AND PRESSURE DISTRIBUTIONS FOR LAMINAR SEPARATED FLOWS DOWNSTREAM OF REARWARD-FACING STEPS WITH AND WITHOUT MASS SUCTION	August 1974
	6. Performing Organization Code
7. Author(s)	8. Performing Organization Report No.
Ronald D. Brown and Antoni K. Jakubowski	L-8790
	10. Work Unit No.
9. Performing Organization Name and Address	502-37-02-01
NASA Langley Research Center Hampton, Va. 23665	11. Contract or Grant No.
	13. Type of Report and Period Covered
12. Sponsoring Agency Name and Address	Technical Note
National Aeronautics and Space Administration Washington, D.C. 20546	14. Sponsoring Agency Code

15. Supplementary Notes

Antoni K. Jakubowski is assistant professor of Aero-Space Engineering, Virginia Polytechnic Institute and State University.

16. Abstract

Heat-transfer and pressure distributions were measured for laminar separated flows downstream of rearward-facing steps with and without mass suction. The flow conditions were such that the boundary-layer thickness was comparable to or larger than the step height. For both suction and no-suction cases, an increase in the step height resulted in a sharp decrease in the initial heat-transfer rates behind the step. Downstream, however, the heat transfer gradually recovered back to less than or near attached-flow values. Mass suction from the step base area increased the local heat-transfer rates; however, this effect was relatively weak for the laminar flows considered. Even removal of the entire approaching boundary layer raised the post-step heat-transfer rates only about 10 percent above the flat-plate values.

Post-step pressure distributions were found to depend on the entrainment conditions at separation. In the case of the solid-faced step, a sharp pressure drop behind the step was followed by a very short plateau and a relatively fast recompression. For the slotted-step connected to a large plenum but without suction, the pressure drop at the base was much smaller and the downstream recompression more gradual than that for the solid-faced step.

17. Key Words (Suggested by Author(s))	18. Distribution Statement
Heat transfer Rearward-facing steps Mass suction	Unclassified – Unlimited STAR Category 12

19. Security Classif. (of this report)	20. Security Classif. (of this page)	21. No. of Pages	22. Price*
Unclassified	Unclassified	67	$3.75

*For sale by the National Technical Information Service, Springfield, Virginia 22151

HEAT-TRANSFER AND PRESSURE DISTRIBUTIONS FOR LAMINAR SEPARATED FLOWS DOWNSTREAM OF REARWARD-FAC. STEPS WITH AND WITHOUT MASS SUCTION

By Ronald D. Brown and Antoni K. Jakubowski*
Langley Research Center

SUMMARY

Heat-transfer and pressure distributions were measured for laminar separated flows downstream of rearward-facing steps with and without mass suction. The flow conditions were such that the boundary-layer thickness was comparable to or larger than the step height. For both suction and no-suction cases, an increase in the step height resulted in a sharp decrease in the initial heat-transfer rates behind the step. Downstream, however, the heat transfer gradually recovered back to less than or near attached-flow values. Mass suction from the step base area increased the local heat-transfer rates; however, this effect was relatively weak for the laminar flows considered. Even removal of the entire approaching boundary layer raised the post-step heat-transfer rates only about 10 percent above the flat-plate values.

Post-step pressure distributions were found to depend on the entrainment conditions at separation. In the case of the solid-faced step, a sharp pressure drop behind the step was followed by a very short plateau and a relatively fast recompression. For the slotted-step connected to a large plenum but without suction, the pressure drop at the base was much smaller and the downstream recompression more gradual than that for the solid-faced step.

INTRODUCTION

The study of the high-speed flow field past a rearward-facing step is of considerable interest in the aerothermodynamic design of various flight configurations, including large lifting entry vehicles. In particular, the possible use of overlapping sliding metallic heat-shield joints calls for a study of the separated region behind a step. The conditions of particular interest are characterized by a thick boundary layer (i.e., the step height h is comparable to or less than the boundary-layer thickness δ) and mass suction from the separated area. The studies of various aspects of a rearward-facing step or wedge are

*Assistant professor of Aero-Space Engineering, Virginia Polytechnic Institute and State University.

numerous, but the vast majority of published works have centered on the case where the boundary-layer thickness is smaller than the step height. Examples of such investigations are Rom and Seginer (ref. 1), Holloway, Sterrett, and Creekmore (ref. 2), Weiss and Weinbaum (ref. 3), Scherberg and Smith (refs. 4, 5), Hama (ref. 6), Adamson (ref. 7), Batt and Kubota (ref. 8), and more recent works by Erdos and Zakkay (ref. 9) and Wu and Su (ref. 10). Experimental information on the case of $h/\delta \leqq 1$ is almost nonexistent and, to our knowledge, no experiments have been made that include mass suction from the separated area.

The purpose of the present investigation was to determine experimentally the heat-transfer and pressure distributions for laminar separated flows downstream of a rearward-facing step with and without mass suction under conditions where the boundary-layer thickness is of the same order as the step height. The program was a joint effort between the Virginia Polytechnic Institute and State University (under an NASA grant) and the NASA Langley Research Center. The experiments were conducted in an arc-heated wind tunnel of the Langley entry structures facility. Apparatus, experimental techniques, and test conditions are described, and data collected during this study are presented, along with a discussion of the basic results.

SYMBOLS

b	width of model
i	enthalpy
h	step height
L	length of surface ahead of step
M	Mach number
$\dot{m}$	mass flow rate
N_{Re}	Reynolds number
$N_{Re_{\infty,h}}$	Reynolds number based on h, $u_\infty h/\nu_\infty$
$N_{Re_{\infty,L}}$	Reynolds number based on L, $u_\infty L/\nu_\infty$

$N_{Re_{\infty,x}}$	Reynolds number based on x, $u_\infty x/\nu_\infty$
N_{St}	Stanton number, $\dot{q}/\rho_\infty u_\infty H$
p	pressure
$\dot{q}$	heat-transfer rate
R	gas constant
T	absolute temperature
u	velocity
w	nondimensional mass suction rate, $\dot{m}_s/\rho_\infty u_\infty bh$
x	distance downstream of leading edge
Δx	distance downstream of step
x_e	distance downstream of nozzle exit
y	transverse distance measured from center line; distance from surface
δ	boundary-layer thickness
δ^*	boundary-layer displacement thickness
ν	kinematic viscosity
ρ	density

Subscripts:

BL	boundary layer
max	maximum value
0	stagnation condition (see fig. 1)

ref	reference condition
s	suction
st	static
step	step location on flat plate
t	total, pitot (see fig. 1)
ts	test section
w	wall condition
∞	free-stream condition

APPARATUS

Figure 1 presents a simplified diagram of the experimental setup used in this investigation. The arc-heated wind tunnel consists of a magnetically stabilized ac arc heater, a plenum chamber, a 15° conical supersonic nozzle, a test section, and a diffuser which exhausts into a vacuum sphere at a minimum pressure of about 1 mm Hg. A multistage steam ejector provides sufficient vacuum for the tunnel operation. The wind tunnel is a free-jet type and has a run duration of about 10 minutes to over 1 hour, depending on the mass flow rate. The test medium was arc-heated air. The water-cooled supersonic nozzle had a 7 cm (2.75 in.) diameter throat and a 22.9 cm (9 in.) diameter exit section. The nominal stagnation pressure and enthalpy were varied from 0.18 to 1.96 atm and from 3.5 MJ/kg to 12.8 MJ/kg (1500 to 5500 Btu/lbm), respectively. The models were mounted on a water-cooled retractable strut.

Models and Instrumentation

Two basic models were used in this investigation. Model I (fig. 2) was designed for tests without suction while model II (fig. 3) was designed and used primarily for tests with suction. Each model was a wedge designed to provide two-dimensional flow on the test surface and had a sharp leading edge, a rearward-facing step, and adjustable test surface heights. Each model was constructed of water-cooled copper.

Model I (fig. 2) had a flat surface preceding the step that was 12.5 cm (4.91 in.) long. This surface was instrumented with a pressure orifice that was located 3.1 cm (1.22 in.) upstream of the step. Another pressure orifice was located in the center of the

rearward-facing step (0.51 cm from the top). The 11.4 cm (4.5 in.) test surface downstream of the step was provided with one of two interchangeable reattachment plates. The heat-transfer plate was 0.74 mm (0.029 in.) thick stainless steel that was instrumented down the center line by spot welding 17 No. 30 gage chromel-alumel thermocouples to the underside. The pressure-distribution plate was 0.635 cm (0.25 in.) thick water-cooled copper and was instrumented by silver-soldering to the pressure orifices 14 stainless-steel tubes 1.2 mm (0.047 in.) inside diameter that were 2.4 m (8 ft) in length. The step height was varied by changing the thickness of the shims beneath the reattachment plates.

Model II (fig. 3) had a flat surface preceding the step that was 10 cm (3.925 in.) long. There was no pressure orifice in this surface because nearly the entire area of the rearward-facing step was used as a suction slot. The heat-transfer plate was identical to that of model I, but the pressure plate was restricted to 12 pressure orifices located immediately downstream of the step.

The heat-transfer data were recorded on a central digital data system at 0.025 sec intervals. The pressure-distribution data were also recorded on the central digital data system but at intervals of approximately 1.0 sec.

Mass-Suction Installation

The experimental test setup used for the suction experiments on model II is shown schematically in figure 1. The hot air removed from the separated region behind the step was passed through the water-cooled strut, through two 7.6 cm (3 in.) diameter flexible hoses that were connected to the two suction outlets of the model, a vacuum pump, an instrumented section to measure the mass flow rate, and then reintroduced into the test section. The vacuum pump was a mechanical blower with a pumping capacity of 1620 liters/sec (3435 standard ft^3/min). The instrumented section was connected to the discharge side of the vacuum pump and equipped with static- and total-pressure sensors and stagnation- and wall-temperature sensors to provide information necessary for evaluation of suction mass flow rates. Pressures were measured by means of strain-gage pressure transducers, and total and wall temperatures were sensed by thermocouple probes. The pressure and temperature data were recorded by a central digital data system. Pressure taps in the suction duct upstream of the vacuum pump provided information to determine that the flow conditions in that section had been stabilized.

The vacuum pump available for these experiments operated at constant speed, and, consequently, there was no convenient way to vary mass suction flow rates at a given test condition. Only small variations of the suction flow rate were obtained by blanking off one of the exhaust ports on the model. The vacuum pump failed before the planned program was completed, and information concerning effects of the mass suction is therefore limited.

PROCEDURES

Flow Conditions

The models were mounted parallel to the supporting strut to minimize blockage and reduce the spillage of the test gas about the diffuser inlet scoop. This arrangement placed the attachment plates approximately parallel to the tunnel viewing ports and precluded any effective use of optical means of flow observation. A nominal zero angle of attack was used throughout the tests.

The stagnation test conditions were varied by changing the tunnel mass flow rate (from 0.045 kg/sec to 0.45 kg/sec) and the power input to the arc heater. Prior to model insertion, the pitot pressure and the stagnation-point heat-transfer rate near the model leading-edge test position were determined by using standard retractable devices (impact pressure probe and hemispherical calorimeter) injected sequentially into the test stream. These measurements, combined with that of the pressure in the plenum chamber, served to establish stagnation and free-stream conditions for each individual run. In addition, during each experiment, several electrical and gas dynamic measurements were performed to provide or supplement information on the conditions of the experiment. These measurements included the arc current, arc voltage, arc power, tunnel-air mass flow rate, test-chamber pressure, temperature of the instrumented plate being tested, and energy balance data on the arc heater. The stagnation enthalpy was calculated from stagnation-point heat-transfer and pressure measurements. The theory of Fay and Riddell (ref. 11) was used. A unit Lewis number and thermodynamic equilibrium at the surface were assumed, and the viscosity from Hansen (ref. 12) was used. The calculated enthalpy and the measured total pressure p_0 (plenum chamber pressure) were used to define the total temperature (plenum) from a Mollier diagram.

Free-stream conditions at any location in the test stream were calculated, based on a frozen isentropic expansion from the total temperature and pressure (plenum) to the local condition defined from a pitot pressure survey. Flat-plate boundary-layer parameters were determined by using frozen flow edge conditions and a finite-rate boundary-layer calculation with an equilibrium catalytic wall. A detailed description of the computation is given in reference 13. Heat-transfer and pressure measurements for all test conditions are listed in tables I to VI. The nominal range of test and model conditions is as follows:

Stagnation pressure, p_0, atm	0.18 to 1.96
Stagnation enthalpy, H_0, MJ/kg	3.5 to 12.8
Stagnation temperature, T_0, K	2700 to 5500
Mach number, M_∞	3.95 to 4.27

Reynolds number per unit length, N_{Re_∞} per cm	100 to 2200
Reynolds number based on prestep surface length, $N_{Re_{\infty,L}}$	2.9×10^3 to 2.9×10^4
Reynolds number based on step height, $N_{Re_{\infty,h}}$	0 to 2200
Ratio of wall temperature to free-stream stagnation temperature, T_w/T_0	0.055 to 0.11
Step height, h, cm	0 to 1.02
Ratio of step height to boundary-layer thickness, h/δ	0.1 to 2.4
Dimensionless mass suction rate, w	0.1 to 0.8

Flow Uniformity

Pitot pressure surveys along the center line of the test stream revealed the presence of an axial pressure gradient in the jet (underexpansion) as shown in figure 4. The presence of the pressure gradient was accounted for in establishing free-stream conditions and boundary-layer parameters along the surface of the models.

To examine transverse uniformity or two dimensionality of the flow along the instrumented sections of the models, transverse surveys of pressure distribution were made at a few stations along the instrumented section. The results of this examination, shown in figures 5(a) to 5(b) for $h = 0$ cm and $h = 0.97$ cm, indicate that the flow near the center line was essentially two dimensional over a distance of at least 6.5 cm (2.5 in.). In view of the longitudinal pressure gradient in the jet and the limited width of the models, great caution must be exercised when interpreting data collected far downstream of the step ($\Delta x > 6.5$ cm (2.5 in.)). In addition, under some flow conditions, the rear part of the model was influenced by back pressure effects from a shock-wave system generated by the supporting strut. Since the main object of this investigation was to study the separated flow region immediately downstream of the step, the flow structure downstream of the reattachment was of secondary interest.

Mass-Suction Experiments

In the experiments involving mass suction (model II), the vacuum pump in the suction circuit was started before the model was injected into the jet. For most of the tests, less than 0.8 sec was needed to stabilize pressures in the suction circuit after the model had been injected.

The suction mass flow rate $\dot{m}_s$ was calculated from the mass-balance equation

$$\dot{m}_s = A\sqrt{\left(2p_{st}/RT_0\right)\left(p_t - p_{st}\right)} \tag{1}$$

where A is the flow area of the instrumented section, and T_0, p_{st}, and p_t are total temperature, static pressure, and average total pressure in that section. The absolute value of $(p_t - p_{st})$ was very small (on the order of 0.1 mm Hg for some tests) and difficult to measure. In addition, the available pressure measuring system had a slow response time and experienced some zero drift when cycling to atmospheric pressure for model changes. To minimize these problems, a calibration procedure was applied before and after each series of runs. The procedure consisted of checking zero intercepts and slopes near zero pressure of the transducers involved in measuring $p_t - p_{st}$ and comparing the outputs against a calibrated pressure gage.

Heat-Transfer Tests

Heat-transfer data were obtained from measurements of transient skin temperatures resulting from a stepwise increase in stagnation temperature. The model, initially at room temperature, was suddenly (in less than 0.25 sec) exposed to the hot air flow where it remained from 1 to 3 sec. Skin temperatures were recorded at a rate of 40 measurements per sec. Heat-transfer data were computed by using the simplified heat-balance equation

$$\dot{q} = c_w \rho_w d_w \frac{dT_w}{dt} \tag{2}$$

where c_w is the specific heat of the wall material, ρ_w is the density of the wall material, d_w is the wall thickness, T_w is the wall temperature, and t is time. Equation (2) presupposes a constant temperature through the model skin, negligible lateral heat flow, negligible heat flow to the interior of the model, and no heat losses through radiation. The experiments with the mass suction from the separated area involved a time delay required to stabilize pressures in the suction circuit. Consequently, the heat-transfer measurements taken after the flow conditions were stabilized might be affected by the lateral heat conduction in the plate. To examine this possibility, plots of skin temperature against time were checked for several test conditions. The results showed that the slope dT_w/dt remained very nearly constant for at least 3 seconds, that is, for a period longer than that required to stabilize the flow in the suction duct (less than 0.8 sec). Therefore, it was concluded that the heat conduction did not have any significant effect on the heat-transfer measurements. The overall error of the heat-transfer measurements was estimated to be about 10 percent.

Pressure Tests

The strain-gage pressure transducers were mounted outside the test section for protection from the hot gases in the tunnel and were connected to the pressure taps on the

model by 1.2 mm (0.047 in.) i.d. tubing that was 2.4 m (8 ft) in length. Thus, the response time of the pressure measuring system was slow, ranging from 20 sec to about 2 min. Consequently, the model with pressure-instrumented reattachment plate had to be kept in the jet for relatively long periods, and the plate was water cooled.

RESULTS AND DISCUSSION

Heat-Transfer Distribution on Model I (No Suction)

The heat-transfer data obtained at all model stations and test points are presented in table V. The stagnation and free-stream conditions for each test can be determined from table I by using the run number.

The classical laminar flat-plate heat-transfer correlation of Stanton number and Reynolds number is shown in figure 6 with experimental heat-transfer data from model I. The correlation between the experiment and classical theory is good over the Reynolds number range of 3×10^3 to 3×10^4. Therefore, the undisturbed flow in these tests is clearly laminar.

The typical effect of step height on the heat-transfer distribution along the center line of the reattachment plate is shown in figure 7. For the different step heights, free-stream conditions were similar but not necessarily identical. The dashed lines indicate data that may be influenced by side effects or disturbance in the external flow. The figure shows that an increase in step height produces a decrease in heat transfer just behind the step. In all cases this drop is followed by a gradual increase in heating to a value less than or nearly equal to that for attached flow. The maximum heat-transfer rate occurs at a distance from the step that varies from 6 step heights for the largest step (1.02 cm) to about 14 step heights for the smallest step (0.16 cm). The same general trends shown in figure 7 held for the other test results contained in table V.

These tests demonstrate that for a small rearward-facing step in laminar flow without suction no significant increase in heating occurs downstream of the step. This indicates that metallic heat-shield systems which would have small steps on the order of typical material thickness will not cause excess heating downstream of the joints between panels, provided the joint is sealed against air inflow.

The range of conditions where peak heating downstream of the step is less than heating on the plate approaching the step can be inferred from figure 8. This figure includes data obtained by Rom and Seginer (ref. 1), Smith (ref. 5), and several points evaluated on the basis of measurements reported by Holloway, Sterrett, and Creekmore (ref. 2), as well as data from the present investigation. It should be noted that the abscissa on figure 8 $\left(N_{Re_{\infty},h}\right)$ is proportional to the square of the ratio of step height to

boundary-layer thickness. This follows because, for a given geometry L/h and free-stream Mach number M_∞, the Reynolds number $N_{Re_{\infty,h}}$ varies approximately as $\left(\frac{h}{\delta}\right)^2$ $\left(\text{in laminar flow, } N_{Re_{\infty,h}} \approx \frac{L}{h}\left(\frac{h}{\delta}\right)^2\right)$.

Pressure-Distribution on Model I (No Suction)

The wall pressure distributions normalized by the reference pressure measured upstream of the step (p_{ref}) are displayed in figures 9(a) to 9(g). The pressure at the step location ($\Delta x = 0$) was measured on the perpendicular surface of the step. This pressure was not measured for the small step ($h = 0.2$ cm) because the pressure port was below the pressure plate. The pressure distribution indicates a small region of low pressure along the surface immediately downstream of the step. The length of this region increases with step height h and with free stream Reynolds number $N_{Re_{\infty,L}}$. Downstream of the low pressure "plateau" the pressure increases in a few step heights to approximately the attached flow value of the flat plate.

Heat-Transfer Distribution on Model II (Suction)

Heat-transfer data obtained from model II on the 1.02 cm and 0.6 cm steps are tabulated in table VI, and representative points are shown in figures 10(a) to 10(j) and figures 11(a) and 11(d), respectively. The stagnation and free-stream conditions for each test are listed by run number in table II. The suction and no-suction results obtained with model II are compared with heat-transfer distributions for a flat-plate configuration under similar free-stream conditions. The mass suction rate w is defined as the ratio of the average mass flux through the slot $\dot{m}_s/bh$ to a free-stream mass flux. The mass suction rates w varied between 0.2 and 0.5 for the 1.02 cm step and between 0.1 and 0.8 for the 0.6 cm step. In terms of the entire mass flow rate throughout the boundary layer $\left(\dot{m}_{BL} = \int_0^\delta \rho u \, dy\right)$, the mass flow rate $\dot{m}_s$ ranged from 40 percent to 120 percent of $\dot{m}_{BL}$ for the 1.02 cm step and 0.6 cm step, respectively. The no-suction experiments were made with the suction duct blanked off at the flexible hose coupling, thus leaving a large internal cavity connected to the suction slot. As a result, the entrainment conditions at separation in the no-suction tests on model II were different from those in the no-suction tests on model I.

Figure 10(a) shows that the effects of suction on the heat transfer downstream of a 1.02 cm step is negligible for $w = 0.25$ and N_{Re_∞} per cm = 250. From figure 10(a) to figure 10(b) the Reynolds number is doubled for approximately the same relative suction and again the increased heating is negligible. From figures 10(b) to 10(d) stagnation

enthalpy is increased with the same relative suction and Reynolds number. Figures 10(b), 10(c), and 10(d) show a small increase in heat transfer just downstream of the step and the effect diminishes in about 3 or 4 step heights. From figures 10(c) to 10(e) the suction is increased with the Reynolds number and the enthalpy constant. The relative increase in heating is the largest just downstream of the step and approaches the flat-plate heat-transfer value at about 8 step heights. From figures 10(e) to 10(f) the Reynolds number is doubled at the same suction rate, and again the relative increase in heating is the largest just downstream of the step but the heat transfer does not recover to the flat-plate value.

A comparison of figures 10(g) and 10(h) indicates that the repeatability is good at a relative suction rate of $w \approx 0.34$. In figure 10(i), a comparison of two suction rates ($w = 0.36$ and 0.41) indicates that the increase in suction gives an increase in heating just downstream of the step. The lower suction value was obtained by blanking off one of the exhaust ports of the model, as previously discussed. In figure 10(j), the two relative suction rates were calculated to be equal, but the lower heat-transfer points were obtained with one port on the model blanked off. Thus, it must be concluded that the suction flow measurement is only an approximation.

The heat-transfer data presented in figure 10 indicate that suction causes a large percentage increase in the heat transfer just downstream of the step. In addition, for a constant step height and relative suction rate the location downstream of the step where the heating approaches the flat-plate value appears to be a function of the Reynolds number.

Figure 11(a) shows that a small relative suction rate ($w = 0.12$) does affect the relative heat transfer just downstream of the 0.6 cm step but the effect diminishes in about 3 or 4 step heights. In figure 11(b), an increase in the relative suction ($w = 0.61$) carries downstream to approximately 10 step heights where the heat transfer approaches the flat-plate value. The lower relative suction value ($w = 0.59$) was obtained with the one exhaust port blanked, as previously discussed. It appears that the sonic point was in the duct in the strut so that a factor of 2 in the exhaust area made only a slight difference in the measured suction mass flow rate (they were equal when the measurement accuracy is considered). From figures 11(b) to 11(c), the enthalpy is increased without any effect on the relative heat-transfer distribution or on the location of the point where the heat transfer approaches the flat-plate value. From figures 11(b) to 11(d) the Reynolds number was doubled, and at the highest relative suction value ($w = 0.79$) the heat transfer reached the flat-plate value at approximately 7 to 8 step heights and exceeded the flat-plate value downstream of this location.

Additional heat-transfer data with suction in table VI show the same general trends. Mass suction through the slotted step increases the local heat transfer. The relative

increase, referenced to the no-suction case, depends on (1) the step height, (2) the mass-suction rate, and (3) the location behind the step. The relative increase is most significant a few step heights immediately behind the step. Location of the maximum heating rate varied between 4 and 6 step heights behind the 1.02 cm step and between 7 and 9 step heights behind the 0.6 cm step. In terms of the maximum heating rates, even large suction rates applied in this investigation did not produce any spectacular peaks, and the effect of mass suction seems to be weaker than might be expected. Nevertheless, at the largest value of w applied in this investigation ($w = 0.8$ in run 190-5-24, see fig. 11(d)), local heat-transfer rates exceeded the flat-plate values over a significant length of the reattachment plate.

Pressure Distribution on Model II (Suction)

Pressure distributions downstream of the 1.02 cm slotted step with and without mass suction are presented in figures 12(a) to 12(j). The results are compared with those for the flat-plate configuration. Pressure data with mass suction were obtained only on the 1.02 cm step because of the failure of the vacuum pump.

As can be seen in figure 12(a), the low total pressure (small Reynolds number) suction data practically coincided with the no-suction data. An increase in total pressure (approximately $1\frac{1}{2}$ from fig. 12(a) to fig. 12(b)) gives a corresponding increase in flat-plate pressure, but the step suction and no-suction results coincide at approximately the absolute pressure level of figure 12(a) immediately behind the step. The pressure then gradually increases to the flat-plate value at approximately 7 step heights. The pressure exceeds the flat-plate pressure data beyond 7 step heights. The increase in pressure downstream of the step is more gradual for the slotted step with no suction than for the solid step (see fig. 9(b)). This may be explained in terms of the large entrainment volume because the suction exhaust ports were capped.

From figures 12(b) to 12(d), the total enthalpy was increased with only small changes in the Reynolds number and total pressure, and again the suction and no suction data coincide. From figures 12(b) to 12(e), the total pressure, thus Reynolds number, is increased by a factor of about 2 at the same enthalpy, and the suction data begin to deviate from the no-suction data. The mass suction moves the point that the pressure recovers to the flat-plate value upstream approximately 1.5 to 2.0 step heights.

For figures 12(e) to 12(g), the total enthalpy was increased with small changes in Reynolds number and total pressure, with the same type of result that was obtained at the lower enthalpy. Comparison of figure 12(f) with figure 12(h) shows that as the total pressure and Reynolds number are increased by about 2, the effects of the suction become quite pronounced. At about 3 step heights downstream of the step, the pressure with

suction exceeds the pressure with no suction and approaches the flat-plate value at approximately 7 step heights. From figures 12(h) to 12(i), an increase in enthalpy gives the same general results.

It should be noted that the absolute pressure measured at the first pressure port downstream of the step with suction was approximately the same regardless of total pressure or Reynolds number level (varied over approximately a factor of 8).

Figure 12 shows the effects of suction on the pressure distribution downstream of the 1.02 cm step. The suction distorts the pressure distribution so that the pressure is less than the no-suction pressure just downstream of the step but approaches the no-suction pressure at approximately 3 to 4 step heights and remains above the no-suction pressure for the remainder of the instrumented section of the plate.

CONCLUSIONS

Measurements of heat-transfer and pressure distributions for laminar separated flow downstream of a step with and without suction demonstrate the following effects:

1. For both suction and no-suction cases, an increase in the step height results in a sharp drop in the initial heating rates behind the step. Downstream of the step, the heat-transfer rates gradually recover back to values less than or near attached flow values. The height of the step controls the heat-transfer rates at the step base and dominates the effects of stagnation enthalpy and pressure.

2. Mass suction from the step base area increases the local heating rates, the relative increase being most significant immediately behind the step. In general, however, the effect of mass suction on heat transfer in laminar flow can be termed as weak, and removal of the entire boundary layer raised the post-step heat-transfer rates only about 10 percent above the flat-plate values.

3. Pressure distribution downstream of the step was found to depend on the entrainment conditions at separation. In the no-suction solid-step case, pressure dropped sharply immediately behind the step to a level strongly dependent on the step height. This drop was followed by a short pressure plateau and then by a recompression in a short distance. The recompression without suction on the slotted step required a longer distance than with a corresponding solid-step configuration. With mass suction applied, the pressure level at the step base was roughly the same for all Reynolds numbers and suction rates in these experiments.

Langley Research Center,
National Aeronautics and Space Administration,
Hampton, Va., April 17, 1974.

REFERENCES

1. Rom, Josef; and Seginer, Arnan: Laminar Heat Transfer to a Two-Dimensional Backward Facing Step From the High-Enthalpy Supersonic Flow in the Shock Tube. AIAA J., vol. 2, no. 2, Feb. 1964, pp. 251-255.

2. Holloway, Paul F.; Sterrett, James R.; and Creekmore, Helen S.: An Investigation of Heat Transfer Within Regions of Separated Flow at a Mach Number of 6.0. NASA TN D-3074, 1965.

3. Weiss, Robert F.; and Weinbaum, Sheldon: Hypersonic Boundary-Layer Separation and the Base Flow Problem. AIAA J., vol. 4, no. 8, Aug. 1966, pp. 1321-1330.

4. Scherberg, Max G.; and Smith, Howard E.: An Experimental Study of Supersonic Flow Over a Rearward Facing Step. AIAA J., vol. 5, no. 1, Jan. 1967, pp. 51-56.

5. Smith, Howard E.: The Flow Field and Heat Transfer Downstream of a Rearward Facing Step in Supersonic Flow. ARL 67-0056, U.S. Air Force, Mar. 1967. (Available from DDC as AD 655 370.)

6. Hama, Francis R.: Experimental Studies on the Lip Shock. AIAA J., vol. 6, no. 2, Feb. 1968, pp. 212-219.

7. Adamson, T. C.: Solutions for Supersonic Rotational Flow Around a Corner Using a New Co-Ordinate System. J. Fluid Mech., vol. 34, pt. 4, Dec. 23, 1968, pp. 735-758.

8. Batt, Richard G.; and Kubota, Toshi: Experimental Investigation of Laminar Near Wakes Behind 20° Wedges at $M_{\infty} = 6$. AIAA J., vol. 6, no. 11, Nov. 1968, pp. 2077-2083.

9. Erdos, John I.; and Zakkay, Victor: Inviscid Solution of the Steady, Hypersonic Near Wake by a Time-Dependent Method. AIAA J., vol. 9, no. 7, July 1971, pp. 1287-1293.

10. Wu, J. M.; and Su, M. W.: Measurements on Separated Supersonic Boundary Layer Flows After an Expansion Corner. Proceedings of the Ninth International Symposium on Space Technology and Science, AGNE Pub. Inc. (Tokyo), 1971, pp. 357-372.

11. Fay, J. A.; and Riddell, F. R.: Theory of Stagnation Point Heat Transfer in Dissociated Air. J. Aeronaut. Sci., vol. 25, no. 2, Feb. 1958, pp. 73-85, 121.

12. Hansen, C. Frederick: Approximations for the Thermodynamic and Transport Properties of High-Temperature Air. NASA TR R-50, 1959. (Supersedes NACA TN 4150.)

13. Jakubowski, Antoni K.; and Lewis, Clark H.: Rearward-Facing Steps in Laminar Supersonic Flows With and Without Suction. AIAA Paper No. 73-667, July 1973.

TABLE I.- TEST CONDITIONS FOR HEAT-TRANSFER MEASUREMENTS ON MODEL I

RUN	MODEL CONDITIONS		STAGNATION CONDITIONS			FREESTREAM CONDITIONS AT THE STEP LOCATION*							BOUNDARY LAYER AT THE STEP **		
	h, cm	T_w/T_0	p_0, atm	H_0, MJ/kg	T_0, K	p_∞, atm $\times 10^3$	ρ_∞, kg/m3 $\times 10^3$	T_∞, K	u_∞, m/sec	M_∞	$N_{Re_\infty,L}$ $\times 10^{-3}$	$N_{Re_\infty,h}$ $\times 10^{-3}$	δ, cm	δ^*, cm	h/δ
180-03-03	0.0	0.103	0.178	3.95	2900	0.91	0.39	790	2279	4.01	3.11	0.0	1.25	0.47	0.0
180-03-06	0.0	0.088	0.205	6.28	3400	1.01	0.37	854	2531	4.09	3.11	0.0	1.29	0.48	0.0
180-03-09	0.0	0.077	0.221	6.97	3900	1.03	0.32	897	2770	4.22	2.83	0.0	1.33	0.50	0.0
180-03-12	0.0	0.073	0.233	7.90	4100	0.96	0.30	922	2855	4.27	2.75	0.0	1.36	0.52	0.0
180-03-15	0.0	0.064	0.253	10.23	4660	1.16	0.31	1071	3051	4.19	2.73	0.0	1.40	0.53	0.0
180-03-18	0.0	0.058	0.265	11.62	5200	1.17	0.29	1150	3260	4.25	2.53	0.0	1.48	0.56	0.0
180-03-21	0.0	0.055	0.277	12.79	5500	1.22	0.28	1168	3389	4.29	2.52	0.0	1.43	0.55	0.0
180-03-24	0.0	0.093	0.360	4.88	3230	1.62	0.64	831	2445	4.12	5.28	0.0	0.99	0.35	0.0
180-03-27	0.0	0.087	0.380	5.81	3430	1.84	0.67	874	2535	4.09	5.54	0.0	0.98	0.37	0.0
180-03-30	0.0	0.081	0.400	6.51	3700	1.84	0.63	897	2667	4.15	5.41	0.0	0.99	0.37	0.0
180-03-33	0.0	0.071	0.440	7.90	4200	1.99	0.60	979	2876	4.19	5.25	0.0	1.01	0.39	0.0
180-03-36	0.0	0.066	0.467	9.30	4550	2.07	0.58	1024	3010	4.21	5.05	0.0	1.03	0.40	0.0
180-03-39	0.0	0.061	0.495	10.46	4950	2.14	0.53	1158	3240	4.24	4.62	0.0	0.99	0.37	0.0
180-04-03	0.0	0.104	0.645	3.49	2880	3.17	1.38	792	2264	4.02	10.89	0.0	0.69	0.27	0.0
180-04-06	0.0	0.095	0.686	4.18	3160	3.34	1.33	856	2392	4.03	10.57	0.0	0.67	0.25	0.0
180-04-09	0.0	0.092	0.722	4.88	3250	3.50	1.30	869	2437	4.04	10.72	0.0	0.68	0.25	0.0
180-04-12	0.0	0.082	0.775	6.16	3640	3.66	1.25	918	2623	4.11	10.45	0.0	0.70	0.27	0.0
180-04-15	0.0	0.076	0.810	6.51	3925	3.75	1.25	930	2679	4.13	10.56	0.0	0.72	0.27	0.0
180-04-18	0.0	0.070	0.870	7.90	4300	3.99	1.24	974	2809	4.16	21.70	0.0	0.73	0.29	0.0
180-11-03	0.0	0.094	1.360	4.53	3175	6.75	2.63	873	2391	4.02	20.61	0.0	0.51	0.19	0.0
180-11-06	0.0	0.090	1.420	5.11	3350	7.00	2.57	907	2469	4.03	20.37	0.0	0.50	0.19	0.0
180-11-09	0.0	0.082	1.490	6.04	3650	7.18	2.43	948	2611	4.08	19.72	0.0	0.43	0.19	0.0
180-05-06	0.16	0.094	0.210	6.28	3175	1.06	0.41	835	2415	4.04	3.36	0.04	1.26	0.47	0.126
180-05-09	0.16	0.088	0.225	7.21	3400	1.11	0.41	858	2529	4.08	3.41	0.04	1.43	0.57	0.111
180-05-12	0.16	0.080	0.238	8.14	3750	1.17	0.38	898	2695	4.14	3.30	0.04	1.28	0.48	0.124
180-05-15	0.16	0.066	0.258	10.23	4575	1.20	0.33	1058	3018	4.18	2.86	0.04	1.37	0.51	0.115
180-05-18	0.16	0.063	0.270	9.76	4775	1.26	0.33	1100	3091	4.19	2.86	0.04	1.51	0.62	0.105
180-05-21	0.16	0.059	0.283	12.55	5050	1.30	0.32	1143	3196	4.21	2.81	0.04	1.37	0.53	0.116
180-06-03	0.16	0.100	0.364	4.88	3000	1.90	0.78	825	2318	3.99	6.13	0.08	0.93	0.35	0.170
180-06-06	0.16	0.094	0.385	5.58	3200	1.97	0.76	858	2415	4.02	6.06	0.08	1.00	0.37	0.159
180-06-09	0.16	0.088	0.407	6.39	3400	2.35	0.82	917	2498	3.96	6.53	0.08	0.98	0.37	0.162
180-06-12	0.16	0.078	0.448	7.90	3850	2.09	0.68	925	2730	4.15	5.90	0.07	1.05	0.39	0.151
180-06-15	0.16	0.068	0.473	9.18	4400	2.16	0.62	1025	2950	4.19	5.40	0.07	1.01	0.39	0.157
180-06-18	0.16	0.063	0.501	10.23	4750	2.28	0.60	1096	3079	4.20	5.23	0.07	0.96	0.36	0.166
180-06-21	0.16	0.111	0.639	3.49	2700	3.24	1.18	749	2180	4.00	11.83	0.15	0.66	0.25	0.239
180-06-24	0.16	0.103	0.680	4.07	2900	3.48	1.49	806	2269	4.00	11.63	0.15	0.68	0.26	0.233
180-06-27	0.16	0.094	0.710	4.88	3175	3.58	1.39	866	2396	4.02	11.02	0.14	0.74	0.27	0.214
180-06-30	0.16	0.086	0.766	6.04	3475	3.78	1.34	909	2540	4.06	10.91	0.14	0.73	0.28	0.216
180-06-33	0.16	0.080	0.808	6.97	3750	3.76	1.31	931	2673	4.13	10.61	0.13	0.71	0.27	0.224
180-06-36	0.16	0.075	0.850	7.90	4025	3.87	1.21	966	2796	4.17	10.42	0.13	0.72	0.28	0.220
180-10-03	0.16	0.092	1.360	4.65	3250	6.74	2.56	866	2425	4.03	20.15	0.26	0.51	0.19	0.312
180-10-06	0.16	0.087	1.420	5.23	3450	6.95	2.48	922	2517	4.05	19.82	0.25	0.44	0.19	0.364
180-10-09	0.16	0.082	1.490	6.00	3675	7.12	2.40	951	2624	4.09	19.58	0.25	0.52	0.19	0.306

*Free-stream conditions based on frozen flow model.

**Boundary-layer predictions based on nonequilibrium flow-equilibrium catalytic wall conditions.

TABLE I.- TEST CONDITIONS FOR HEAT-TRANSFER MEASUREMENTS ON MODEL I – Concluded

RUN	MODEL CONDITIONS		STAGNATION CONDITIONS			FREESTREAM CONDITIONS AT THE STEP LOCATION*							BOUNDARY LAYER AT THE STEP **		
	h, cm	T_w/T_0	p_0, atm	H_0, MJ/kg	T_0, K	p_∞, atm $\times 10^3$	ρ_∞, kg/m3 $\times 10^3$	T_∞, K	u_∞, m/sec	M_∞	$N_{Re_\infty,L}$ $\times 10^{-3}$	$N_{Re_\infty,h}$ $\times 10^{-3}$	δ, cm	δ^*, cm	h/δ
180-07-03	0.51	0.110	0.183	4.18	2725	0.90	0.42	742	2200	4.03	3.33	0.14	1.22	0.45	0.417
180-07-06	0.51	0.097	0.202	6.04	3100	1.03	0.41	826	2377	4.03	3.32	0.13	1.20	0.44	0.424
180-07-09	0.51	0.090	0.214	7.09	3350	1.06	0.39	852	2505	4.08	3.29	0.13	1.26	0.47	0.405
180-07-12	0.51	0.080	0.224	8.14	3750	1.07	0.36	896	2696	4.14	3.11	0.13	1.42	0.57	0.358
180-07-15	0.51	0.069	0.246	9.53	4350	1.23	0.35	1032	2926	4.12	3.00	0.12	1.33	0.50	0.381
180-07-18	0.51	0.061	0.259	11.62	4900	1.20	0.31	1120	3139	4.20	2.66	0.11	1.44	0.55	0.354
180-07-21	0.51	0.059	0.273	12.79	5075	1.26	0.31	1147	3206	4.21	2.70	0.11	1.37	0.53	0.372
180-07-24	0.51	0.102	0.365	4.65	2950	1.90	0.80	815	2294	3.99	5.87	0.25	0.94	0.36	0.538
180-07-27	0.51	0.095	0.380	5.35	3150	1.96	0.76	852	2391	4.01	6.09	0.25	1.00	0.38	0.508
180-07-30	0.51	0.092	0.395	6.04	3275	2.00	0.75	868	2453	4.03	6.09	0.25	0.99	0.38	0.513
180-07-33	0.51	0.080	0.431	7.67	3750	2.10	0.70	921	2686	4.11	5.92	0.24	0.93	0.34	0.546
180-07-36	0.51	0.070	0.457	9.07	4300	2.10	0.62	1005	2912	4.18	5.36	0.22	1.00	0.38	0.507
180-07-39	0.51	0.067	0.484	9.42	4500	2.21	0.63	1057	3002	4.18	5.47	0.22	1.01	0.39	0.501
180-07-42	0.51	0.109	0.640	3.60	2750	3.33	1.51	768	2200	3.98	11.75	0.48	0.67	0.25	0.761
180-07-45	0.51	0.100	0.680	4.30	3000	3.51	1.44	832	2313	3.99	11.27	0.46	0.66	0.24	0.775
180-07-48	0.51	0.094	0.711	4.88	3175	3.01	1.22	825	2415	4.14	10.04	0.41	0.70	0.26	0.728
180-07-51	0.51	0.086	0.760	6.04	3475	3.74	1.33	897	2540	4.06	10.81	0.44	0.70	0.26	0.728
180-07-54	0.51	0.081	0.797	6.97	3725	3.13	1.11	884	2681	4.30	9.65	0.39	0.70	0.26	0.728
180-07-57	0.51	0.075	0.832	7.90	4025	3.78	1.19	965	2796	4.17	10.20	0.41	0.72	0.27	0.703
180-09-03	0.51	0.096	1.360	4.18	3125	6.76	2.68	862	2368	4.02	20.96	0.85	0.50	0.26	1.010
180-09-06	0.51	0.086	1.420	5.35	3475	6.91	2.46	925	2530	4.05	19.65	0.80	0.52	0.19	0.986
180-09-09	0.51	0.076	1.500	6.97	3950	6.98	2.21	980	2750	4.13	18.49	0.75	0.54	0.20	0.936
180-01-03	1.02	0.111	0.178	3.95	2700	0.93	0.43	747	2182	3.99	3.38	0.27	1.24	0.45	0.819
180-01-06	1.02	0.098	0.207	5.81	3075	1.05	0.43	825	2363	4.02	3.44	0.28	1.20	0.44	0.846
180-01-09	1.02	0.092	0.226	6.74	3275	1.13	0.43	848	2465	4.06	3.53	0.29	1.40	0.56	0.726
180-01-12	1.02	0.081	0.240	7.90	3700	1.15	0.39	891	2672	4.14	3.37	0.27	1.26	0.48	0.807
180-01-15	1.02	0.067	0.254	9.76	4450	1.19	0.33	1034	2971	4.18	2.92	0.24	1.35	0.50	0.754
180-01-18	1.02	0.063	0.265	11.16	4800	1.23	0.32	1103	3101	4.19	2.79	0.23	1.42	0.54	0.717
180-01-21	1.02	0.058	0.276	13.25	5150	1.24	0.30	1150	3238	4.23	2.65	0.22	1.37	0.53	0.739
180-01-24	1.02	0.102	0.358	4.65	2950	1.87	0.78	815	2294	3.99	6.14	0.50	0.95	0.45	1.068
180-01-27	1.02	0.094	0.380	5.58	3200	2.01	0.77	861	2416	4.00	6.10	0.50	1.01	0.39	1.001
180-01-30	1.02	0.092	0.402	6.04	3275	2.01	0.77	870	2455	4.03	6.21	0.50	0.93	0.34	1.093
180-02-03	1.02	0.072	0.470	8.60	4150	2.17	0.66	976	2854	4.17	5.73	0.47	0.98	0.37	1.038
180-02-06	1.02	0.064	0.500	10.60	4700	2.27	0.61	1086	3061	4.20	5.27	0.43	0.95	0.36	1.065
180-02-09	1.02	0.105	0.640	3.95	2850	2.80	1.43	792	2246	4.00	11.17	0.91	0.67	0.25	1.508
180-02-12	1.02	0.102	0.680	4.18	2950	3.48	1.46	818	2291	4.00	11.42	0.93	0.68	0.26	1.488
180-02-15	1.02	0.094	0.710	4.88	3200	3.58	1.38	870	2408	4.02	10.92	0.89	0.70	0.27	1.449
180-02-18	1.02	0.087	0.760	5.81	3450	3.82	1.36	911	2526	4.04	10.99	0.89	0.75	0.28	1.355
180-02-24	1.02	0.073	0.860	8.14	4125	3.89	1.19	981	2838	4.18	10.28	0.84	0.73	0.28	1.389
180-08-03	1.02	0.093	1.400	4.53	3225	6.94	2.66	883	2413	4.02	20.87	1.70	0.50	0.19	2.033
180-08-06	1.02	0.087	1.460	5.23	3450	7.12	2.55	922	2517	4.05	20.33	1.65	0.50	0.18	2.020
180-08-09	1.02	0.080	1.530	6.28	3750	7.24	2.40	953	2658	4.10	19.71	1.60	0.52	0.19	1.972

*Free-stream conditions based on frozen flow model.

**Boundary-layer predictions based on nonequilibrium flow-equilibrium catalytic wall conditions.

TABLE II.- TEST CONDITIONS FOR PRESSURE MEASUREMENTS ON MODEL I

RUN	MODEL CONDITIONS		STAGNATION CONDITIONS			FREESTREAM CONDITIONS AT THE STEP LOCATION*							BOUNDARY LAYER AT THE STEP **		
	h, cm	T_w/T_0	p_0, atm	H_0, MJ/kg	T_0, K	p_∞, atm $\times 10^3$	ρ_∞, kg/m^3 $\times 10^3$	T_∞, K	u_∞, m/sec	M_∞	$N_{Re_\infty,L}$ $\times 10^{-3}$	$N_{Re_\infty,h}$ $\times 10^{-3}$	δ, cm	δ^*, cm	h/δ
200-04-09	0.0	0.094	0.378	5.58	3200	1.95	0.75	860	2415	4.02	5.98	0.0	1.02	0.40	0.0
200-04-12	0.0	0.076	0.439	8.14	3925	2.04	0.65	924	2762	4.15	5.68	0.0	0.98	0.37	0.0
200-04-15	0.0	0.098	0.697	4.53	3075	3.53	1.42	845	2349	4.00	11.15	0.0	0.72	0.28	0.0
200-04-18	0.0	0.086	0.780	6.16	3500	3.79	1.34	910	2553	4.07	10.97	0.0	0.73	0.27	0.0
200-04-21	0.0	0.084	1.500	5.70	3575	7.19	2.49	938	2577	4.07	20.13	0.0	0.73	0.89	0.0
200-04-24	0.0	0.079	1.590	6.28	3775	7.49	2.47	962	2669	4.10	20.30	0.0	0.51	0.19	0.0
200-04-27	0.0	0.081	1.905	5.81	3700	9.39	3.11	971	2626	4.06	25.07	0.0	0.49	0.18	0.0
200-07-09	0.20	0.093	0.380	5.81	3225	1.95	0.74	862	2428	4.02	5.96	0.09	1.01	0.39	0.195
200-07-12	0.20	0.075	0.432	8.25	4000	2.01	0.63	949	2793	4.16	5.50	0.09	1.06	0.42	0.187
200-07-15	0.20	0.098	0.700	4.42	3050	3.52	1.43	838	2339	4.01	11.05	0.18	0.72	0.27	0.274
200-07-18	0.20	0.086	0.785	6.04	3475	3.90	1.38	912	2538	4.05	11.21	0.18	0.72	0.27	0.275
200-07-21	0.20	0.082	1.505	5.99	3675	7.31	2.45	955	2621	4.07	19.93	0.32	0.53	0.20	0.374
200-07-24	0.20	0.081	1.640	6.04	3725	7.78	2.59	959	2645	4.09	21.19	0.34	0.51	0.19	0.392
200-03-09	0.51	0.080	0.380	6.04	3750	1.83	0.61	913	2685	4.12	5.22	0.21	1.09	0.43	0.467
200-03-12	0.51	0.070	0.428	9.07	4275	2.00	0.59	1004	2901	4.16	5.10	0.21	1.10	0.43	0.463
200-03-15	0.51	0.102	0.700	4.18	2950	3.58	1.50	818	2291	4.00	11.74	0.48	0.71	0.27	0.715
200-03-18	0.51	0.087	0.788	5.93	3450	3.86	1.39	905	2528	4.06	11.23	0.46	0.69	0.26	0.734
200-03-21	0.51	0.086	1.520	5.35	3500	7.28	2.58	927	2542	4.06	20.71	0.84	0.49	0.18	1.029
200-03-24	0.51	0.080	1.605	6.04	3750	7.73	2.55	965	2655	4.08	20.82	0.85	0.50	0.19	1.010
200-03-27	0.51	0.087	1.960	5.00	3450	10.27	3.60	948	2504	3.99	28.10	1.14	0.46	0.15	1.104
200-08-09	0.71	0.092	0.389	5.99	3250	2.01	0.76	869	2439	4.02	6.09	0.35	1.00	0.39	0.711
200-08-12	0.71	0.079	0.447	7.90	3800	2.11	0.70	921	2688	4.14	5.98	0.34	1.05	0.42	0.680
200-08-15	0.71	0.097	0.700	4.65	3100	3.57	1.42	852	2360	4.01	11.15	0.63	0.72	0.27	0.985
200-08-18	0.71	0.086	0.788	6.04	3475	3.91	1.39	912	2538	4.05	11.25	0.64	0.72	0.27	0.993
200-08-21	0.71	0.087	1.510	5.23	3450	7.34	2.63	922	2517	4.05	20.96	1.19	0.50	0.19	1.414
200-08-24	0.71	0.080	1.595	6.28	3750	7.68	2.53	965	2655	4.08	20.70	1.18	0.51	0.19	1.397
200-08-27	0.71	0.081	1.925	5.81	3725	9.25	3.07	968	2640	4.08	24.88	1.42	0.46	0.17	1.535
200-01-09	1.02	0.092	0.379	5.81	3250	1.93	0.73	864	2441	4.03	5.89	0.48	1.01	0.39	1.001
200-01-12	1.02	0.073	0.440	8.60	4125	2.02	0.62	969	2845	4.17	5.39	0.44	1.01	0.39	1.004
200-01-15	1.02	0.098	0.695	4.42	3050	3.50	1.42	838	2339	4.01	11.17	0.91	0.70	0.27	1.449
200-01-18	1.02	0.086	0.780	6.04	3475	3.88	1.38	912	2538	4.05	11.15	0.91	0.73	0.28	1.395
200-01-21	1.02	0.084	1.500	5.70	3575	7.19	2.49	938	2577	4.07	20.13	1.64	0.50	0.19	2.020
200-01-24	1.02	0.080	1.590	6.16	3750	7.66	2.53	965	2655	4.08	20.64	1.68	0.51	0.19	1.996
200-01-27	1.02	0.082	1.900	5.58	3650	9.15	3.10	958	2606	4.07	24.96	2.03	0.49	0.18	2.083

*Free-stream conditions based on frozen flow model.

**Boundary-layer predictions based on nonequilibrium flow-equilibrium catalytic wall conditions.

TABLE III.- TEST CONDITIONS FOR HEAT-TRANSFER MEASUREMENTS ON MODEL II

RUN	MODEL CONDITIONS			STAGNATION CONDITIONS			FREESTREAM CONDITIONS AT THE STEP LOCATION*							BOUNDARY LAYER AT THE STEP **		
	h, cm	w	T_w/T_0	p_0, atm	H_0, MJ/kg	T_0, K	p_∞, atm $\times 10^3$	ρ_∞, kg/m^3 $\times 10^3$	T_∞, K	u_∞, m/sec	M_∞	$N_{Re_\infty,L}$ $\times 10^{-3}$	$N_{Re_\infty,h}$ $\times 10^{-3}$	δ, cm	δ^*, cm	h/δ
190-10-03	0.0	0.0	0.082	0.226	7.90	3650	1.13	0.39	894	2645	4.10	2.61	0.0	1.24	0.45	0.0
190-10-06	0.0	0.0	0.063	0.253	10.93	4750	1.24	0.32	1110	3076	4.15	2.19	0.0	1.24	0.45	0.0
190-10-12	0.0	0.0	0.092	0.385	5.81	3250	2.06	0.77	877	2435	3.99	4.87	0.0	0.79	0.30	0.0
190-10-15	0.0	0.0	0.078	0.450	7.90	3850	2.24	0.72	943	2722	4.10	4.87	0.0	0.82	0.31	0.0
190-10-18	0.0	0.0	0.069	0.477	9.18	4375	2.32	0.66	1038	2933	4.18	4.47	0.0	0.86	0.33	0.0
190-10-21	0.0	0.0	0.103	0.695	3.95	2900	3.78	1.59	819	2262	3.96	9.72	0.0	0.58	0.22	0.0
190-10-24	0.0	0.0	0.087	0.775	5.93	3450	4.08	1.44	922	2520	4.01	9.08	0.0	0.60	0.22	0.0
190-10-27	0.0	0.0	0.081	0.815	6.97	3725	4.05	1.34	944	2655	4.08	8.78	0.0	0.61	0.23	0.0
190-10-30	0.0	0.0	0.077	0.875	7.44	3900	4.24	1.35	965	2735	4.11	8.99	0.0	0.61	0.23	0.0
190-05-03	0.60	0.119	0.081	0.221	7.90	3694	1.13	0.38	905	2663	4.09	2.55	0.15	1.23	0.49	0.487
190-09-03	0.60	0.0	0.082	0.222	7.90	3650	1.11	0.38	894	2645	4.10	2.57	0.15	1.12	0.42	0.534
190-04-09	0.60	0.708	0.063	0.240	11.39	4800	1.16	0.30	1116	3096	4.16	2.04	0.12	1.21	0.44	0.493
190-09-06	0.60	0.0	0.063	0.252	11.16	4775	1.24	0.32	1116	3084	4.15	2.17	0.13	1.22	0.46	0.491
190-04-12	0.60	0.613	0.095	0.355	5.58	3166	1.91	0.73	862	2395	3.99	4.59	0.28	0.82	0.30	0.728
190-05-12	0.60	0.588	0.093	0.375	5.81	3237	2.00	0.75	873	2429	3.99	4.75	0.29	0.82	0.30	0.731
190-09-12	0.60	0.0	0.093	0.383	5.81	3225	2.10	0.79	878	2420	3.98	4.93	0.30	0.87	0.34	0.687
190-04-15	0.60	0.668	0.084	0.410	7.21	3560	2.10	0.73	907	2589	4.06	4.76	0.29	0.82	0.30	0.728
190-05-15	0.60	0.593	0.081	0.432	7.56	3700	2.16	0.72	921	2656	4.08	4.82	0.29	0.84	0.31	0.712
190-09-15	0.60	0.0	0.078	0.439	7.90	3850	2.19	0.70	943	2723	4.10	4.73	0.29	0.83	0.31	0.720
190-05-18	0.60	0.512	0.070	0.460	9.07	4315	2.23	0.64	1025	2911	4.14	4.37	0.26	0.86	0.33	0.694
190-04-21	0.60	0.700	0.102	0.644	4.07	2928	3.52	1.46	827	2275	3.95	8.95	0.54	0.59	0.22	1.004
190-05-21	0.60	0.733	0.102	0.680	4.07	2935	3.71	1.54	828	2278	3.95	9.41	0.57	0.59	0.22	1.015
190-09-21	0.60	0.0	0.103	0.691	3.95	2900	3.76	1.58	819	2262	3.96	9.67	0.58	0.58	0.22	1.031
190-04-24	0.60	0.725	0.087	0.720	5.88	3437	3.80	1.34	919	2515	4.01	8.50	0.51	0.62	0.23	0.969
190-04-27	0.60	0.719	0.082	0.760	6.74	3657	3.89	1.30	941	2622	4.05	8.44	0.51	0.62	0.23	0.960
190-09-24	0.60	0.0	0.087	0.770	5.81	3450	4.06	1.43	922	2520	4.01	9.03	0.54	0.60	0.22	0.999
190-05-24	0.60	0.786	0.086	0.770	6.04	3470	4.03	1.41	923	2530	4.01	8.96	0.54	0.60	0.22	0.999
190-09-27	0.60	0.0	0.083	0.818	6.39	3600	4.09	1.40	930	2596	4.06	9.05	0.55	0.60	0.22	0.999
190-04-30	0.60	0.777	0.077	0.818	7.44	3875	3.96	1.27	958	2725	4.11	8.46	0.51	0.62	0.23	0.965
190-09-30	0.60	0.0	0.077	0.870	7.44	3900	4.22	1.34	965	2735	4.11	8.94	0.54	0.61	0.23	0.984
190-08-03	1.02	0.0	0.081	0.222	7.90	3695	1.13	0.38	905	2664	4.09	2.56	0.26	1.42	0.57	0.717
188-05-03	1.02	0.251	0.082	0.227	7.90	3675	1.07	0.37	882	2664	4.14	2.53	0.26	1.23	0.49	0.829
190-07-12	1.02	0.224	0.093	0.348	5.81	3217	1.89	0.71	872	2419	3.98	4.48	0.46	0.90	0.38	1.130
190-08-12	1.02	0.0	0.094	0.379	5.52	3185	2.04	0.78	867	2403	3.98	4.88	0.50	0.88	0.34	1.153
190-07-15	1.02	0.284	0.084	0.402	7.15	3580	2.09	0.71	912	2598	4.05	4.68	0.48	0.84	0.31	1.212
190-03-06	1.02	0.404	0.076	0.425	8.14	3958	2.11	0.66	960	2769	4.11	4.47	0.46	0.90	0.31	1.134
190-07-18	1.02	0.264	0.068	0.430	9.30	4405	2.08	0.59	1042	2946	4.14	3.99	0.41	0.91	0.34	1.119
190-08-15	1.02	0.0	0.078	0.435	7.90	3846	2.17	0.70	942	2721	4.10	4.70	0.48	0.83	0.31	1.225
190-08-18	1.02	0.0	0.069	0.465	9.07	4320	2.26	0.65	1026	2913	4.14	4.39	0.45	0.86	0.32	1.186
188-06-15	1.02	0.337	0.099	0.620	4.42	3030	3.35	1.34	848	2323	3.96	8.27	0.85	0.68	0.25	1.502
190-07-21	1.02	0.346	0.100	0.645	4.30	2990	3.45	1.41	837	2305	3.97	8.66	0.89	0.60	0.22	1.692
190-08-21	1.02	0.0	0.104	0.690	3.95	2894	3.75	1.58	817	2260	3.96	9.67	0.99	0.58	0.22	1.754

*Free-stream conditions based on frozen flow model.

**Boundary-layer predictions based on nonequilibrium flow-equilibrium catalytic wall conditions.

TABLE III.- TEST CONDITIONS FOR HEAT-TRANSFER MEASUREMENTS ON MODEL II – Concluded

RUN	MODEL CONDITIONS			STAGNATION CONDITIONS			FREESTREAM CONDITIONS AT THE STEP LOCATION*							BOUNDARY LAYER AT THE STEP **		
	h, cm	w	T_w/T_0	p_0, atm	H_0, MJ/kg	T_0, K	p_∞, atm $\times 10^3$	ρ_∞, kg/m^3 $\times 10^3$	T_∞, K	u_∞, m/sec	M_∞	$N_{Re_\infty,L}$ $\times 10^{-3}$	$N_{Re_\infty,h}$ $\times 10^{-3}$	δ, cm	δ^*, cm	h/δ
190-07-24	1.02	0.358	0.088	0.714	5.88	3420	3.74	1.33	915	2508	4.01	8.42	0.86	0.62	0.23	1.642
190-02-18	1.02	0.407	0.089	0.750	5.58	3375	3.95	1.42	911	2485	4.00	8.95	0.92	0.60	0.22	1.701
190-07-27	1.02	0.396	0.080	0.755	6.97	3732	3.87	1.27	951	2656	4.06	8.28	0.85	0.63	0.23	1.603
190-08-24	1.02	0.0	0.087	0.766	5.81	3440	4.02	1.42	920	2516	4.01	8.98	0.92	0.60	0.22	1.701
190-07-30	1.02	0.435	0.076	0.802	7.67	3936	3.91	1.23	968	2751	4.11	8.23	0.84	0.63	0.24	1.610
190-03-12	1.02	0.491	0.079	0.805	7.15	3775	3.88	1.28	943	2681	4.10	8.48	0.87	0.62	0.23	1.634
190-08-27	1.02	0.0	0.080	0.815	6.97	3750	4.02	1.32	946	2667	4.08	8.71	0.89	0.61	0.23	1.675
188-02-09	1.02	0.442	0.077	0.865	7.56	3900	4.20	1.34	965	2735	4.11	8.90	0.91	0.61	0.23	1.667
190-08-30	1.02	0.0	0.077	0.870	7.56	3920	4.25	1.34	970	2742	4.10	8.94	0.92	0.61	0.23	1.658

*Free-stream conditions based on frozen flow model.

**Boundary-layer predictions based on nonequilibrium flow-equilibrium catalytic wall conditions.

TABLE IV.- TEST CONDITIONS FOR PRESSURE MEASUREMENTS ON MODEL II

RUN	MODEL CONDITIONS			STAGNATION CONDITIONS			FREESTREAM CONDITIONS AT THE STEP LOCATION*							BOUNDARY LAYER AT THE STEP **		
	h, cm	w	T_w/T_0	p_0, atm	H_0, MJ/kg	T_0, K	p_∞, atm $\times 10^3$	ρ_∞, kg/m^3 $\times 10^3$	T_∞, K	u_∞, m/sec	M_∞	$N_{Re_\infty,L}$ $\times 10^{-3}$	$N_{Re_\infty,h}$ $\times 10^{-3}$	δ, cm	δ^*, cm	h/δ
197-05-06	0.0	0.0	0.071	0.236	9.24	4250	1.18	0.34	1009	2889	4.12	2.33	0.0	1.19	0.45	0.0
197-05-12	0.0	0.0	0.094	0.360	5.52	3175	1.94	0.74	865	2399	3.98	4.65	0.0	0.82	0.30	0.0
197-05-15	0.0	0.0	0.076	0.421	8.14	3925	2.08	0.66	951	2756	4.11	4.45	0.0	0.86	0.32	0.0
197-05-18	0.0	0.0	0.070	0.451	9.07	4300	2.11	0.61	1010	2910	4.16	4.23	0.0	0.87	0.33	0.0
197-05-21	0.0	0.0	0.101	0.680	4.18	2960	3.68	1.52	832	2290	3.96	9.28	0.0	0.58	0.22	0.0
197-05-24	0.0	0.0	0.087	0.770	5.93	3450	4.06	1.43	922	2520	4.01	9.03	0.0	0.60	0.22	0.0
197-05-27	0.0	0.0	0.081	0.813	6.80	3700	4.14	1.37	947	2641	4.06	8.91	0.0	0.61	0.23	0.0
197-05-30	0.0	0.0	0.097	1.423	4.18	3080	7.65	3.02	870	2339	3.96	18.38	0.0	0.42	0.16	0.0
197-05-36	0.0	0.0	0.082	1.570	5.81	3675	7.99	2.65	968	2615	4.04	16.84	0.0	0.44	0.16	0.0
197-05-39	0.0	0.0	0.085	1.895	5.35	3550	9.69	3.32	958	2553	4.02	20.78	0.0	0.46	0.16	0.0
197-04-03	1.02	0.276	0.082	0.226	7.90	3650	1.13	0.39	894	2639	4.10	2.61	0.27	1.23	0.49	0.829
197-01-03	1.02	0.237	0.094	0.240	6.22	3200	1.28	0.49	856	2419	4.00	3.11	0.32	1.10	0.43	0.926
197-03-06	1.02	0.0	0.077	0.242	8.37	3900	1.20	0.38	936	2753	4.12	2.62	0.27	1.10	0.41	0.921
197-01-12	1.02	0.318	0.101	0.362	4.77	2980	2.00	0.81	834	2302	3.95	5.01	0.51	0.79	0.29	1.292
197-03-12	1.02	0.0	0.098	0.364	5.00	3050	1.99	0.79	846	2337	3.96	4.90	0.50	0.80	0.30	1.272
197-04-12	1.02	0.384	0.094	0.368	5.70	3200	2.00	0.76	872	2410	3.98	4.75	0.49	0.80	0.30	1.263
197-01-15	1.02	0.386	0.085	0.422	6.97	3530	2.12	0.74	900	2577	4.07	4.87	0.50	0.81	0.30	1.248
197-03-15	1.02	0.0	0.082	0.425	7.32	3650	2.15	0.73	916	2632	4.07	4.81	0.49	0.83	0.30	1.221
197-04-15	1.02	0.430	0.078	0.431	7.90	3825	2.14	0.69	937	2713	4.10	4.66	0.48	0.84	0.31	1.217
197-01-18	1.02	0.461	0.069	0.450	9.13	4350	2.19	0.62	1033	2924	3.98	4.25	0.44	0.88	0.34	1.149
197-03-18	1.02	0.0	0.075	0.453	8.37	4020	2.23	0.69	969	2795	4.12	4.66	0.48	0.81	0.30	1.258
197-04-18	1.02	0.474	0.070	0.455	9.07	4300	2.21	0.64	1021	2906	4.14	4.34	0.44	0.87	0.36	1.161
197-03-21	1.02	0.0	0.103	0.675	4.07	2920	3.68	1.54	825	2271	3.95	9.39	0.96	0.59	0.22	1.736
197-01-21	1.02	0.385	0.106	0.680	3.84	2825	3.68	1.60	798	2229	3.96	9.78	1.00	0.58	0.22	1.754
197-04-21	1.02	0.383	0.101	0.680	4.18	2960	3.68	1.52	832	2290	3.96	9.28	0.95	0.58	0.22	1.745
197-01-24	1.02	0.391	0.092	0.762	5.11	3250	4.06	1.52	893	2424	3.98	9.42	0.97	0.58	0.21	1.764
197-03-24	1.02	0.0	0.090	0.765	5.46	3350	3.91	1.43	900	2472	4.02	9.02	0.93	0.59	0.22	1.736
197-04-24	1.02	0.381	0.087	0.768	5.93	3450	4.05	1.42	922	2520	4.01	9.01	0.92	0.60	0.22	1.701
197-01-27	1.02	0.417	0.086	0.800	5.99	3475	4.18	1.46	925	2532	4.02	9.28	0.95	0.59	0.22	1.718
197-03-27	1.02	0.0	0.084	0.810	6.34	3575	4.22	1.44	938	2580	4.03	9.20	0.94	0.59	0.22	1.709
197-04-27	1.02	0.379	0.081	0.810	6.97	3700	4.12	1.37	947	2641	4.06	8.88	0.91	0.61	0.23	1.667
197-03-30	1.02	0.0	0.090	1.495	4.88	3350	7.76	2.82	921	2464	4.00	17.44	1.79	0.43	0.16	2.381
197-01-30	1.02	0.422	0.092	1.500	4.65	3250	7.80	2.92	901	2418	3.99	18.01	1.85	0.41	0.15	2.451
197-04-30	1.02	0.410	0.087	1.505	5.23	3460	7.87	2.76	942	2513	4.00	17.16	1.76	0.44	0.16	2.331
197-01-36	1.02	0.482	0.083	1.565	5.81	3630	7.93	2.67	962	2595	4.03	16.91	1.73	0.44	0.16	2.331
197-04-33	1.02	0.412	0.080	1.585	6.28	3750	8.01	2.61	977	2650	4.05	16.68	1.71	0.44	0.16	2.331
197-03-33	1.02	0.0	0.083	1.595	5.75	3630	8.07	2.71	962	2595	4.04	17.20	1.76	0.45	0.16	2.252
197-04-36	1.02	0.360	0.085	1.900	5.23	3525	9.95	3.41	960	2539	4.00	21.20	2.17	0.46	0.16	2.193
197-03-36	1.02	0.0	0.086	1.905	5.11	3480	9.90	3.45	951	2518	4.00	21.40	2.20	0.45	0.15	2.237

*Free-stream conditions based on frozen flow model.

**Boundary-layer predictions based on nonequilibrium flow-equilibrium catalytic wall conditions.

TABLE V.- HEAT-TRANSFER MEASUREMENTS OBTAINED FOR MODEL I

Run	Step, cm	Heat-transfer rate $\times 10^{-4}$, watts/m^2, at thermocouple –																
		1	2	3	4	5	6	7	8	9	10	11	12	13	14	15	16	17
(a) p_0 = 0.18 atm; T_0 = 2800 K																		
180-3-3	0.00	---	2.28	2.20	2.14	2.05	2.02	1.80	1.88	1.92	1.84	1.69	1.62	1.63	---	1.59	1.57	1.57
180-7-3	0.51	1.05	1.57	1.94	1.95	1.86	1.82	1.73	1.84	1.74	1.81	2.05	2.03	1.99	1.82	1.82	1.81	1.82
180-1-3	1.02	---	0.65	0.77	0.79	0.80	0.90	0.91	0.89	0.91	0.82	0.90	0.92	0.92	---	0.97	0.91	0.92
(b) p_0 = 0.20 atm; T_0 = 3200 K																		
180-3-6	0.00	3.58	3.52	3.64	3.60	3.27	3.29	3.03	3.02	2.96	3.04	2.72	2.84	2.76	---	2.68	2.51	2.46
180-5-6	0.16	2.85	3.00	3.19	3.11	2.85	2.62	2.56	2.51	2.44	2.57	3.25	3.35	3.18	---	2.05	2.23	2.39
180-7-6	0.51	1.63	2.31	2.77	2.84	2.73	2.84	2.84	2.87	2.85	2.81	---	3.05	2.96	2.71	2.73	2.68	2.69
180-1-6	1.02	0.38	0.85	1.25	1.48	1.59	1.70	1.73	1.70	1.73	1.83	1.84	1.84	1.70	---	1.70	1.67	1.62
(c) p_0 = 0.22 atm; T_0 = 3400 K																		
180-3-9	0.00	4.42	4.29	4.53	4.33	4.01	4.02	3.51	3.69	3.68	3.75	3.41	3.26	3.37	---	3.33	3.02	3.02
180-5-9	0.16	3.55	3.91	4.21	3.99	3.72	3.47	3.17	3.14	3.09	3.27	3.76	3.93	3.76	---	2.82	2.84	2.85
180-7-9	0.51	2.13	3.02	3.51	3.70	3.52	3.58	3.64	3.64	3.59	3.53	3.63	3.64	3.59	3.39	3.42	3.34	3.30
180-1-9	1.02	0.57	1.35	1.89	2.15	2.23	2.45	2.53	2.61	2.62	2.72	2.70	2.72	2.73	---	2.43	2.40	2.39
(d) p_0 = 0.24 atm; T_0 = 3800 K																		
180-3-12	0.00	5.35	5.13	5.33	5.17	4.67	4.60	4.24	4.34	4.38	4.36	4.12	3.86	3.96	---	3.93	3.59	3.56
180-5-12	0.16	4.57	4.61	5.01	4.84	4.65	4.28	3.94	3.96	3.87	3.97	4.59	4.61	4.50	---	3.76	3.61	3.51
180-7-12	0.51	2.44	3.52	4.15	4.33	4.80	---	4.21	4.33	4.16	4.36	4.26	4.21	4.10	3.97	4.02	3.97	3.88
180-1-12	1.02	0.80	1.58	2.17	2.61	2.63	2.90	3.06	3.14	3.19	3.22	3.25	3.23	3.25	---	3.14	---	3.02
(e) p_0 = 0.25 atm; T_0 = 4500 K																		
180-3-15	0.00	6.80	6.58	6.69	6.58	6.18	6.13	5.75	5.75	5.64	5.56	5.35	5.10	5.10	---	4.93	4.67	4.64
180-5-15	0.16	5.56	5.95	6.23	6.09	5.69	5.46	5.35	5.30	5.33	5.35	5.28	5.28	5.25	---	4.65	4.44	4.36
180-7-15	0.51	2.95	4.38	5.16	5.35	5.13	5.22	5.18	5.32	5.28	5.30	5.33	5.31	5.20	4.98	5.10	4.95	4.92
180-1-15	1.02	1.06	2.05	2.82	3.36	3.44	3.72	3.88	---	3.96	3.97	3.97	3.94	3.99	---	3.79	3.68	3.64
(f) p_0 = 0.27 atm; T_0 = 5000 K																		
180-3-18	0.00	8.01	7.65	7.70	7.62	7.16	7.23	6.78	6.80	6.69	6.50	6.29	6.15	5.92	---	5.74	5.47	5.35
180-5-18	0.16	6.61	6.96	7.22	7.18	6.66	6.72	6.32	6.43	6.37	6.26	6.24	6.21	6.09	---	5.60	5.47	5.30
180-7-18	0.51	3.59	5.15	6.09	6.32	6.10	6.10	6.12	6.22	6.08	6.06	6.26	6.21	6.07	5.81	5.87	5.67	5.68
180-1-18	1.02	1.31	2.52	3.48	4.09	4.21	4.65	4.78	4.85	4.89	4.94	1.14	4.90	4.87	---	4.66	4.53	4.44

TABLE V.- HEAT-TRANSFER MEASUREMENTS OBTAINED FOR MODEL I – Continued

Run	Step, cm	Heat-transfer rate $\times 10^{-4}$, watts/m^2, at thermocouple –																
		1	2	3	4	5	6	7	8	9	10	11	12	13	14	15	16	17
(g) p_0 = 0.28 atm; T_0 = 5200 K																		
180-3-21	0.00	9.17	8.91	8.84	8.63	8.05	8.09	7.86	7.78	7.57	7.46	7.10	6.95	6.88	---	6.70	6.38	6.15
180-5-21	0.16	7.46	8.03	8.36	8.31	7.82	7.72	7.40	7.46	7.18	7.13	7.32	7.27	7.08	---	6.61	6.46	6.26
180-7-21	0.51	4.10	5.77	6.92	7.00	6.82	6.84	6.87	7.05	6.83	6.83	7.06	7.06	6.92	6.54	6.47	6.36	6.38
180-1-21	1.02	1.61	3.07	4.23	4.98	5.24	5.73	5.81	5.84	5.92	5.98	5.92	5.87	5.81	---	5.69	5.58	5.42
(h) p_0 = 0.36 atm; T_0 = 3000 K																		
180-3-24	0.00	3.84	3.52	3.54	3.47	3.25	3.28	2.96	3.05	2.96	2.96	2.85	2.62	2.68	---	2.71	2.51	2.45
180-6-3	0.16	2.73	2.96	3.19	3.07	2.96	2.85	2.62	2.62	2.56	2.60	2.79	2.85	2.87	---	2.41	2.33	2.24
180-7-24	0.51	1.40	2.11	2.64	2.76	2.73	2.73	2.73	2.82	2.76	2.77	2.93	3.02	2.82	2.85	2.82	2.73	2.71
180-1-24	1.02	0.46	0.93	1.37	1.71	1.80	1.99	2.04	2.05	2.10	2.05	2.12	2.11	2.10	---	2.13	2.05	2.04
(i) p_0 = 0.38 atm; T_0 = 3200 K																		
180-3-27	0.00	4.56	4.26	4.33	4.27	3.87	3.94	3.47	3.66	3.62	3.55	3.30	3.11	3.22	---	3.25	3.00	2.94
180-6-6	0.16	3.51	3.70	4.05	3.95	3.64	3.53	3.25	3.30	3.19	3.30	3.59	3.68	3.53	---	3.14	2.96	2.85
180-7-27	0.51	1.79	2.62	3.19	3.34	3.26	3.29	3.25	3.38	3.37	3.36	3.59	3.62	3.53	3.33	3.35	3.22	3.20
180-1-27	1.02	---	1.28	1.82	2.16	2.24	2.41	2.57	2.61	2.66	2.61	2.62	2.61	2.70	---	2.71	---	2.61
(j) p_0 = 0.40 atm; T_0 = 3400 K																		
180-3-30	0.00	5.64	5.20	5.27	5.24	4.73	4.81	4.30	4.38	4.34	4.37	4.07	3.85	4.03	---	3.91	3.59	3.63
180-6-9	0.16	4.10	4.36	4.82	4.70	4.33	3.99	3.84	3.85	3.82	3.89	4.27	4.35	4.16	---	3.64	3.53	3.45
180-7-30	0.51	2.06	3.07	3.80	3.96	3.85	3.91	4.04	4.10	4.01	4.02	4.20	4.28	4.16	3.93	4.02	3.87	3.89
180-1-30	1.02	---	1.49	2.06	2.45	2.53	2.88	3.03	3.07	3.05	3.05	3.06	3.09	3.09	---	3.07	2.96	2.93
(k) p_0 = 0.44 atm; T_0 = 3800 K																		
180-3-33	0.00	7.40	6.95	6.95	6.86	6.32	6.18	6.07	---	5.84	5.79	5.39	5.17	5.36	---	5.17	4.81	4.87
180-6-12	0.16	5.80	6.04	6.59	6.55	5.98	5.68	5.30	5.35	5.38	5.35	5.81	5.92	5.73	---	5.01	4.81	4.67
180-7-33	0.51	2.64	4.04	4.93	5.15	5.07	5.17	5.13	5.23	5.14	5.17	5.26	5.27	5.22	4.93	4.94	4.76	4.78
(l) p_0 = 0.47 atm; T_0 = 4400 K																		
180-3-36	0.00	9.00	8.52	8.60	8.26	7.66	7.74	7.23	7.27	7.12	6.99	6.64	6.40	6.47	---	6.37	5.92	5.81
180-6-15	0.16	6.83	7.40	7.82	7.74	7.27	7.06	6.74	6.78	6.66	6.58	6.81	6.79	6.72	---	6.15	5.91	5.72
180-7-36	0.51	3.30	5.24	6.26	6.51	6.32	6.56	6.61	6.59	6.58	6.49	6.53	6.45	6.39	6.13	5.75	6.09	6.09
180-2-3	1.02	1.10	2.12	3.05	3.69	3.87	4.27	4.37	4.46	4.54	4.73	4.78	4.70	4.67	---	4.67	4.44	4.46

TABLE V.- HEAT-TRANSFER MEASUREMENTS OBTAINED FOR MODEL I – Continued

Run	Step, cm	Heat-transfer rate $\times 10^{-4}$, watts/m^2, at thermocouple –																
		1	2	3	4	5	6	7	8	9	10	11	12	13	14	15	16	17
(m) p_0 = 0.50 atm; T_0 = 4700 K																		
180-3-39	0.00	10.5	10.0	9.79	9.57	9.34	9.09	8.61	8.62	8.43	8.31	7.95	7.63	7.52	---	7.40	7.04	6.97
180-6-18	0.16	8.53	9.13	9.62	9.64	9.05	9.17	8.83	8.83	8.66	8.60	8.47	8.43	8.20	---	7.74	7.52	7.40
180-7-39	0.51	3.99	6.21	7.38	7.68	7.40	7.70	7.63	7.74	7.65	---	7.63	7.63	7.54	7.18	7.23	7.07	7.11
180-2-6	1.02	1.37	2.78	4.10	4.89	5.09	5.63	5.67	5.88	5.84	6.04	6.00	5.93	5.90	---	5.85	5.67	5.57
(n) p_0 = 0.64 atm; T_0 = 2800 K																		
180-4-3	0.00	3.47	3.30	3.22	3.15	2.93	2.95	2.77	2.73	2.62	2.53	2.43	2.38	2.36	---	2.29	2.28	2.20
180-6-21	0.16	2.45	2.68	2.85	2.88	2.73	2.72	2.62	2.56	2.53	2.56	2.50	2.61	2.64	---	2.60	2.72	2.96
180-7-42	0.51	0.93	1.78	2.27	2.39	2.39	2.45	2.49	2.51	2.53	2.56	2.65	2.64	---	2.51	2.52	2.52	2.62
180-2-9	1.02	0.38	0.69	0.97	1.25	1.48	1.64	1.72	1.80	1.81	1.86	1.91	1.90	1.87	---	1.92	1.83	1.82
(o) p_0 = 0.68 atm; T_0 = 3000 K																		
180-4-6	0.00	4.36	4.18	4.11	4.05	3.77	3.80	3.51	3.47	3.44	3.42	3.21	3.15	3.14	---	3.07	2.96	2.94
180-6-24	0.16	3.19	3.64	3.87	3.82	3.59	3.52	3.37	3.44	3.42	3.36	3.49	3.64	3.55	---	3.15	3.04	3.05
180-7-45	0.51	1.39	2.39	3.04	3.21	3.12	3.22	3.30	3.42	3.33	3.42	3.62	3.64	3.53	3.33	3.31	3.30	3.37
180-2-12	1.02	0.49	0.84	1.37	1.82	1.97	2.20	2.28	2.31	2.37	2.48	2.52	2.53	2.48	---	2.52	2.39	2.37
(p) p_0 = 0.71 atm; T_0 = 3200 K																		
180-4-9	0.00	5.42	5.24	5.39	5.20	4.73	4.81	4.45	4.48	4.40	4.35	4.29	4.02	4.08	---	3.96	3.79	4.35
180-6-27	0.16	3.80	4.27	4.67	4.62	4.35	4.30	4.10	4.15	4.12	4.18	4.30	4.30	4.25	---	3.77	3.68	3.52
180-7-48	0.51	1.71	2.90	3.68	3.87	3.79	3.92	3.96	4.00	4.01	4.02	4.10	4.15	3.97	3.99	3.97	---	3.99
180-2-15	1.02	0.36	0.71	1.09	1.39	1.59	1.72	1.72	1.74	1.72	1.72	1.72	1.72	1.69	---	1.67	1.59	1.58
(q) p_0 = 0.76 atm; T_0 = 3500 K																		
180-4-12	0.00	7.23	6.94	6.97	6.83	6.26	6.36	5.82	5.98	5.82	5.74	5.47	5.24	5.30	---	5.16	4.86	4.84
180-6-30	0.16	5.23	5.80	6.36	6.26	5.81	5.67	5.46	5.47	5.46	5.49	5.84	---	5.69	---	5.01	4.78	4.73
180-7-51	0.51	2.25	3.76	4.78	5.11	4.95	5.07	5.13	5.24	5.18	5.24	5.47	5.58	5.41	5.01	4.98	4.90	4.98
180-2-18	1.02	0.56	1.37	1.84	2.36	2.60	2.84	2.82	2.88	2.85	2.92	2.87	2.72	2.58	---	2.51	2.28	2.16
(r) p_0 = 0.80 atm; T_0 = 3700 K																		
180-4-15	0.00	---	8.49	8.43	8.26	7.54	7.68	7.03	7.19	7.07	---	6.59	6.33	6.40	---	6.21	5.87	5.81
180-6-33	0.16	6.33	7.10	7.66	7.55	7.05	6.95	6.51	6.59	6.44	6.45	6.81	6.79	6.59	---	6.03	5.72	5.64
180-7-54	0.51	2.99	5.07	6.30	6.60	6.47	6.58	6.82	6.89	6.85	6.88	7.11	7.04	6.84	6.56	6.57	6.53	6.53

TABLE V.- HEAT-TRANSFER MEASUREMENTS OBTAINED FOR MODEL I – Concluded

Run	Step, cm	Heat-transfer rate × 10^{-4}, watts/m^2, at thermocouple –																
		1	2	3	4	5	6	7	8	9	10	11	12	13	14	15	16	17
(s) p_0 = 0.85 atm; T_0 = 4000 K																		
180-4-18	0.00	10.9	10.4	10.4	9.97	9.28	9.40	9.04	8.71	8.66	8.46	7.97	7.74	7.78	---	7.65	7.12	6.92
180-6-36	0.16	8.07	8.94	9.42	9.33	8.76	8.66	8.43	8.37	8.31	8.29	8.23	8.23	8.14	---	7.54	7.35	7.15
180-7-57	0.51	3.54	6.04	7.52	7.86	7.72	7.93	8.01	8.12	8.07	8.09	8.36	8.34	8.22	7.74	7.77	7.57	10.1
180-2-24	1.02	0.99	2.07	3.35	4.16	4.51	5.05	5.01	5.20	5.12	5.30	5.07	4.85	4.60	---	4.46	3.84	3.58
(t) p_0 = 1.36 atm; T_0 = 3200 K																		
180-11-3	0.00	6.61	6.31	6.18	5.83	5.56	5.65	5.35	5.36	---	5.24	5.41	5.58	---	5.34	5.33	5.31	6.43
180-10-3	0.16	4.44	5.03	5.38	5.42	5.24	5.16	5.09	5.01	4.90	5.01	5.09	5.10	5.01	4.81	4.87	4.87	4.76
180-9-3	0.51	1.54	2.85	3.87	4.17	4.13	4.33	4.36	4.37	4.38	4.51	4.78	4.77	4.67	4.40	4.44	4.40	4.67
180-8-3	1.02	0.34	0.67	1.20	1.69	1.96	2.58	2.97	3.07	3.11	3.22	3.42	3.54	3.55	3.39	3.37	3.36	4.16
(u) p_0 = 1.42 atm; T_0 = 3500 K																		
180-11-6	0.00	8.09	7.54	7.63	7.40	6.87	6.96	6.59	6.56	6.38	6.55	6.58	6.54	6.38	6.15	6.30	6.25	7.54
180-10-6	0.16	5.34	6.30	6.67	6.72	6.48	6.45	6.32	6.15	5.97	6.15	6.42	6.38	6.15	5.92	6.04	6.04	---
180-9-6	0.51	2.05	3.76	4.84	5.18	5.23	5.31	5.50	5.24	5.09	5.37	5.69	5.61	5.44	5.18	5.06	4.99	5.56
180-8-6	1.02	0.48	0.85	1.71	2.33	2.65	3.20	3.42	3.53	3.60	3.79	4.16	4.20	4.13	3.99	4.07	4.23	5.12
(v) p_0 = 1.50 atm; T_0 = 3800 K																		
180-11-9	0.00	9.62	9.26	9.41	9.05	8.43	8.54	8.02	8.05	7.73	7.80	7.85	7.85	7.68	7.32	7.46	7.37	8.83
180-10-9	0.16	6.96	7.74	8.15	8.19	7.82	7.72	7.63	7.35	7.18	7.35	7.61	7.45	7.35	6.83	6.88	6.95	8.09
180-9-9	0.51	2.45	4.19	5.92	6.32	6.39	6.43	6.49	6.39	6.30	6.61	7.04	7.03	6.81	6.39	6.39	6.48	7.47
180-8-9	1.02	0.57	1.14	2.20	3.01	3.66	4.11	4.33	4.38	4.50	4.90	5.23	5.24	5.12	4.84	4.92	5.26	6.21

TABLE VI.- HEAT-TRANSFER MEASUREMENTS OBTAINED FOR MODEL II

Run	Step, cm	Suction rate, w	Heat-transfer rate $\times 10^{-4}$, watts/m^2, at thermocouple –													
			1	2	3	4	5	6	7	8	9	10	11	12	13	14
(a) p_0 = 0.22 to 0.23 atm; T_0 = 3700 K																
188-5-3	1.02	0.25	0.82	1.56	2.11	2.58	2.91	3.08	3.22	3.24	3.31	3.31	3.25	3.14	3.15	3.10
190-8-3	1.02	0.00	0.89	1.63	2.27	2.62	3.10	3.24	3.37	3.37	3.48	3.22	3.27	3.33	3.34	3.30
190-10-3	0.00	0.00	6.07	5.85	5.64	5.43	5.23	4.94	4.85	4.67	4.49	4.34	4.16	4.03	3.86	3.74
(b) p_0 = 0.35 to 0.38 atm; T_0 = 3200 K																
190-7-12	1.02	0.22	0.61	1.17	1.56	1.85	2.13	2.46	2.49	2.39	2.51	2.39	2.40	2.41	2.54	2.51
190-8-12	1.02	0.00	0.39	0.73	1.23	1.62	2.02	2.32	2.31	2.29	2.50	2.17	2.21	2.39	2.42	2.34
190-10-12	0.00	0.00	4.70	4.51	4.37	4.20	4.07	3.94	3.82	3.67	3.56	3.43	3.34	3.23	3.13	3.06
(c) p_0 = 0.40 to 0.43 atm; T_0 = 3600 to 3900 K																
190-7-15	1.02	0.28	1.07	1.84	2.58	3.11	3.77	4.14	4.13	3.97	4.32	4.06	4.04	4.17	4.24	4.01
190-8-15	1.02	0.00	0.71	1.27	2.01	2.76	3.34	3.83	3.85	3.74	4.16	3.62	3.71	3.97	4.02	3.84
190-10-15	0.00	0.00	7.79	7.51	7.27	7.02	6.78	6.54	6.33	6.08	5.85	5.62	5.42	5.22	5.04	4.83
(d) p_0 = 0.43 atm; T_0 = 3900 K																
190-3-6	1.02	0.40	1.92	2.84	3.63	4.19	4.53	4.66	4.74	4.76	4.89	4.91	4.96	4.84	4.87	5.09
190-8-15	1.02	0.00	0.71	1.27	2.01	2.76	3.34	3.83	3.85	3.74	4.16	3.62	3.71	3.97	4.02	3.84
190-10-15	0.00	0.00	7.79	7.51	7.27	7.02	6.78	6.54	6.33	6.08	5.85	5.62	5.42	5.22	5.04	4.83
(e) p_0 = 0.43 to 0.46 atm; T_0 = 4300 to 4400 K																
190-7-18	1.02	0.26	1.48	2.46	3.51	4.27	4.86	5.12	5.28	5.22	5.31	5.21	5.22	5.24	5.22	5.18
190-8-18	1.02	0.00	0.86	1.85	2.93	3.79	4.39	4.73	4.90	4.87	5.09	4.93	5.06	5.09	5.06	5.13
190-10-18	0.00	0.00	9.83	9.54	9.26	8.95	8.70	8.42	8.18	7.96	7.70	7.48	7.23	7.01	6.77	6.57
(f) p_0 = 0.62 to 0.69 atm; T_0 = 2900 to 3000 K																
188-6-15	1.02	0.34	0.72	1.23	1.66	1.97	2.18	2.21	2.31	2.17	2.18	2.07	2.16	2.17	2.33	2.38
190-8-21	1.02	0.00	0.36	0.65	0.78	0.94	1.34	1.47	1.59	1.64	1.77	1.64	1.65	1.66	1.70	1.61
190-10-21	0.00	0.00	4.52	4.34	4.16	4.82	3.90	3.77	3.64	3.53	3.41	3.30	3.20	3.11	3.01	2.91

TABLE VI.- HEAT-TRANSFER MEASUREMENTS OBTAINED FOR MODEL II – Continued

Run	Step, cm	Suction rate, w	Heat-transfer rate × 10^{-4}, watts/m^2, at thermocouple –													
			1	2	3	4	5	6	7	8	9	10	11	12	13	14
(g) p_0 = 0.65 to 0.69 atm; T_0 = 2900 to 3000 K																
190-7-21	1.02	0.35	0.70	1.10	1.54	1.87	2.15	2.34	2.32	2.20	2.40	2.14	2.19	2.17	2.08	2.96
190-8-21	1.02	0.00	0.36	0.65	0.78	0.94	1.34	1.47	1.59	1.64	1.77	1.64	1.65	1.66	1.70	1.61
190-10-21	0.00	0.00	4.52	4.34	4.16	4.82	3.90	3.77	3.64	3.53	3.41	3.30	3.20	3.11	3.01	2.91
(h) p_0 = 0.71 to 0.77 atm; T_0 = 3400 K																
190-2-18	1.02	0.41	1.38	2.23	2.81	2.73	3.22	3.36	3.45	3.43	3.57	3.43	3.51	3.37	3.37	3.51
190-7-24	1.02	0.36	1.01	1.63	2.27	2.73	3.12	3.55	3.56	3.31	3.58	3.32	3.22	3.36	3.24	3.10
190-8-24	1.02	0.00	0.31	0.69	1.14	1.60	2.20	2.46	2.60	2.63	2.87	2.62	2.71	2.67	2.68	2.59
190-10-24	0.00	0.00	7.24	6.94	6.69	6.45	6.24	6.02	5.81	5.63	5.43	5.26	5.06	4.89	4.72	4.58
(i) p_0 = 0.75 to 0.81 atm; T_0 = 3700 K																
190-7-27	1.02	0.40	1.35	2.11	2.89	3.50	4.13	4.58	4.55	4.38	4.59	4.16	4.18	4.35	4.33	4.05
190-8-27	1.02	0.00	0.42	0.85	1.57	2.21	2.91	3.35	3.49	3.55	3.81	3.43	3.54	3.57	3.58	3.45
190-10-27	0.00	0.00	8.90	8.52	8.22	7.91	7.63	7.37	7.07	6.82	6.55	6.34	6.11	5.85	5.63	5.42
(j) p_0 = 0.80 to 0.87 atm; T_0 = 3900 K																
188-2-9	1.02	0.44	2.07	3.58	4.89	5.59	6.14	6.36	6.53	6.31	6.43	6.24	6.18	5.98	5.97	5.92
190-7-30	1.02	0.44	1.67	2.83	3.96	4.79	5.55	5.90	5.91	5.77	6.01	5.71	5.65	5.63	5.66	5.41
190-8-30	1.02	0.00	0.42	1.04	1.94	2.73	3.64	4.23	4.49	4.48	4.78	4.45	4.50	4.65	4.59	4.33
190-10-30	0.00	0.00	10.6	10.3	9.88	9.61	9.33	9.03	8.77	8.47	8.18	7.89	7.63	7.37	7.09	6.83
(k) p_0 = 0.22 atm; T_0 = 3700 K																
190-5-3	0.60	0.12	2.52	3.20	3.17	3.85	3.95	3.88	4.03	3.97	3.99	4.01	3.82	3.72	3.72	3.82
190-9-3	0.60	0.00	1.32	2.39	2.97	3.58	3.95	3.88	3.74	3.86	4.18	3.92	3.66	3.76	3.69	---
190-10-3	0.00	0.00	6.27	5.98	5.72	5.46	5.22	5.05	4.85	4.68	4.48	4.34	4.17	4.03	3.88	3.75
(l) p_0 = 0.24 to 0.25 atm; T_0 = 4800 K																
190-4-9	0.60	0.71	3.37	4.38	4.48	5.06	5.38	5.30	5.54	5.41	5.50	5.43	5.23	5.21	5.19	5.32
190-9-6	0.60	0.00	2.47	3.85	4.62	5.06	5.54	5.58	5.51	5.49	5.57	5.44	5.42	5.39	5.30	4.87
190-10-6	0.00	0.00	8.62	8.30	7.95	7.61	7.32	7.04	6.77	6.56	6.31	6.11	5.90	5.69	5.49	5.28

TABLE VI.- HEAT-TRANSFER MEASUREMENTS OBTAINED FOR MODEL II – Concluded

Run	Step, cm	Suction rate, w	Heat-transfer rate × 10^{-4}, watts/m^2, at thermocouple –													
			1	2	3	4	5	6	7	8	9	10	11	12	13	14
(m) p_0 = 0.36 to 0.38 atm; T_0 = 3200 K																
190-4-12	0.60	0.61	1.62	2.30	2.67	2.68	2.88	2.88	3.12	3.14	3.22	3.11	3.03	3.07	2.89	3.19
190-5-12	0.60	0.59	1.68	2.31	2.51	2.70	2.86	2.91	3.34	3.34	3.35	3.27	3.19	3.12	2.97	3.23
190-9-12	0.60	0.00	1.06	1.74	2.04	2.32	2.77	3.13	2.87	2.87	3.15	2.75	2.70	2.91	2.94	2.81
190-10-12	0.00	0.00	4.73	4.54	4.38	4.24	3.98	3.95	3.82	3.69	3.54	3.73	3.27	3.20	3.12	3.10
(n) p_0 = 0.41 to 0.44 atm; T_0 = 3600 to 3800 K																
190-4-15	0.60	0.67	2.72	3.87	4.37	4.50	4.69	4.68	5.03	5.20	5.23	5.11	5.10	4.86	4.73	5.13
190-5-15	0.60	0.59	2.92	3.81	4.07	4.53	4.90	4.99	5.22	5.20	5.30	5.11	4.99	4.85	4.77	5.00
190-9-15	0.60	0.00	1.66	2.84	3.53	3.89	4.66	4.90	4.65	4.71	5.05	4.20	4.29	4.75	4.71	4.31
190-10-15	0.00	0.00	7.82	7.65	7.38	7.05	6.78	6.55	6.33	6.00	5.90	5.67	5.45	5.26	5.07	4.89
(o) p_0 = 0.64 to 0.69 atm; T_0 = 2900 K																
190-4-21	0.60	0.70	1.56	2.20	2.49	2.58	2.75	2.81	2.92	2.96	3.04	2.63	2.93	2.84	2.80	2.91
190-5-21	0.60	0.73	1.78	2.47	2.70	2.92	3.05	3.15	3.31	3.27	3.31	3.25	3.22	3.10	3.03	3.10
190-9-21	0.60	0.00	0.54	1.15	1.71	2.06	2.46	2.65	2.63	2.67	2.87	2.62	2.73	2.70	2.70	2.54
190-10-21	0.00	0.00	4.53	4.37	4.17	4.03	3.87	3.76	3.64	3.51	3.40	3.27	3.16	3.10	3.01	2.91
(p) p_0 = 0.72 to 0.77 atm; T_0 = 3400 to 3500 K																
190-4-24	0.60	0.73	2.46	3.58	3.93	4.07	4.36	4.45	4.67	4.74	4.83	4.71	4.66	4.41	4.35	4.54
190-5-24	0.60	0.79	3.43	4.59	5.20	5.50	5.69	5.67	5.84	5.72	5.79	5.74	5.61	5.42	5.38	5.26
190-9-24	0.60	0.00	0.74	1.68	1.48	3.12	3.86	4.22	4.14	4.18	4.41	3.88	4.03	3.63	4.31	3.85
190-10-24	0.00	0.00	7.25	6.93	6.68	6.46	6.24	6.03	5.84	5.62	5.42	5.23	5.09	4.89	4.68	4.50
(q) p_0 = 0.76 to 0.82 atm; T_0 = 3600 K																
190-4-27	0.60	0.72	2.94	4.18	4.70	4.91	5.21	5.33	5.58	5.74	5.69	5.68	5.66	5.35	5.21	5.52
190-9-27	0.60	0.00	0.98	2.12	3.22	3.92	4.77	5.10	5.03	5.13	5.40	4.86	4.97	5.20	5.17	4.76
190-10-27	0.00	0.00	8.81	8.51	8.21	7.91	7.61	7.37	7.09	7.83	6.56	6.32	6.10	5.83	5.62	5.40
(r) p_0 = 0.82 to 0.87 atm; T_0 = 3900 K																
190-4-30	0.60	0.78	3.71	5.39	6.02	6.28	6.68	6.80	6.75	6.79	7.11	7.21	7.29	7.14	7.05	6.78
190-9-30	0.60	0.00	0.64	2.79	4.10	5.01	6.07	6.31	6.32	6.47	6.63	6.11	6.28	6.49	6.48	5.88
190-10-30	0.00	0.00	10.5	10.2	9.85	9.56	9.26	8.95	8.65	8.41	8.12	7.87	7.60	7.11	7.07	6.79

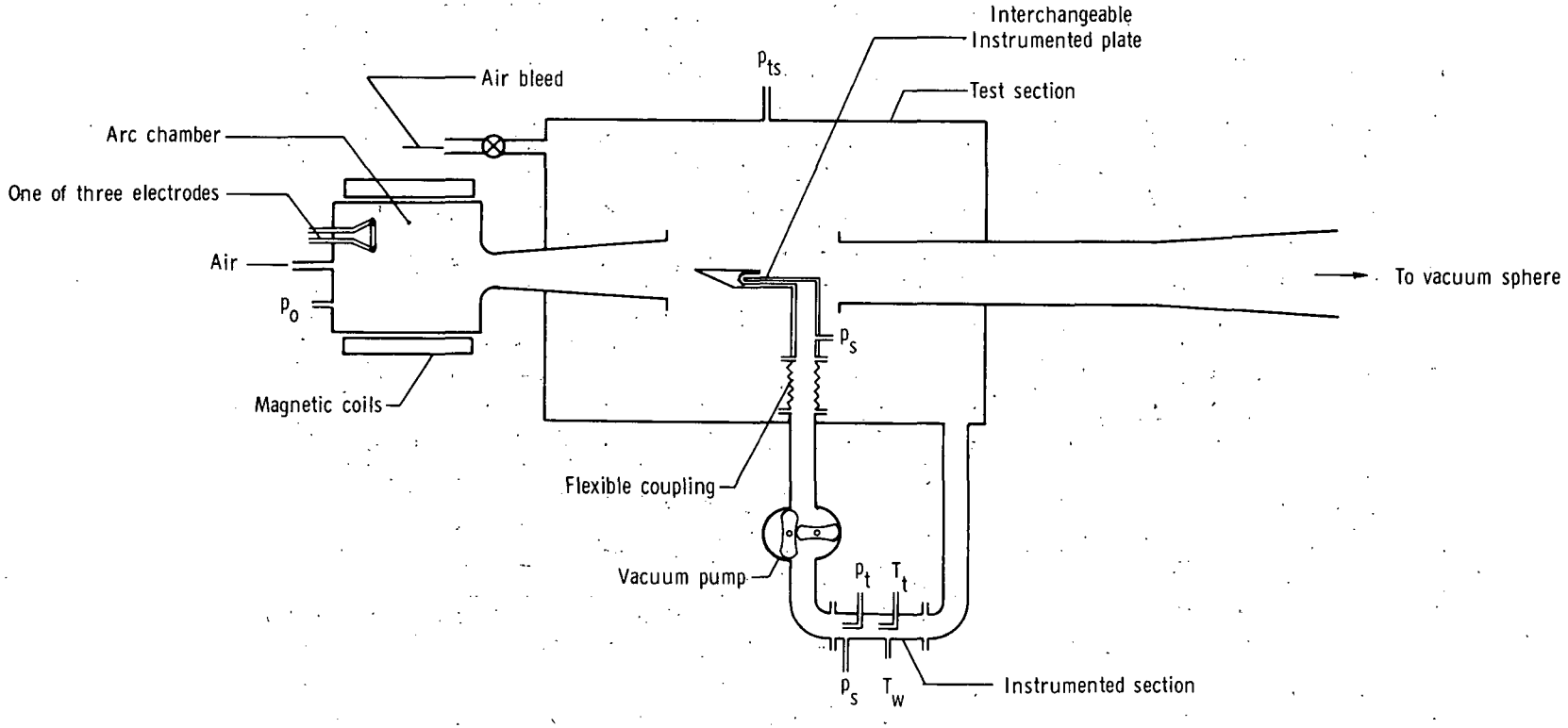

Figure 1.- Schematic diagram of suction experimental setup.

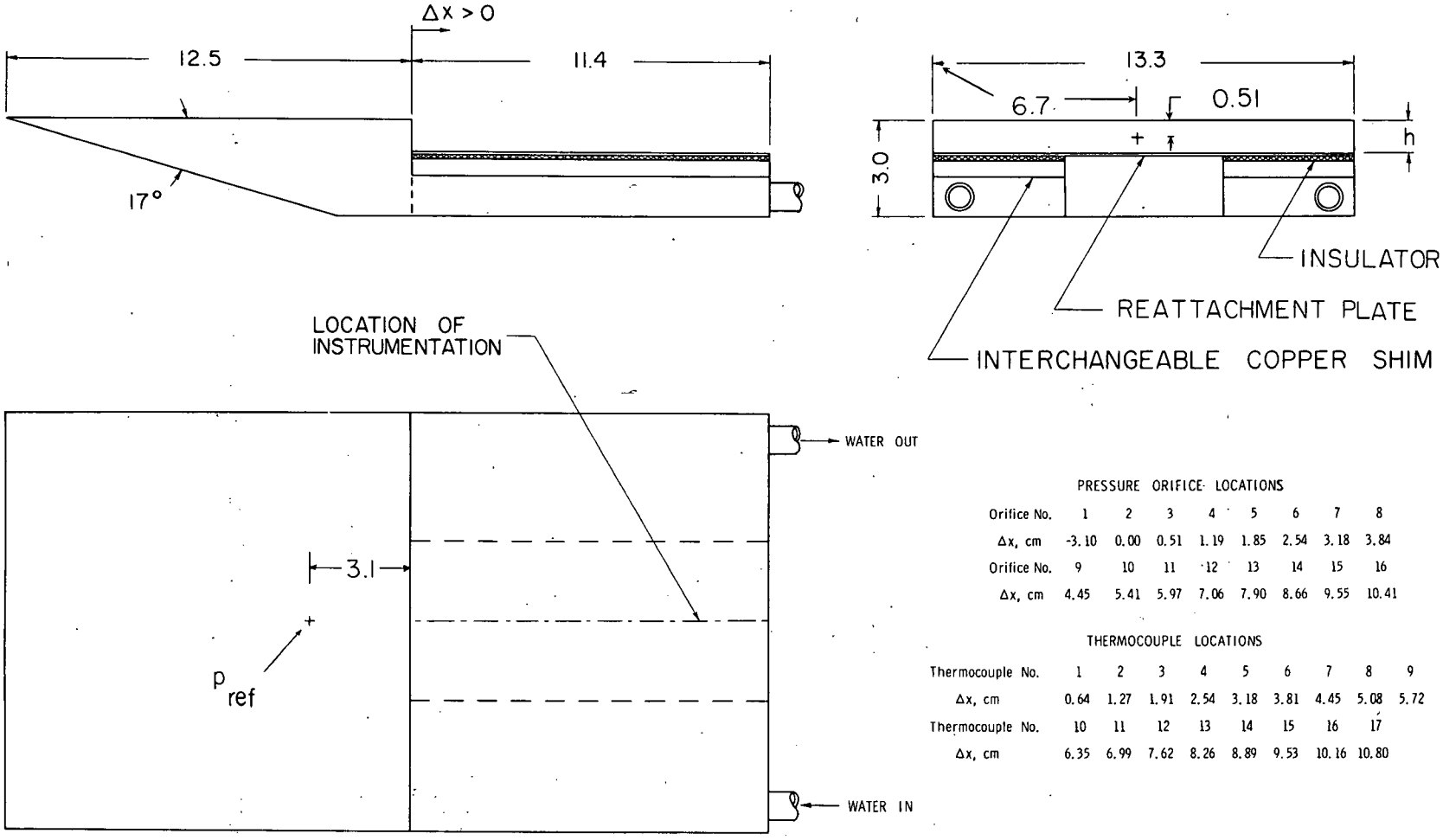

PRESSURE ORIFICE LOCATIONS

Orifice No.	1	2	3	4	5	6	7	8
Δx, cm	-3.10	0.00	0.51	1.19	1.85	2.54	3.18	3.84
Orifice No.	9	10	11	12	13	14	15	16
Δx, cm	4.45	5.41	5.97	7.06	7.90	8.66	9.55	10.41

THERMOCOUPLE LOCATIONS

Thermocouple No.	1	2	3	4	5	6	7	8	9
Δx, cm	0.64	1.27	1.91	2.54	3.18	3.81	4.45	5.08	5.72
Thermocouple No.	10	11	12	13	14	15	16	17	
Δx, cm	6.35	6.99	7.62	8.26	8.89	9.53	10.16	10.80	

Figure 2.- Model I. All dimensions are in centimeters.

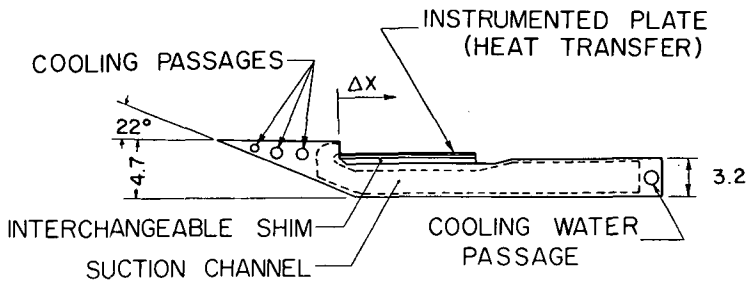

SECTION Z-Z

PRESSURE ORIFICE LOCATIONS (Pressure Instrumented Plate)

Orifice No.	1	2	3	4	5	6
Δx, cm	0.24	0.87	1.51	2.14	2.78	3.42
Orifice No.	7	8	9	10	11	12
Δx, cm	4.37	5.00	5.80	6.58	7.39	8.18

THERMOCOUPLE LOCATIONS (Heat-Transfer Instrumented Plate)

Thermocouple No.	1	2	3	4	5	6
Δx, cm	0.64	1.27	1.91	2.54	3.18	3.81
Thermocouple No.	7	8	9	10	11	12
Δx, cm	4.45	5.08	5.72	6.35	6.99	7.62
Thermocouple No.	13	14	15	16	17	
Δx, cm	8.26	8.89	9.53	10.16	10.80	

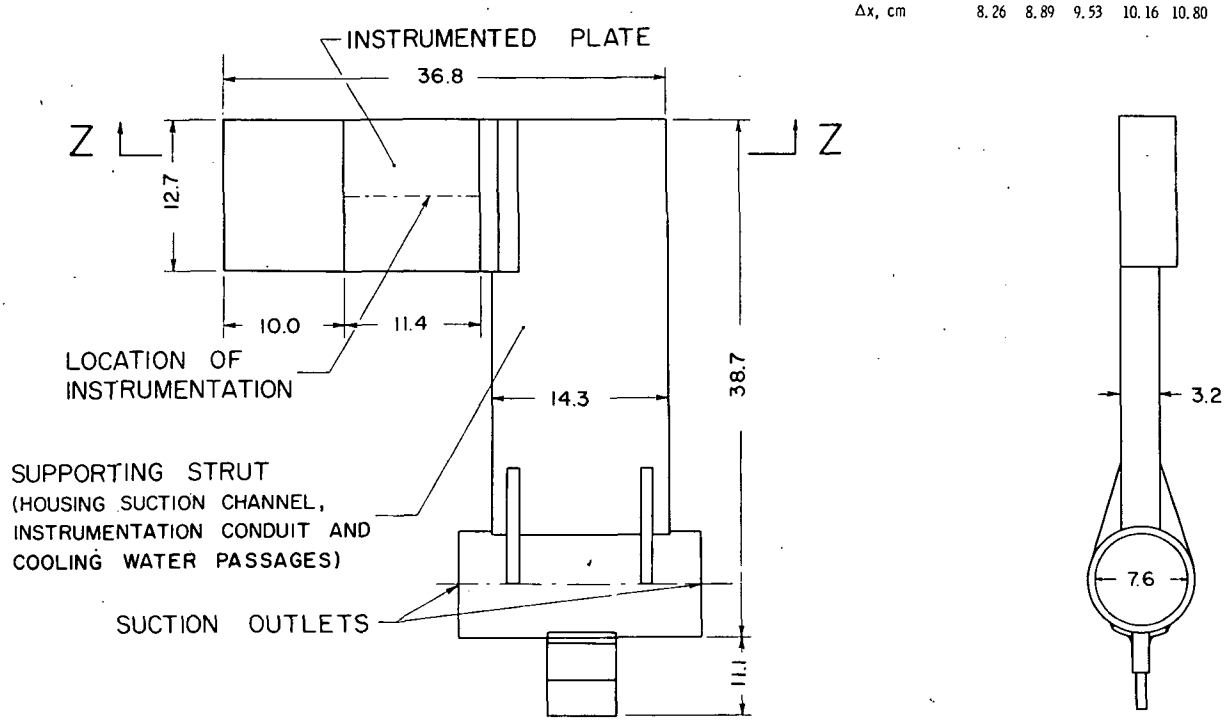

Figure 3.- Model II. All linear dimensions are in centimeters.

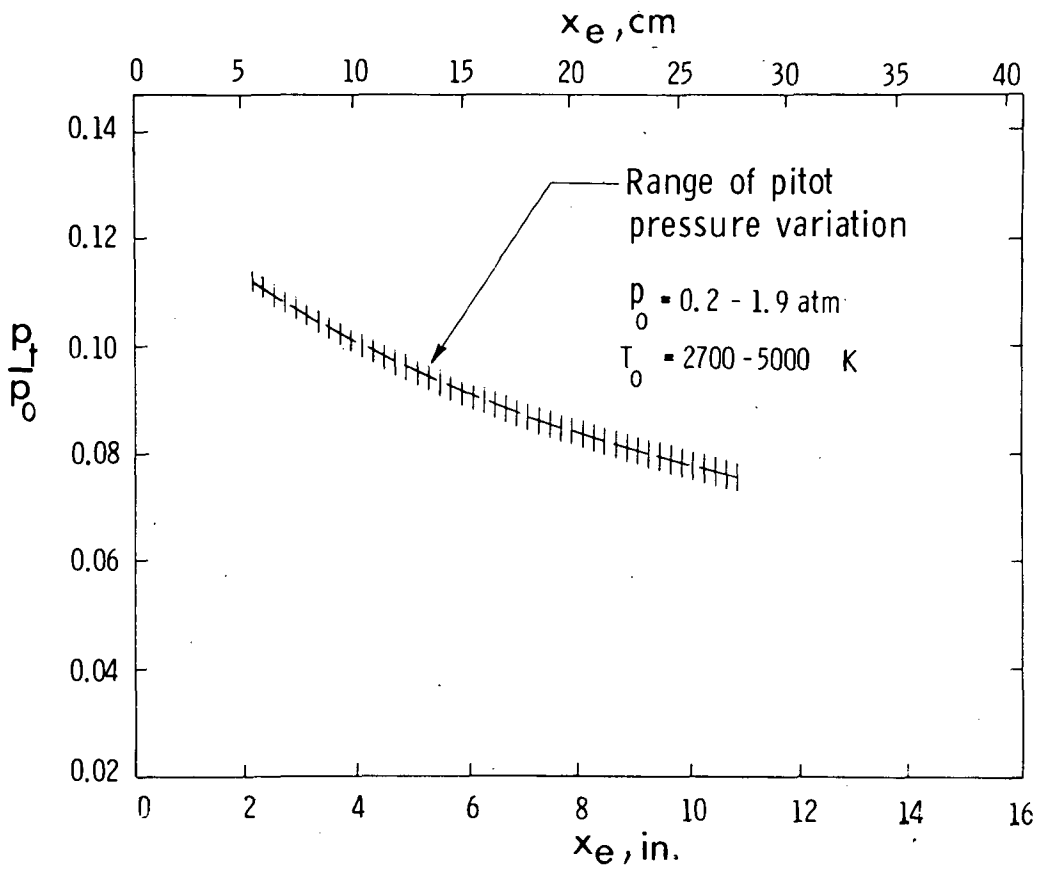

Figure 4.- Axial distribution of pitot pressure in test section.

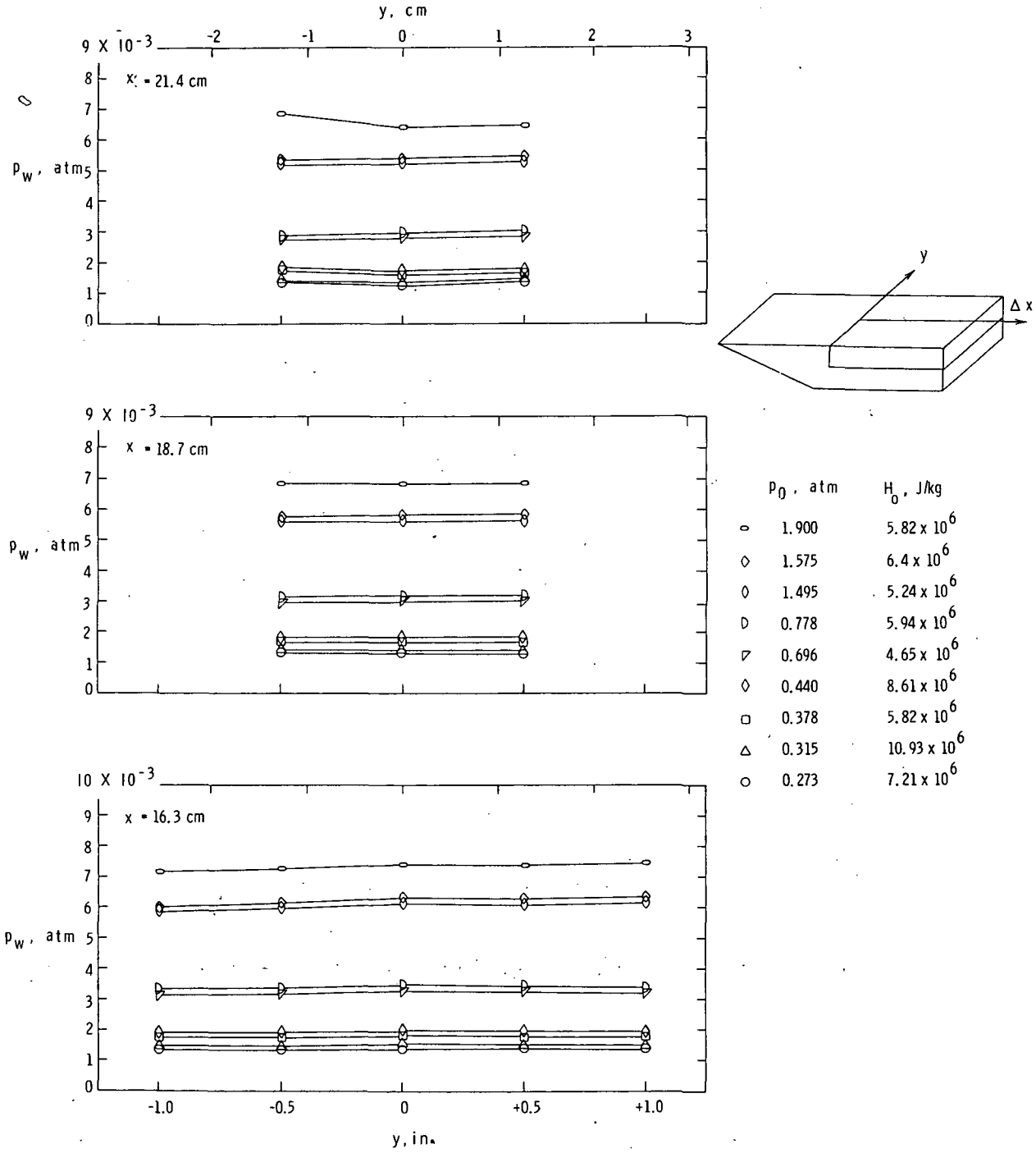

(a) h = 0.

Figure 5.- Transverse surface pressure distribution on model I.

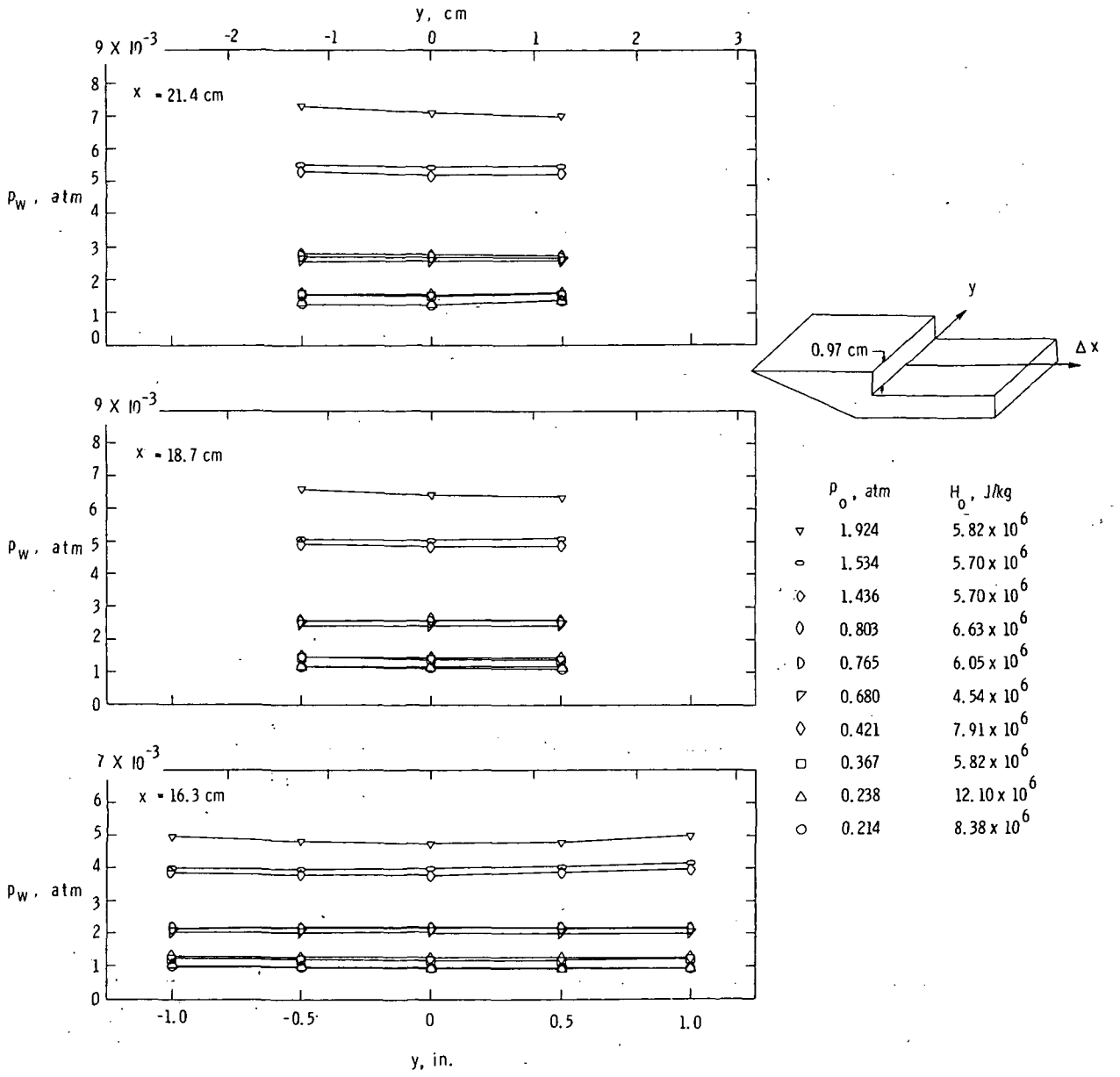

(b) h = 0.97 cm.

Figure 5.- Concluded.

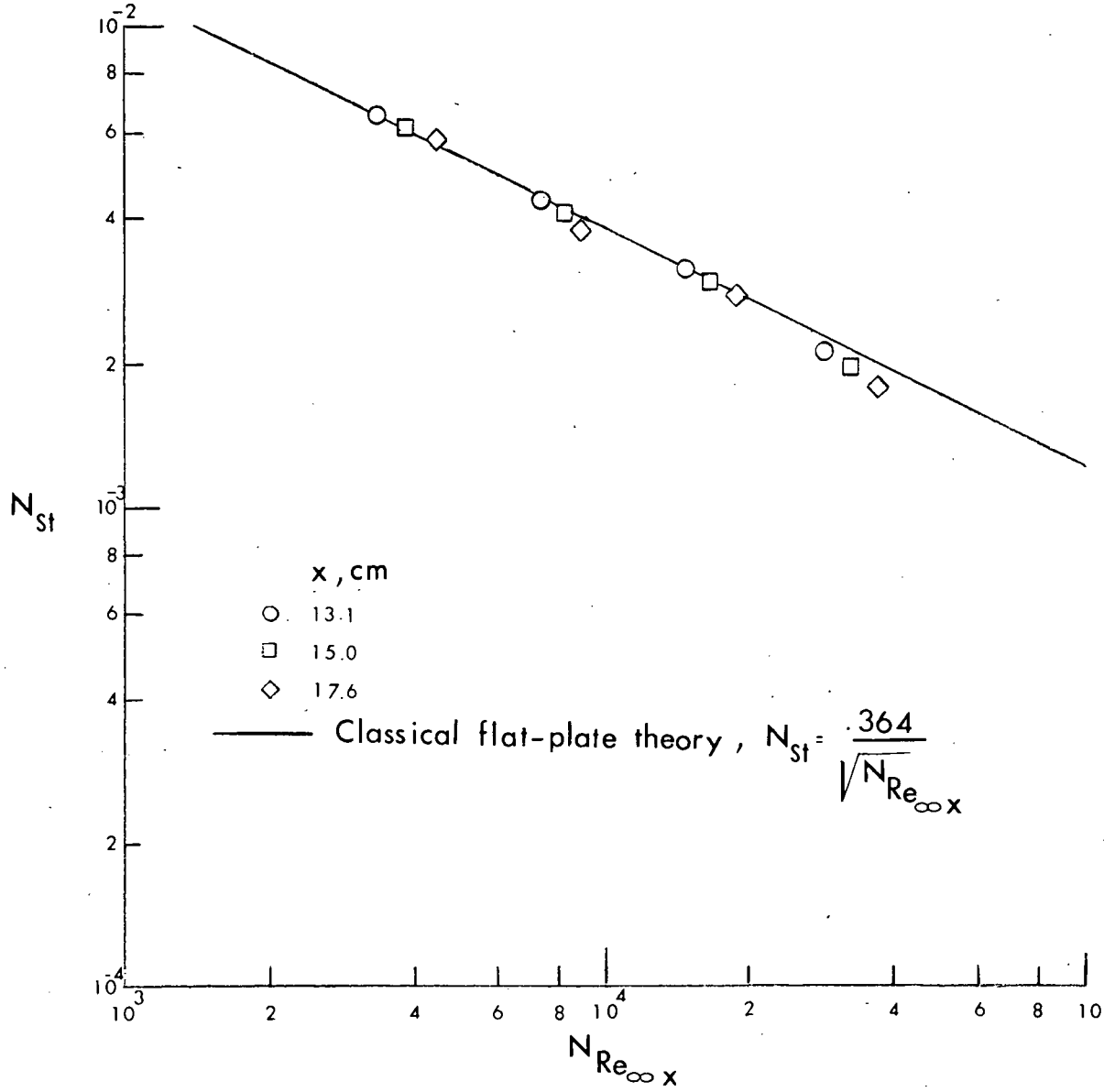

Figure 6.- Stanton number correlation of flat-plate heat-transfer data as a function of Reynolds number.

	Run	h, cm	p_0, atm	T_0, K	N_{Re_∞}/cm	M_∞
●	180-3-21	0.00	0.277	5500	202	4.29
▲	180-5-21	0.16	0.283	5050	224	4.21
◆	180-7-21	0.51	0.273	5075	216	4.21
■	180-1-21	1.02	0.276	5150	212	2.23

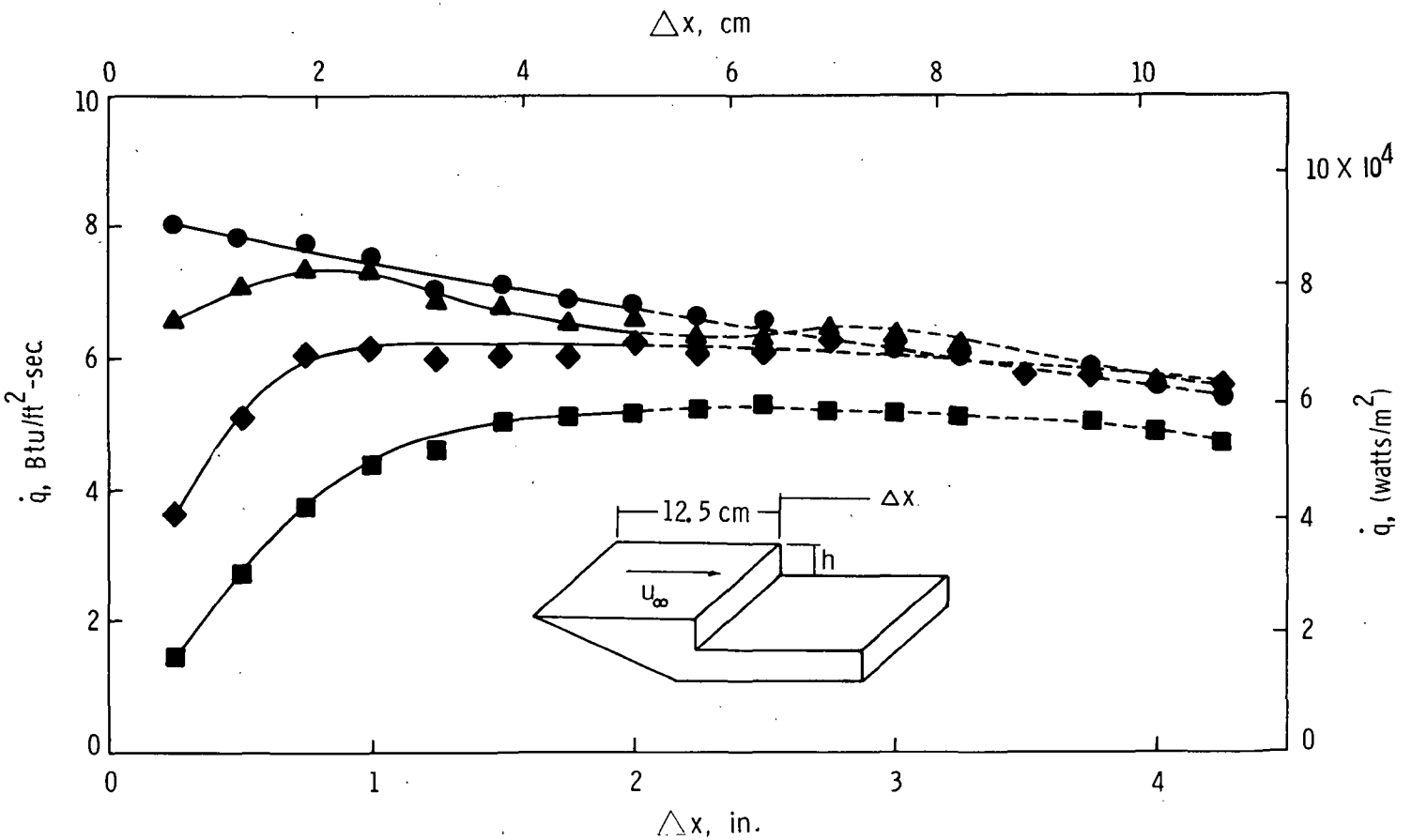

Figure 7.- Effect of step height on heat-transfer distribution downstream of step. Model I (no suction).

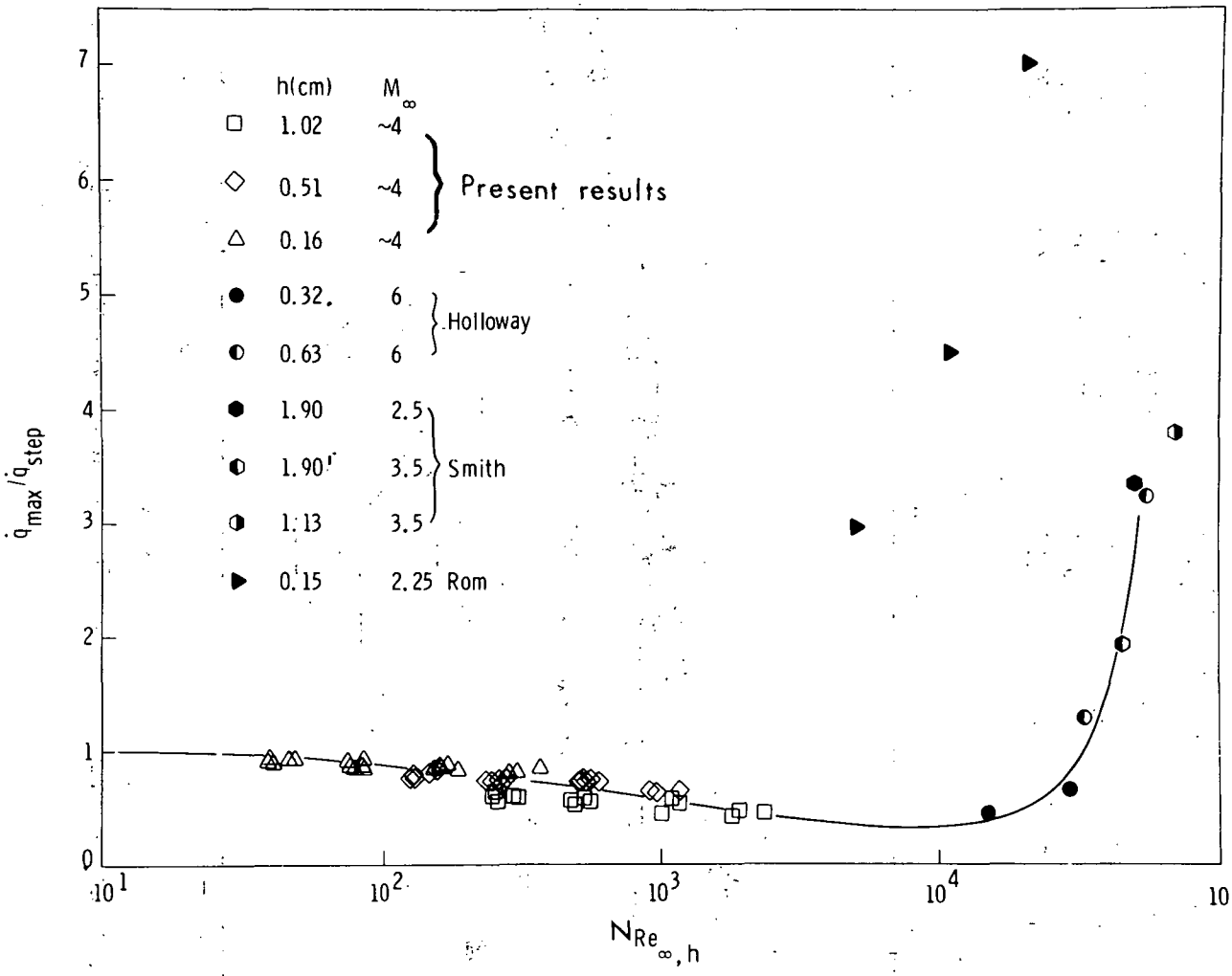

Figure 8.- Maximum heating rate as function of $N_{Re_{\infty,h}}$.

	Run	h, cm	p_o, atm	T_o, K	N_{Re_∞}/cm	M_∞	p_{ref}, mm Hg
○	200-4-9	0.00	0.378	3200	480	4.02	1.58
◺	200-7-9	0.20	0.380	3225	475	4.02	1.41
◇	200-3-9	0.51	0.380	3750	415	4.12	1.58
△	200-8-9	0.71	0.389	3250	485	4.02	1.47
□	200-1-9	1.02	0.379	3250	470	4.03	1.56

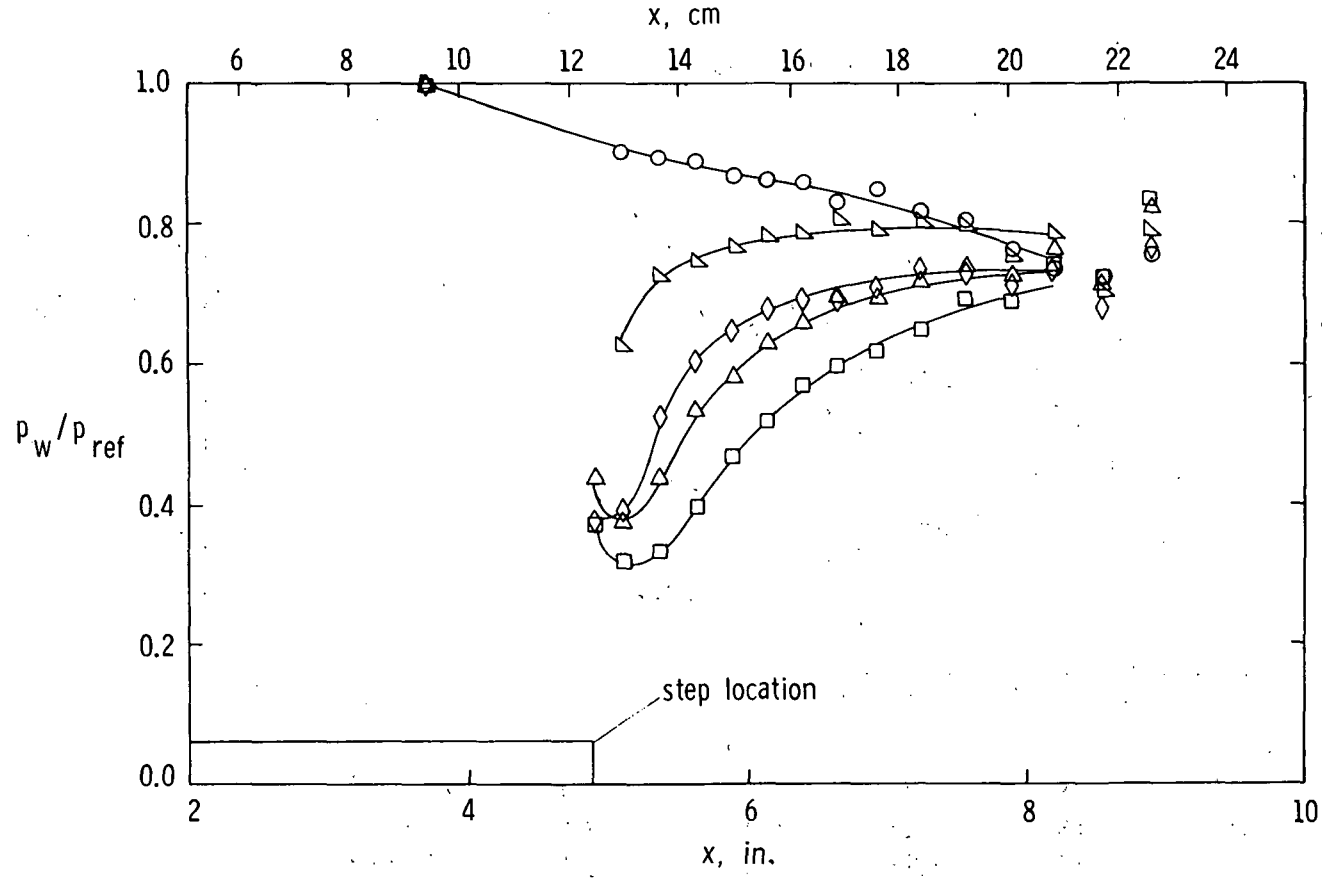

(a) $p_0 \approx 0.38$ atm.

Figure 9.- Normalized wall pressure in the separated region on model I.

	Run	h, cm	p_0, atm	T_0, K	N_{Re_∞}/cm	M_∞	p_{ref}, mm Hg
○	200-4-12	0.00	0.439	3925	455	4.15	1.77
▷	200-7-12	0.20	0.432	4000	440	4.16	1.54
◇	200-3-12	0.51	0.428	4275	410	4.16	1.81
△	200-8-12	0.71	0.447	3800	480	4.14	1.59
□	200-1-12	1.02	0.440	4125	430	4.18	1.90

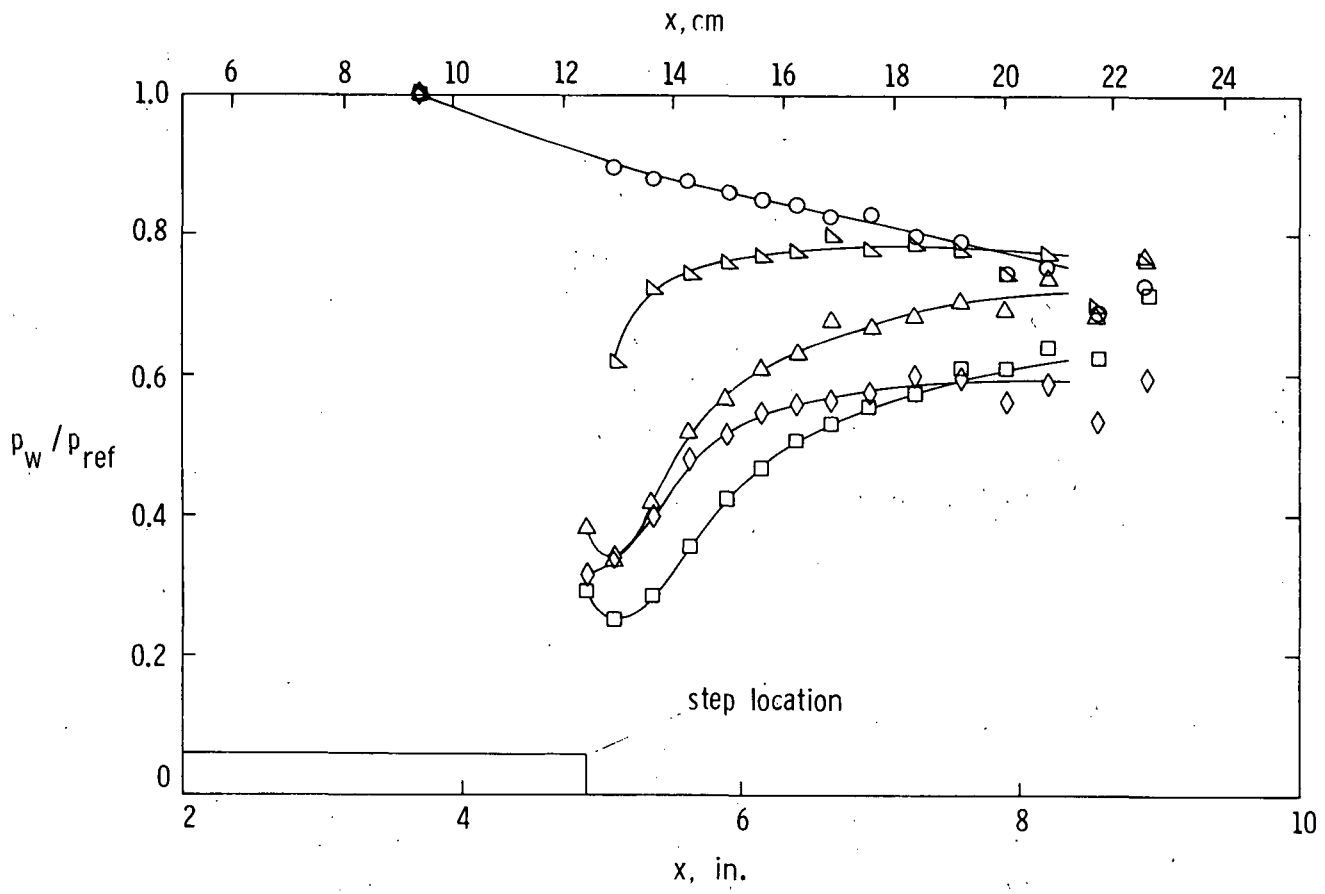

(b) $p_0 \approx 0.44$ atm.

Figure 9.- Continued.

	Run	h, cm	p_0, atm	T_0, K	N_{Re_∞}/cm	M_∞	p_{ref}, mm Hg
○	200-4-15	0.00	0.697	3075	890	4.00	2.85
◺	200-7-15	0.20	0.700	3050	885	4.01	2.58
◇	200-3-15	0.51	0.700	2950	940	4.00	3.14
△	200-8-15	0.71	0.700	3100	890	4.01	2.58
□	200-1-15	1.02	0.695	3050	895	4.01	2.80

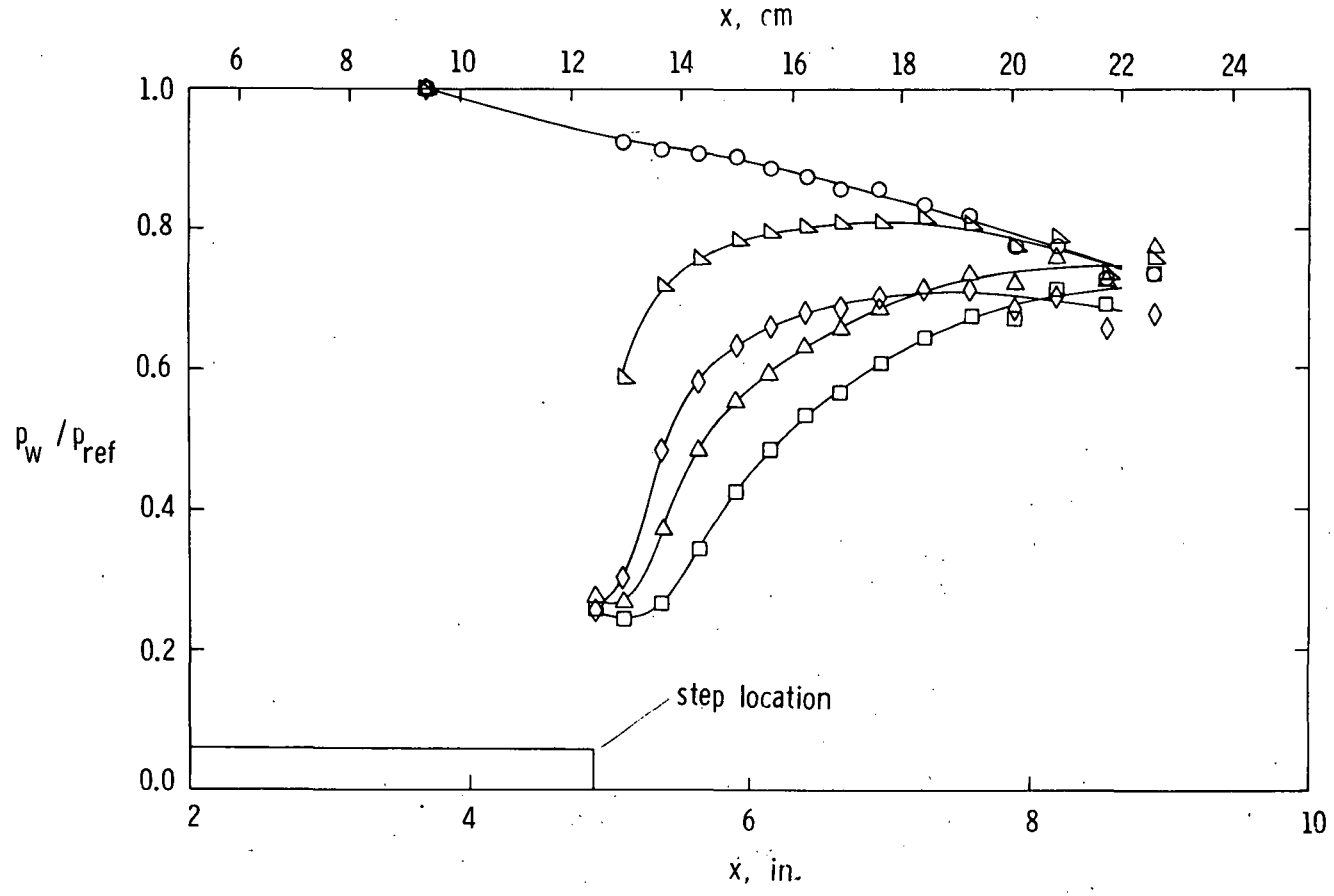

(c) $p_0 \approx 0.70$ atm.

Figure 9.- Continued.

	Run	h, cm	p_0, atm	T_0, K	N_{Re_∞}/cm	M_∞	p_{ref}, mm Hg
○	200-4-18	0.00	0.780	3500	875	4.07	3.12
◁	200-7-18	0.20	0.785	3475	895	4.05	2.84
◇	200-3-18	0.51	0.788	3450	900	4.06	3.38
△	200-8-18	0.71	0.788	3475	900	4.05	2.84
□	200-1-18	1.02	0.780	3475	890	4.05	3.12

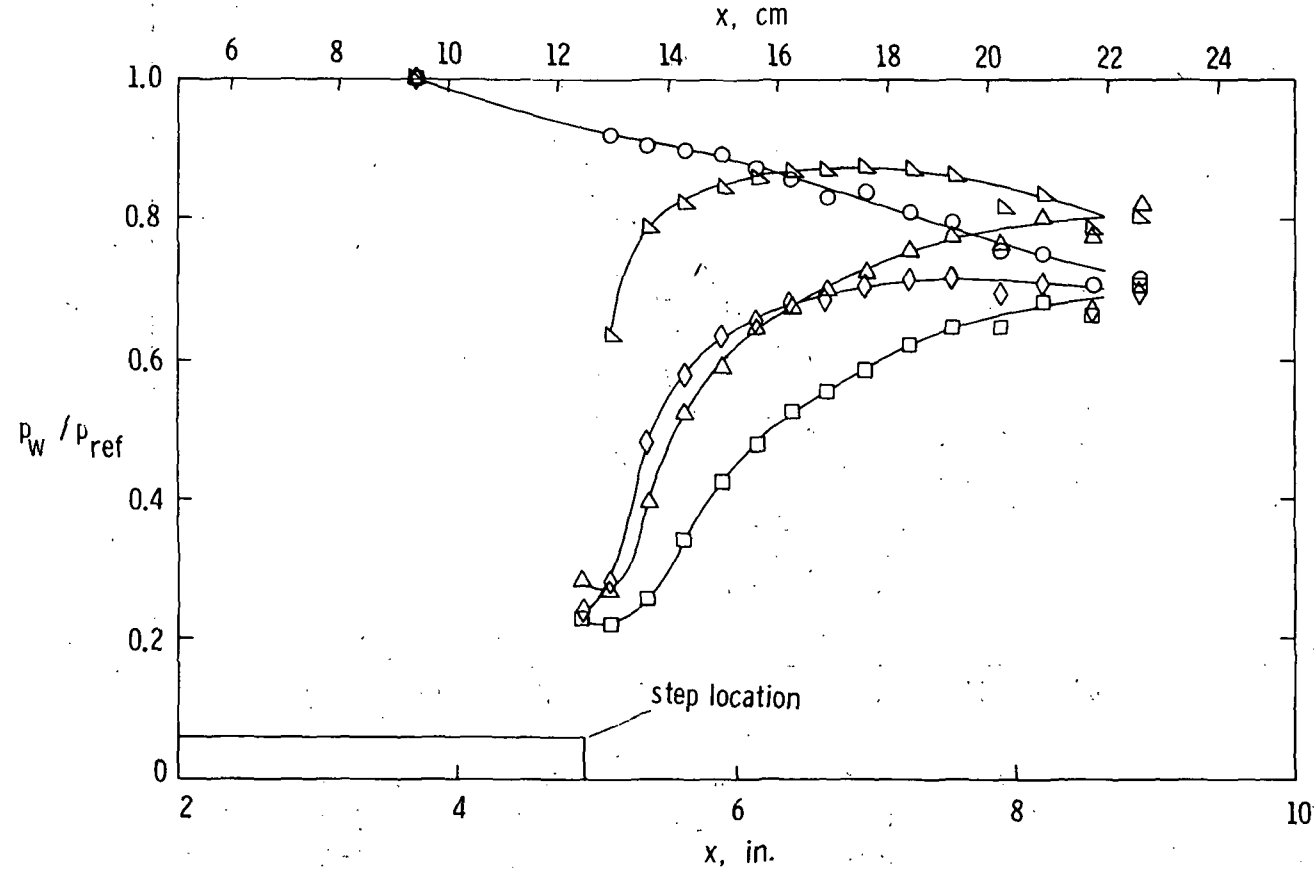

(d) $p_0 \approx 0.78$ atm.

Figure 9.- Continued.

	Run	h, cm	p_0, atm	T_0, K	N_{Re_∞}/cm	M_∞	p_{ref}, mm Hg
○	200-4-21	0.00	1.500	3575	1610	4.07	6.12
◺	200-7-21	0.20	1.505	3675	1595	4.07	5.41
◇	200-3-21	0.51	1.520	3500	1655	4.06	6.75
△	200-8-21	0.71	1.510	3450	1675	4.05	5.61
□	200-1-21	1.02	1.500	3575	1610	4.07	6.48

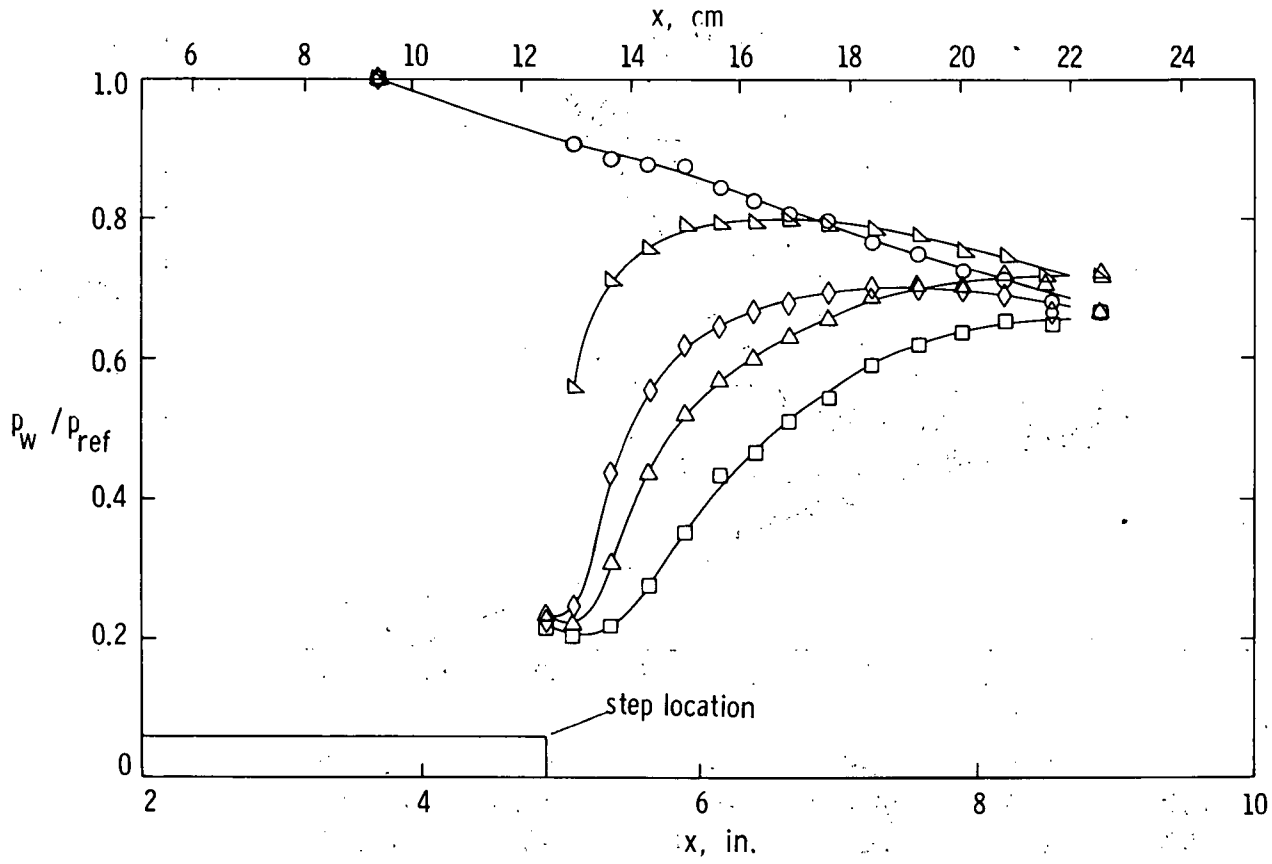

(e) $p_0 \approx 1.50$ atm.

Figure 9.- Continued.

	Run	h, cm	p_0, atm	T_0, K	N_{Re_∞}/cm	M_∞	p_{ref}, mm Hg
○	200-4-24	0.00	1.590	3775	1620	4.10	6.39
▷	200-7-24	0.20	1.640	3725	1695	4.09	7.36
◇	200-3-24	0.51	1.605	3750	1665	4.08	7.36
△	200-8-24	0.71	1.595	3750	1655	4.08	5.78
□	200-1-24	1.02	1.590	3750	1650	4.08	6.39

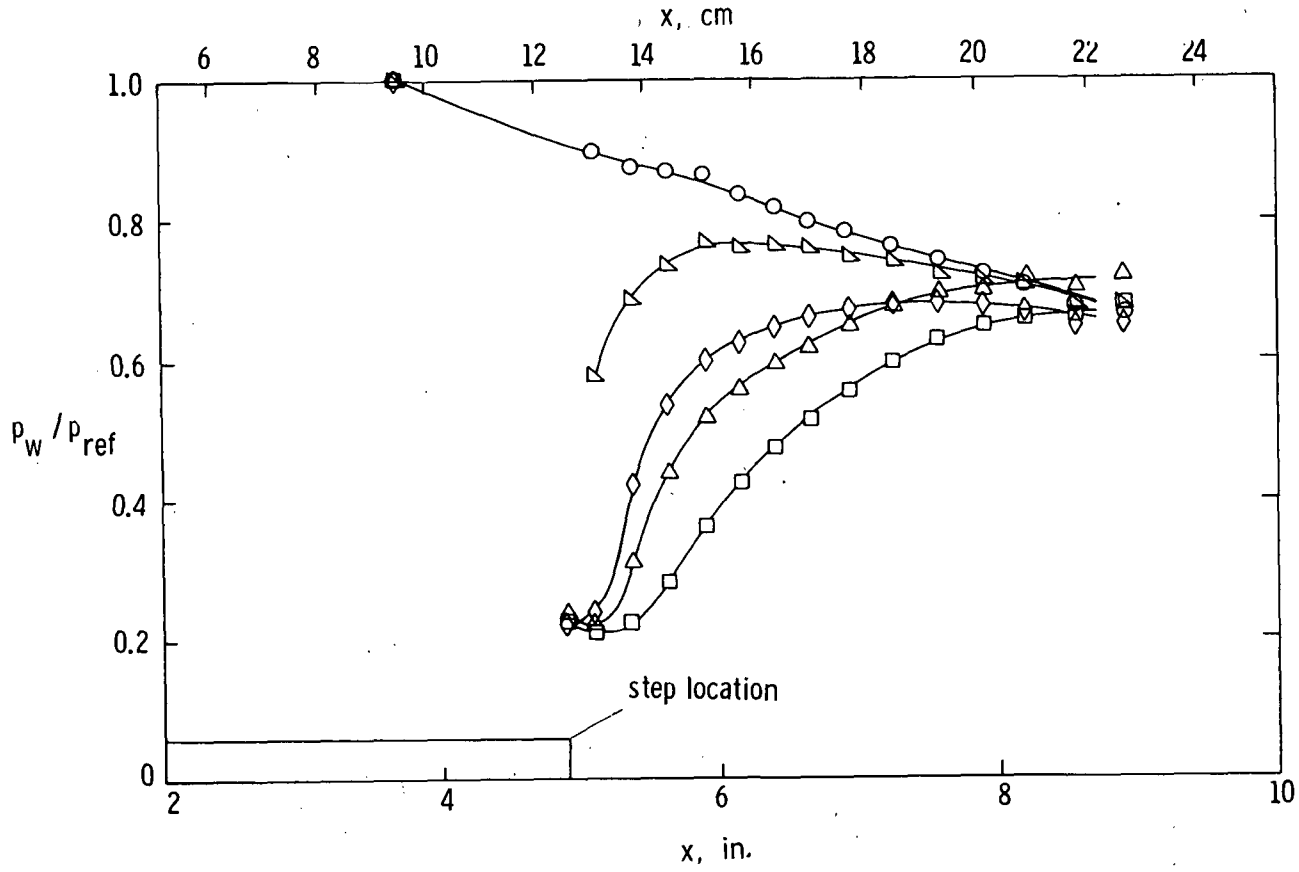

(f) $p_0 \approx 1.60$ atm.

Figure 9.- Continued.

	Run	h, cm	p_0, atm	T_0, K	N_{Re_∞}/cm	M_∞	p_{ref}, mm Hg
○	200-4-27	0.00	1.905	3700	2005	4.06	7.83
◇	200-3-27	0.51	1.960	3450	2245	3.99	8.75
△	200-8-27	0.71	1.925	3725	1995	4.08	7.26
□	200-1-27	1.02	1.900	3650	1995	4.07	7.83

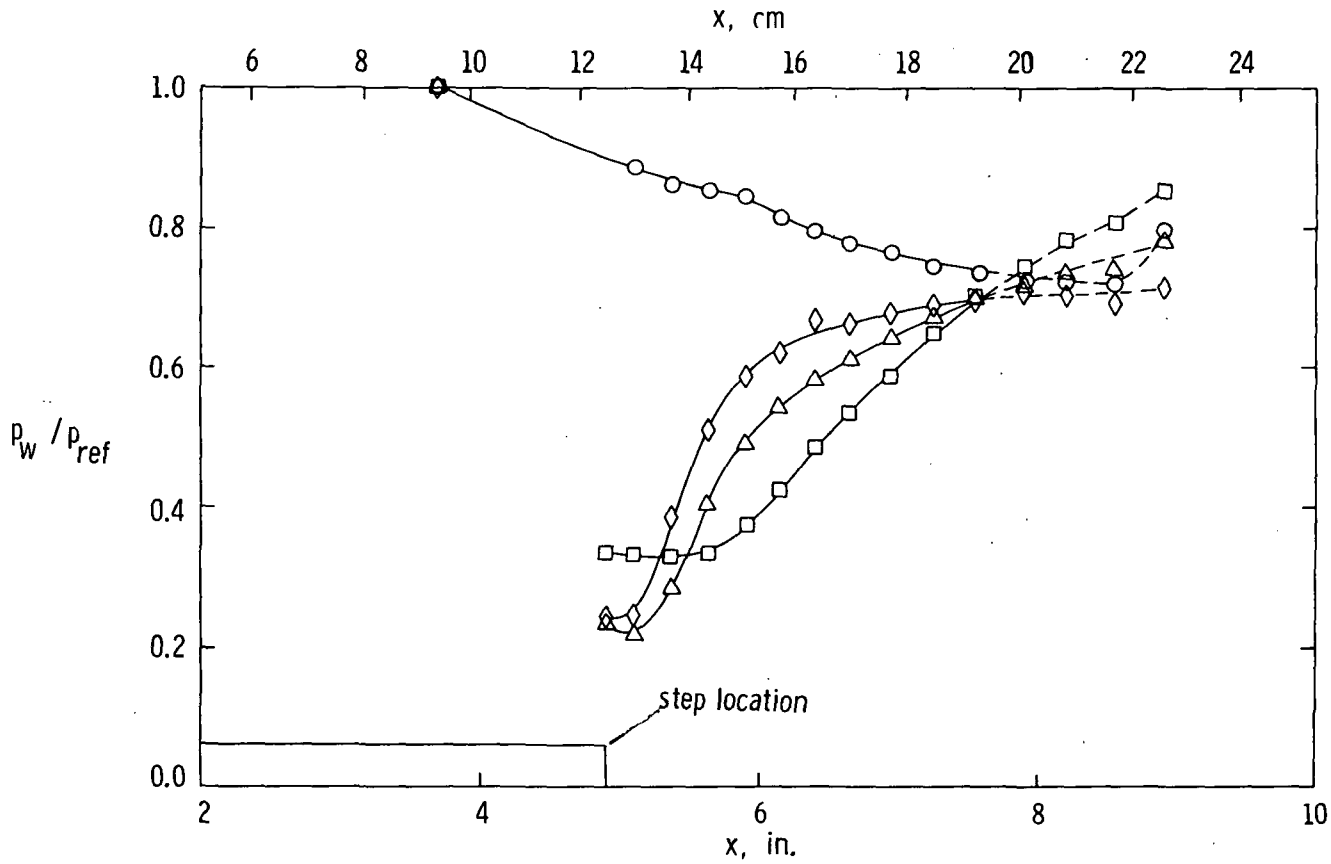

(g) $p_0 \approx 1.90$ atm.

Figure 9.- Concluded.

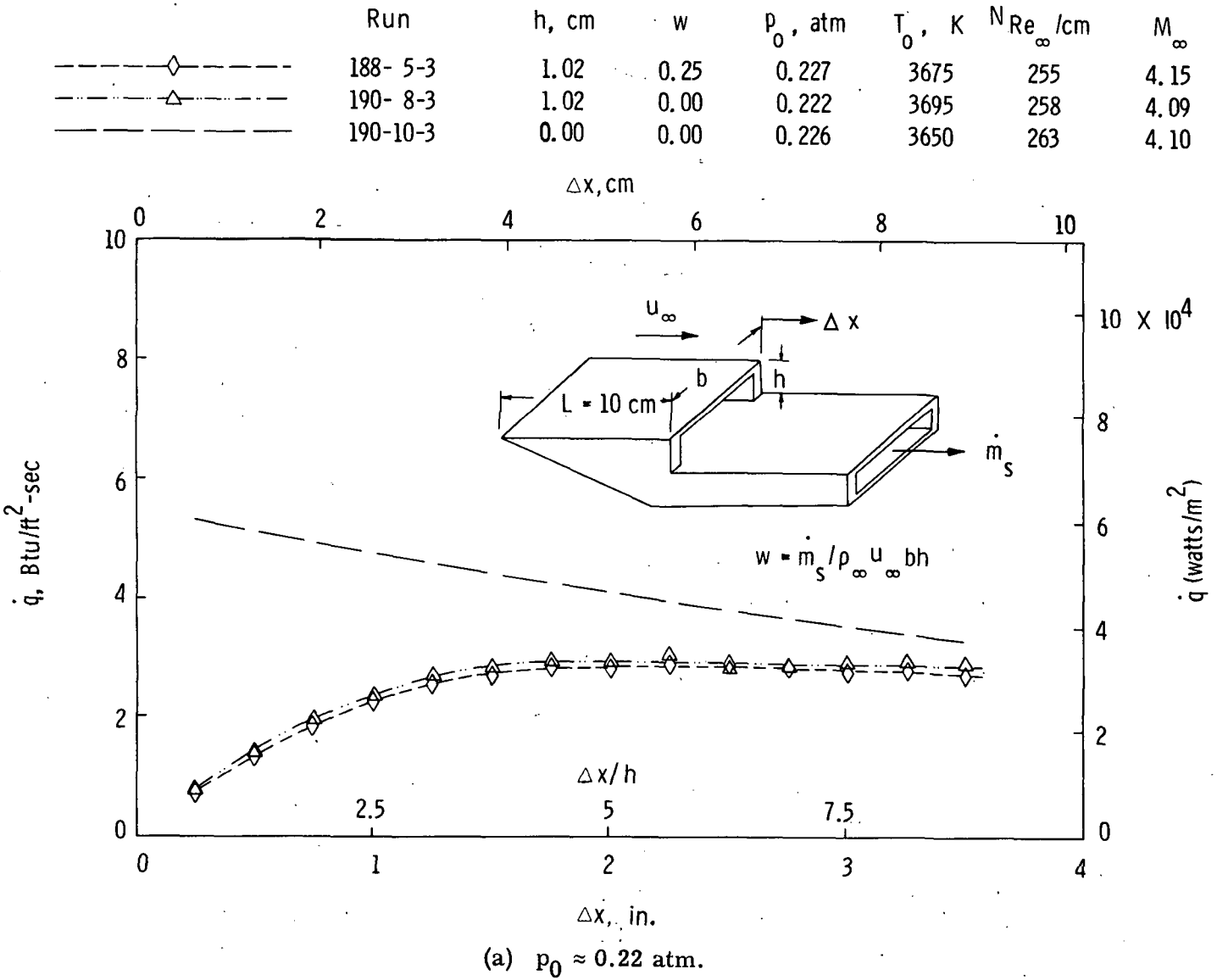

(a) $p_0 \approx 0.22$ atm.

Figure 10.- Effect of mass suction on heat-transfer distribution downstream of a 1.02 cm step.

Run	h, cm	w	p_0, atm	T_0, K	N_{Re_∞}/cm	M_∞
190- 7-12	1.02	0.22	0.348	3220	452	3.98
190- 8-12	1.02	0.00	0.379	3185	492	3.98
190-10-12	0.00	0.00	0.385	3250	491	3.99

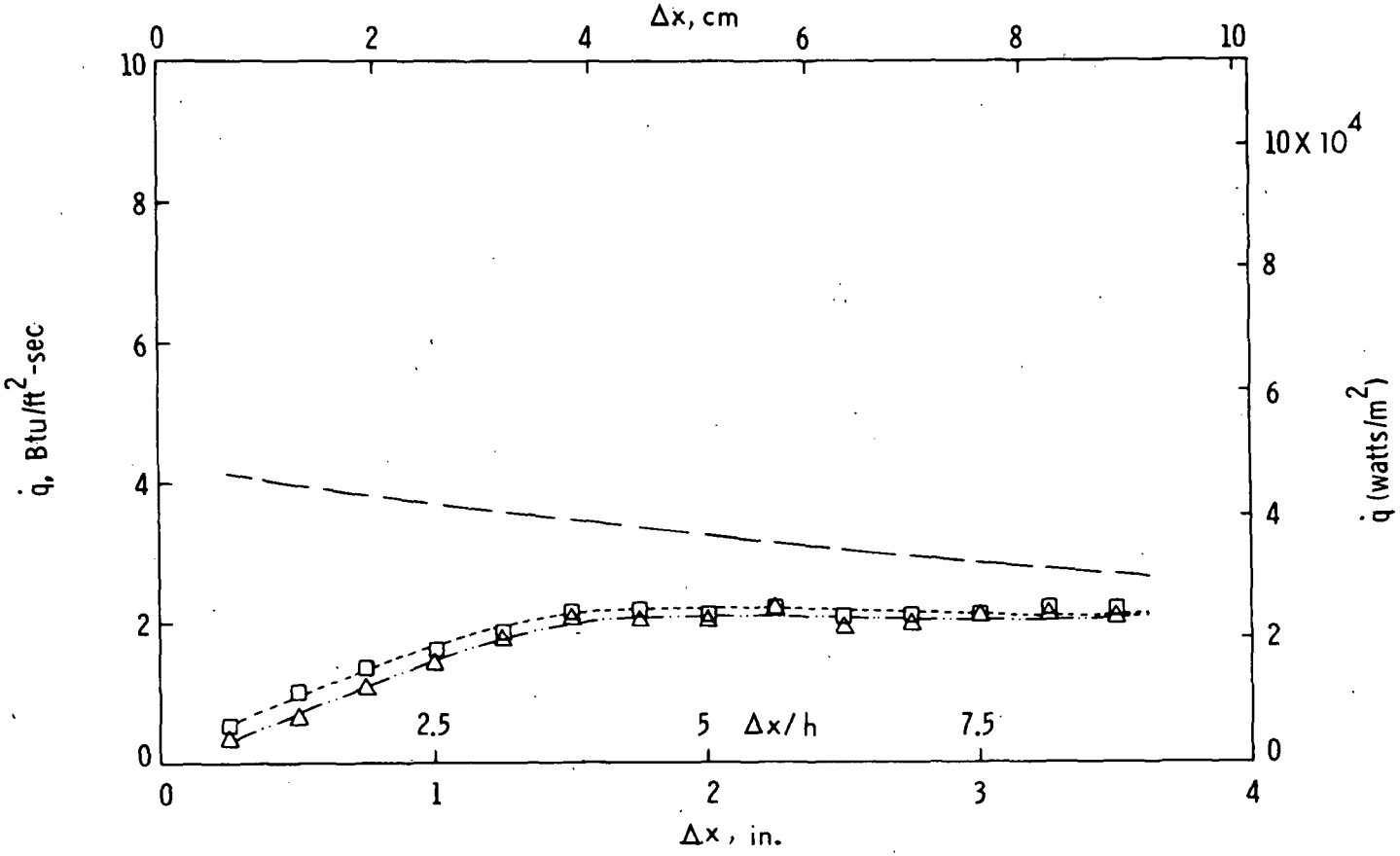

(b) $p_0 \approx 0.38$ atm.

Figure 10.- Continued.

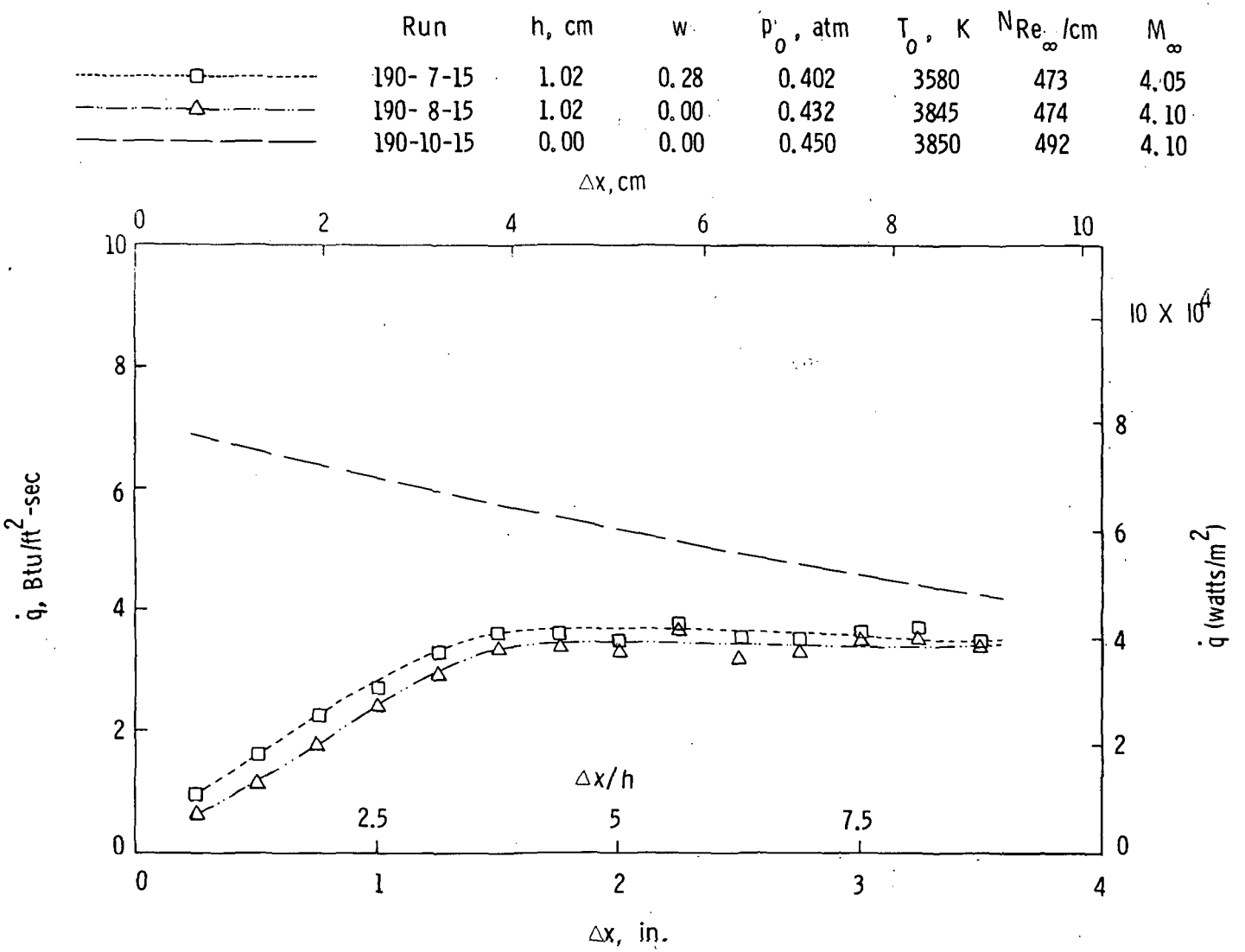

(c) $p_0 \approx 0.40$ atm.

Figure 10.- Continued.

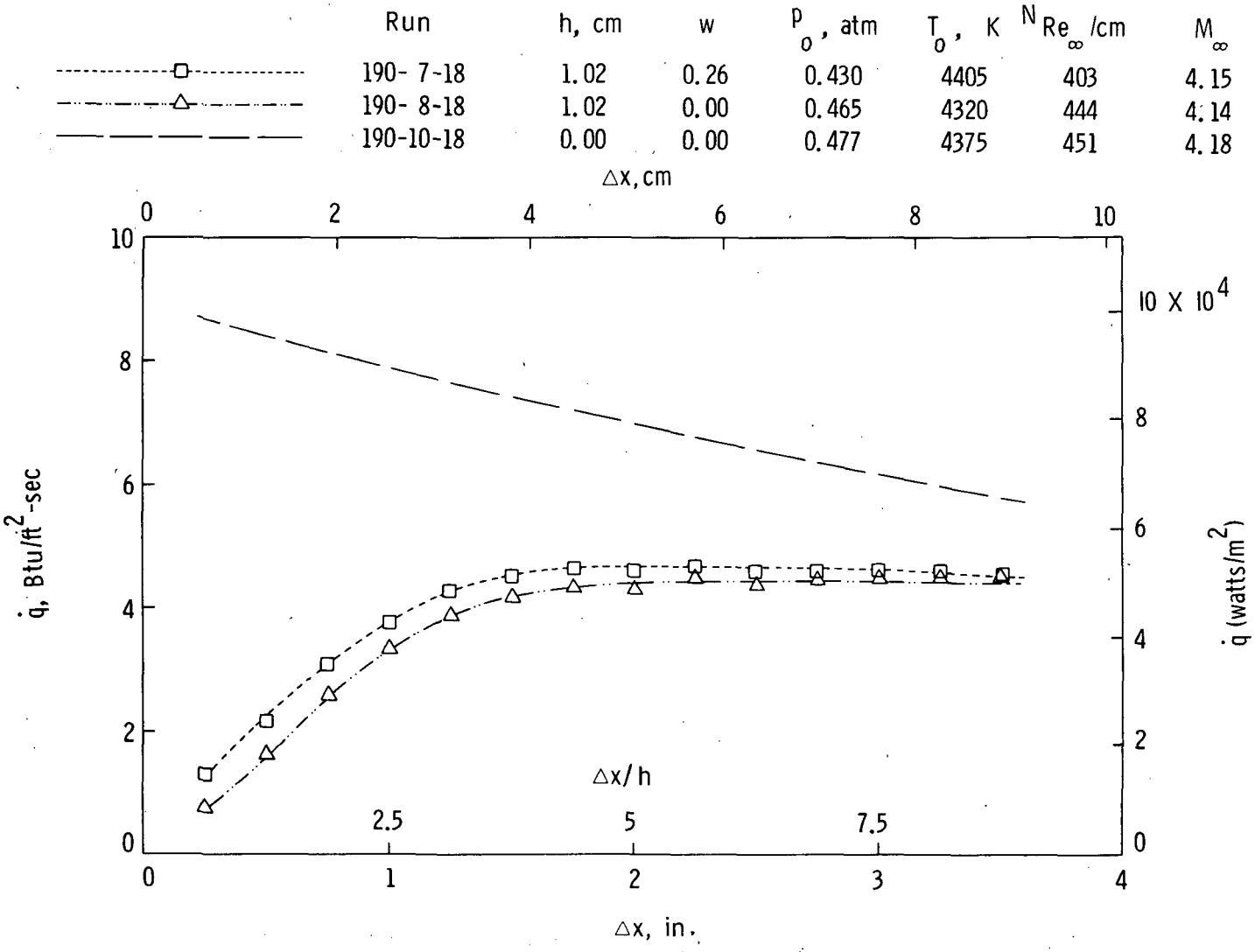

(d) $p_0 \approx 0.46$ atm.

Figure 10.- Continued.

Run	h, cm	w	p_0, atm	T_0, K	N_{Re_∞}/cm	M_∞
190- 3-6	1.02	0.40	0.425	3958	450	4.11
190- 8-15	1.02	0.00	0.432	3845	474	4.10
190-10-15	0.00	0.00	0.450	3850	492	4.10

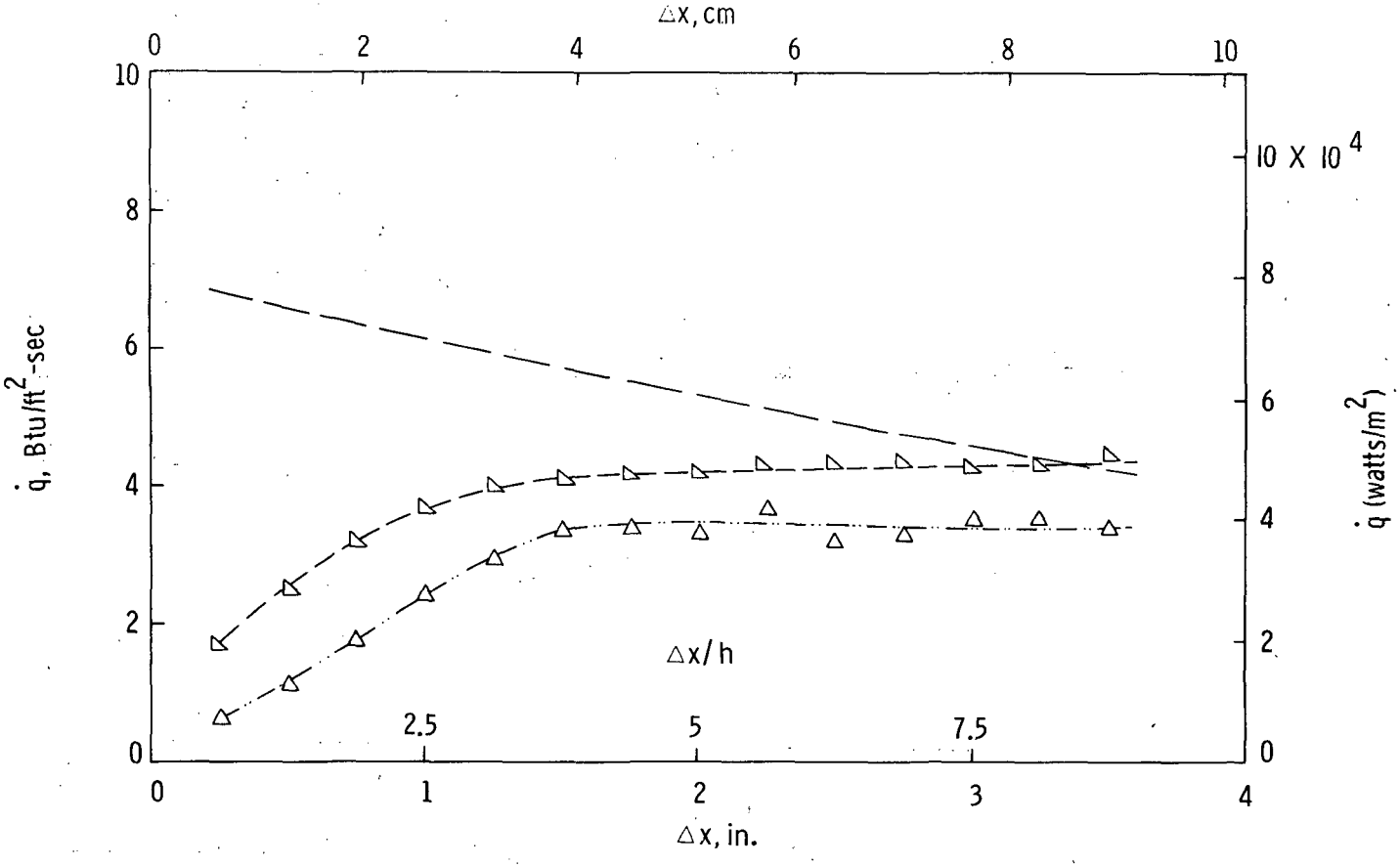

(e) $p_0 \approx 0.43$ atm.

Figure 10.- Continued.

Run	h, cm	w	p_0, atm	T_0, °K	N_{Re_∞}/cm	M_∞
190- 7-27	1.02	0.40	0.755	3730	836	4.06
190- 8-27	1.02	0.00	0.815	3750	880	4.08
190-10-27	0.00	0.00	0.815	3425	886	4.08

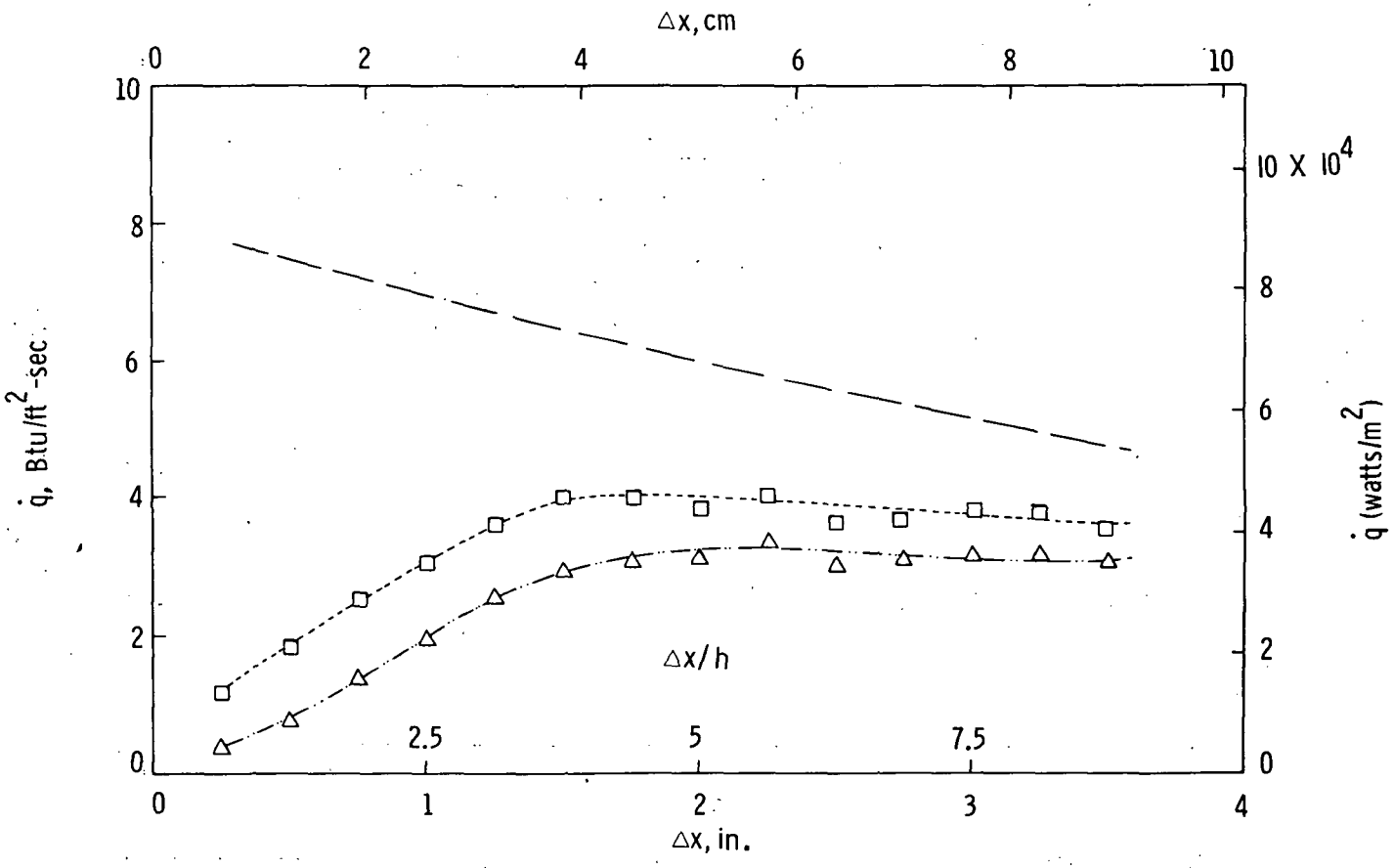

(f) $p_0 \approx 0.81$ atm.

Figure 10.- Continued.

Run	h, cm	w	p_0, atm	T_0, °K	N_{Re_∞}/cm	M_∞
188- 6-15	1.02	0.34	0.620	3030	834	3.97
190- 8-21	1.02	0.00	0.690	2894	976	3.96
190-10-21	0.00	0.00	0.695	2900	981	3.96

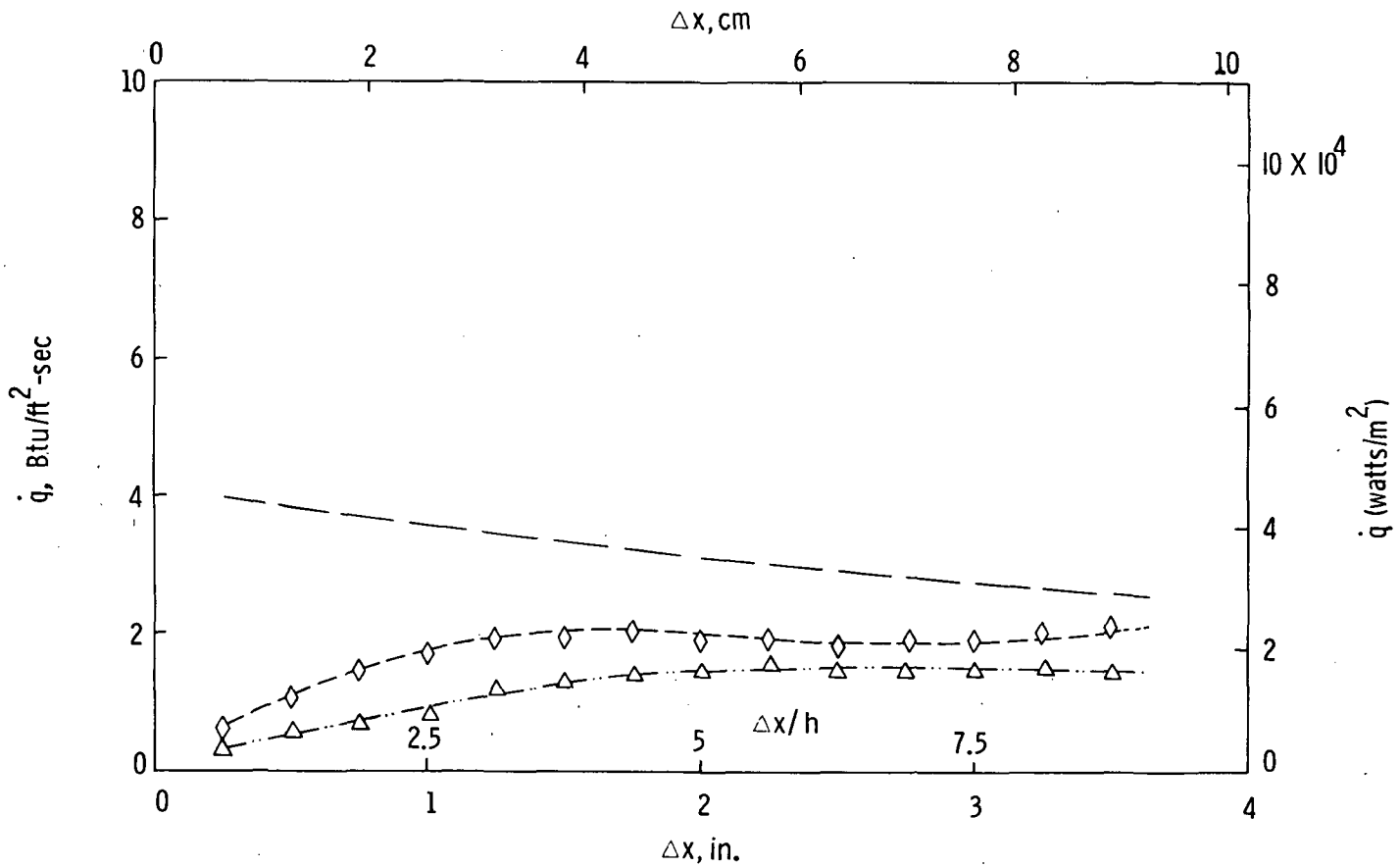

(g) $p_0 \approx 0.69$ atm.

Figure 10.- Continued.

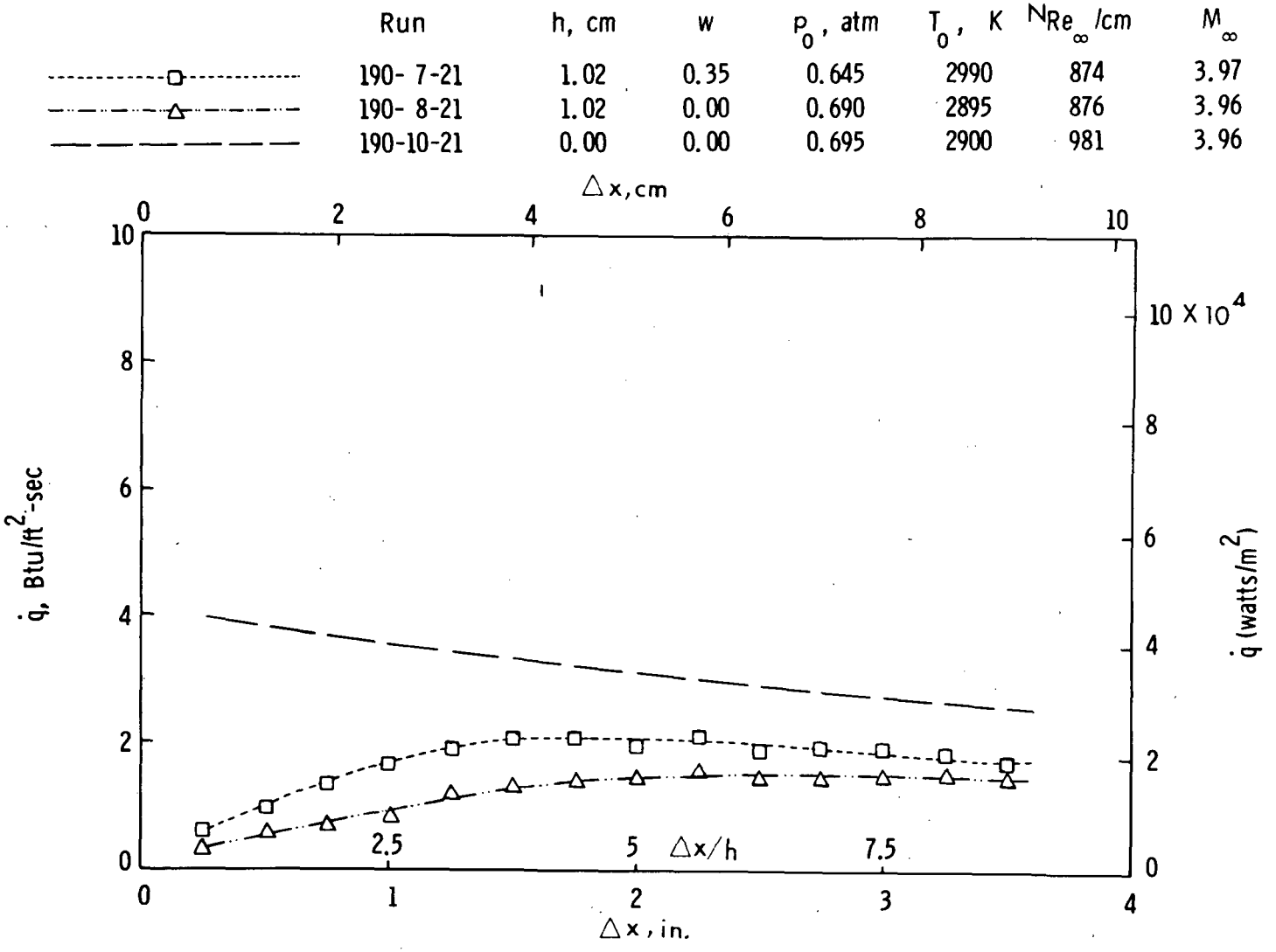

(h) $p_0 \approx 0.64$ atm.

Figure 10.- Continued.

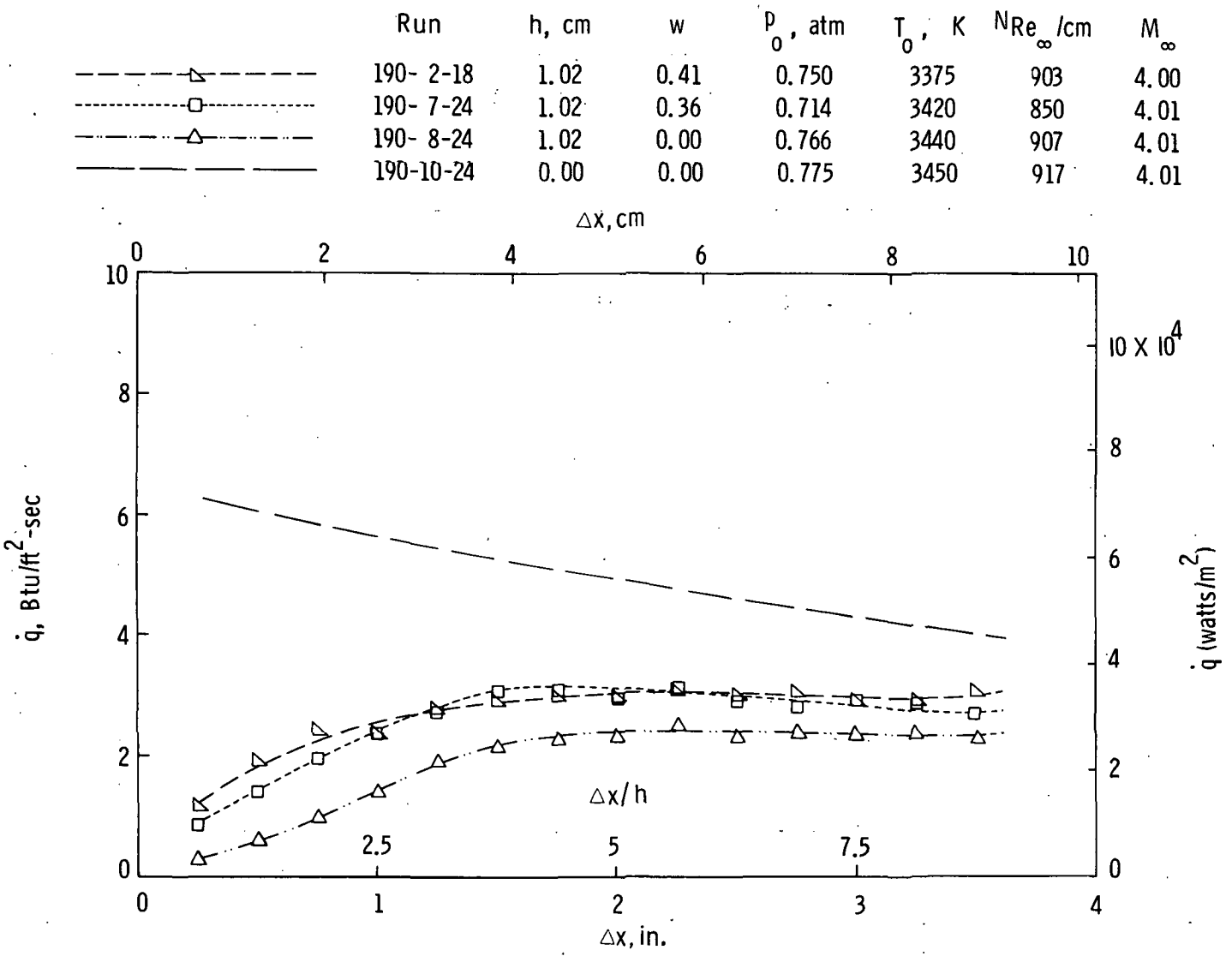

(i) $p_0 \approx 0.75$ atm.

Figure 10.- Continued.

Run	h, cm	w	p_0, atm	T_0, K	N_{Re_∞}/cm	M_∞
188- 2-9	1.02	0.44	0.865	3900	898	4.11
190- 7-30	1.02	0.44	0.802	3936	831	4.11
190- 8-30	1.02	0.00	0.870	3920	902	4.10
190-10-30	0.00	0.00	0.875	3900	907	4.11

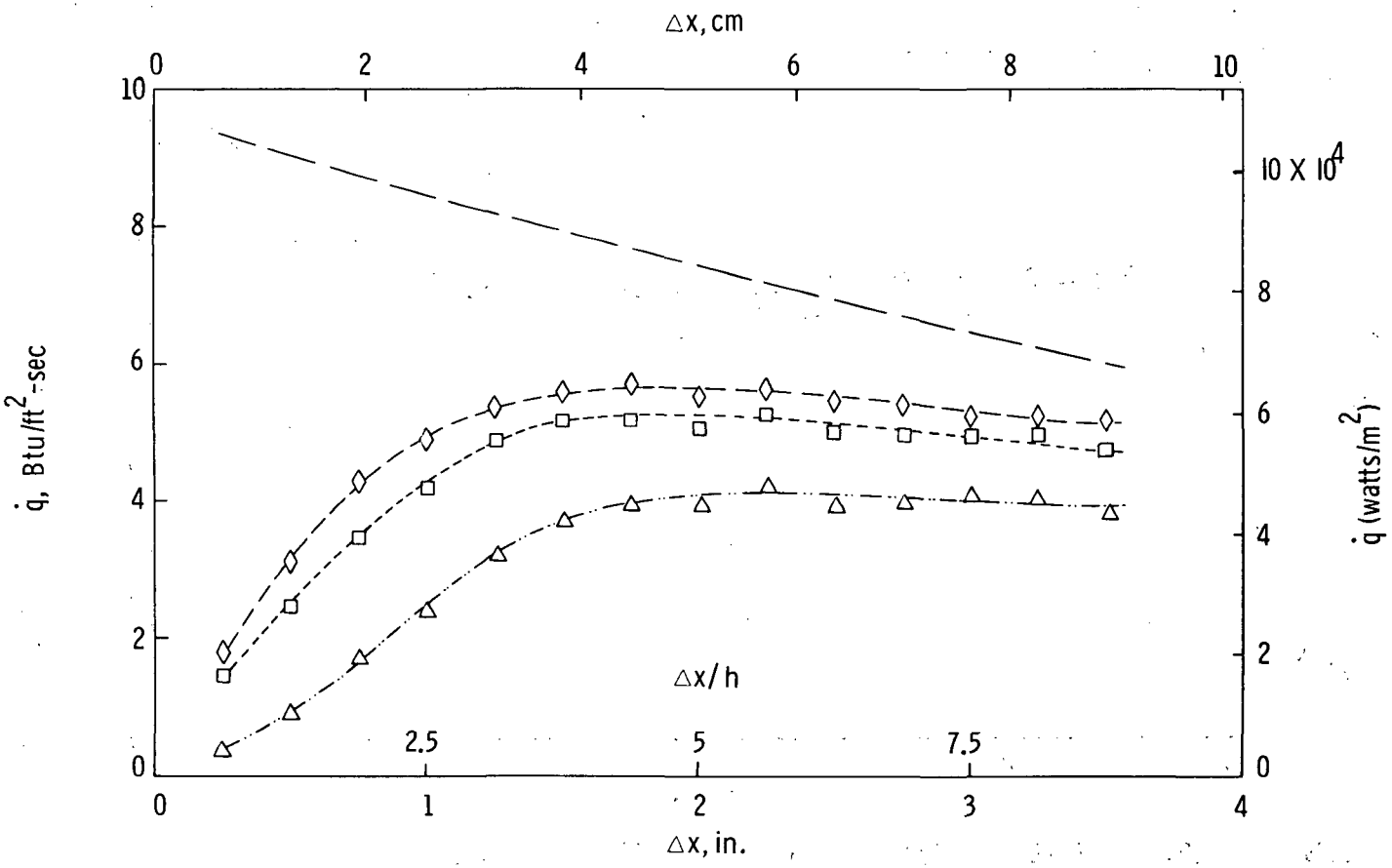

(j) $p_0 \approx 0.87$ atm.

Figure 10.- Concluded.

Run	h, cm	w	p_0, atm	T_0, K	N_{Re_∞}/cm	M_∞
190- 5-3	0.60	0.12	0.221	3695	257	4.09
190- 9-3	0.60	0.00	0.222	3650	259	4.10
190-10-3	0.00	0.00	0.226	3650	263	4.10

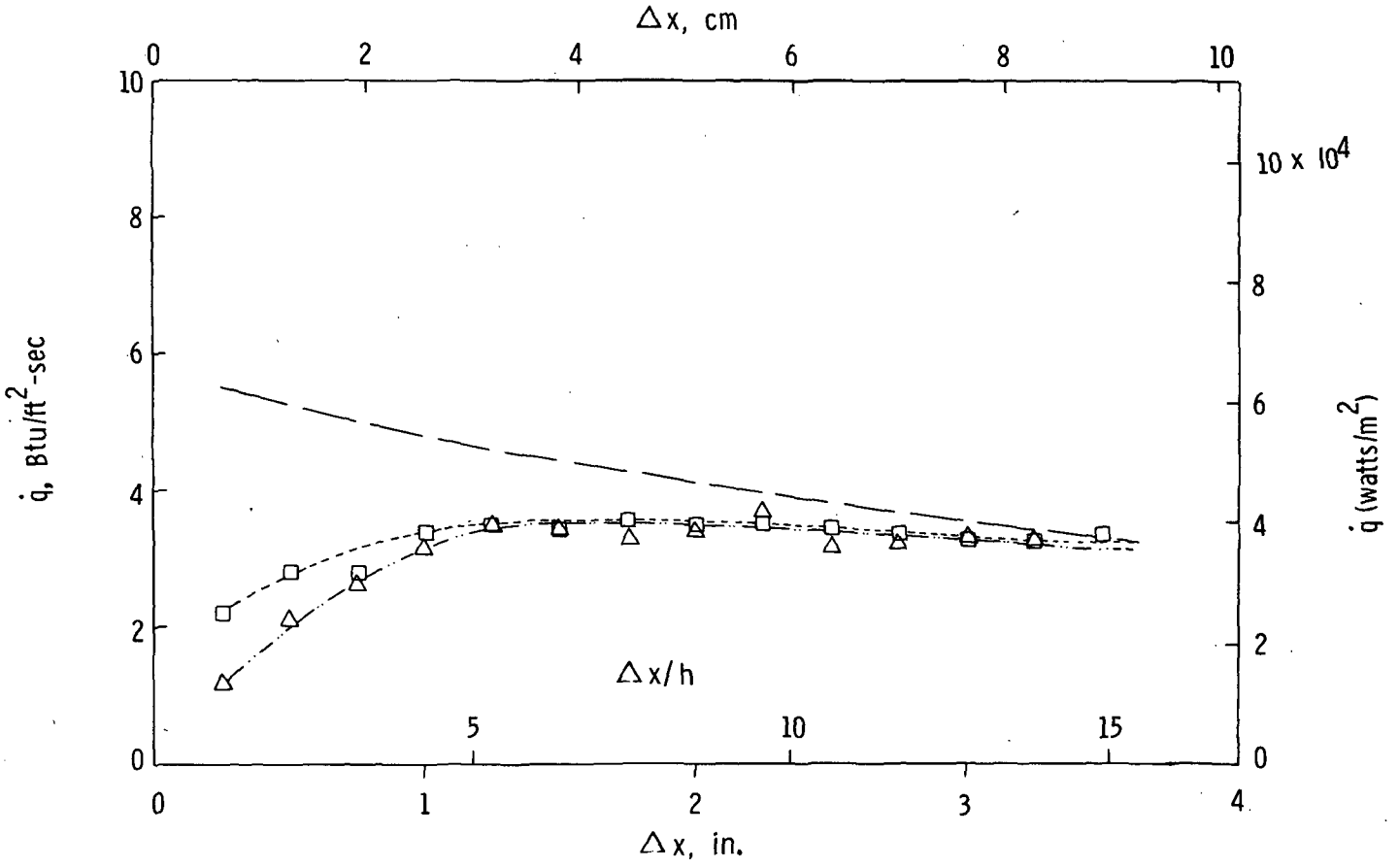

(a) $p_0 \approx 0.22$ atm.

Figure 11.- Effect of mass suction on heat-transfer distribution downstream of a 0.6 cm step.

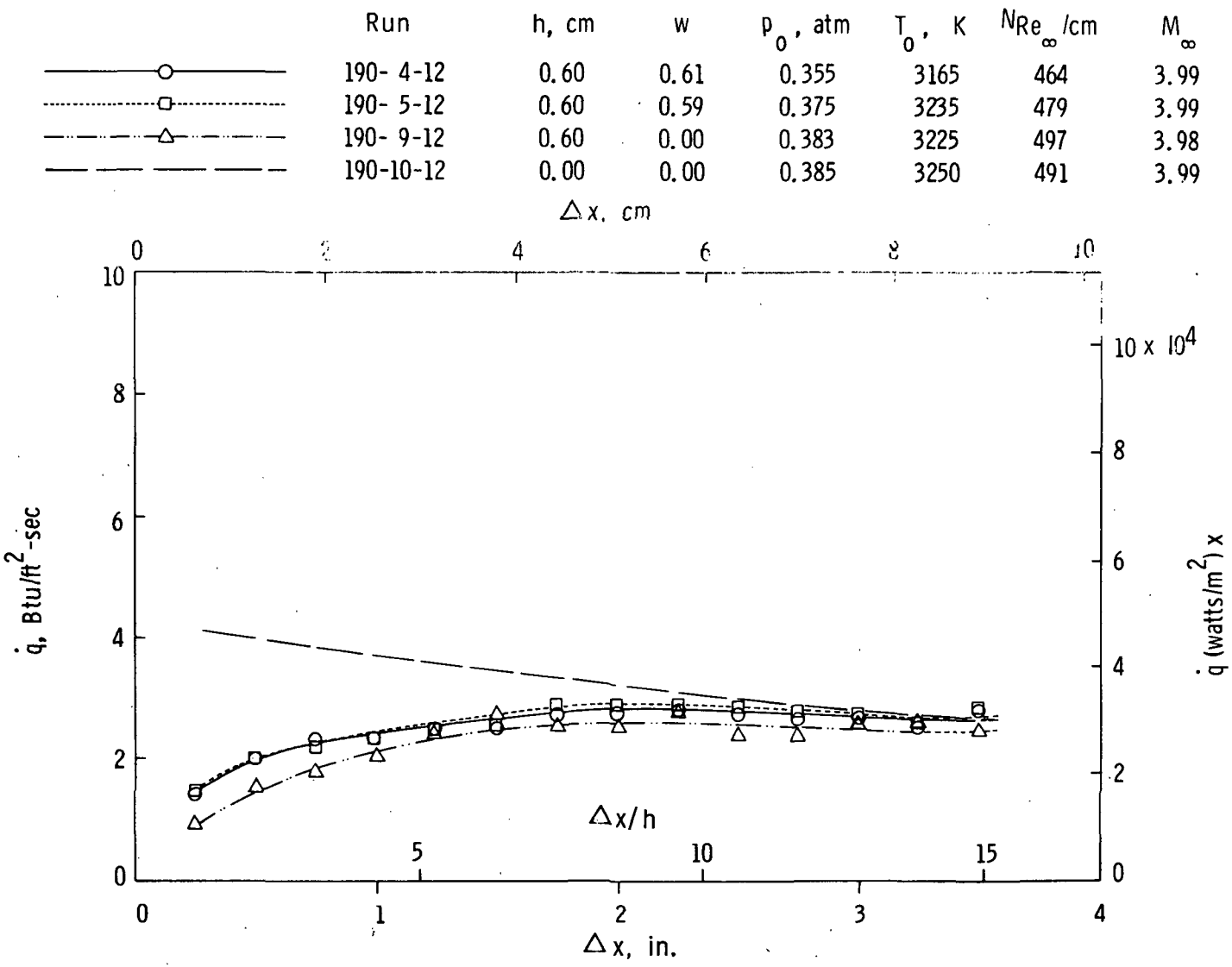

(b) $p_0 \approx 0.38$ atm.

Figure 11.- Continued.

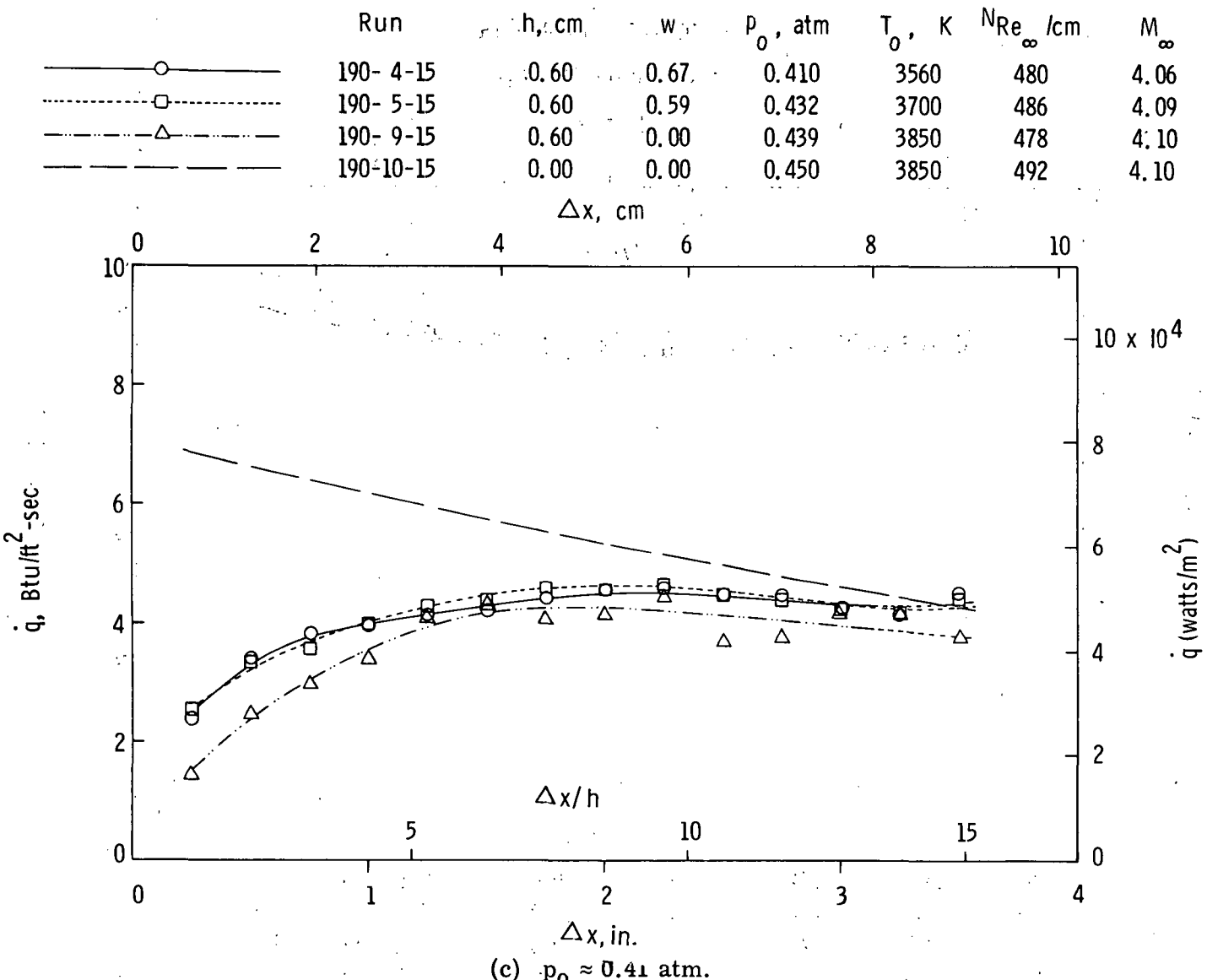

(c) $p_0 \approx 0.41$ atm.

Figure 11.- Continued.

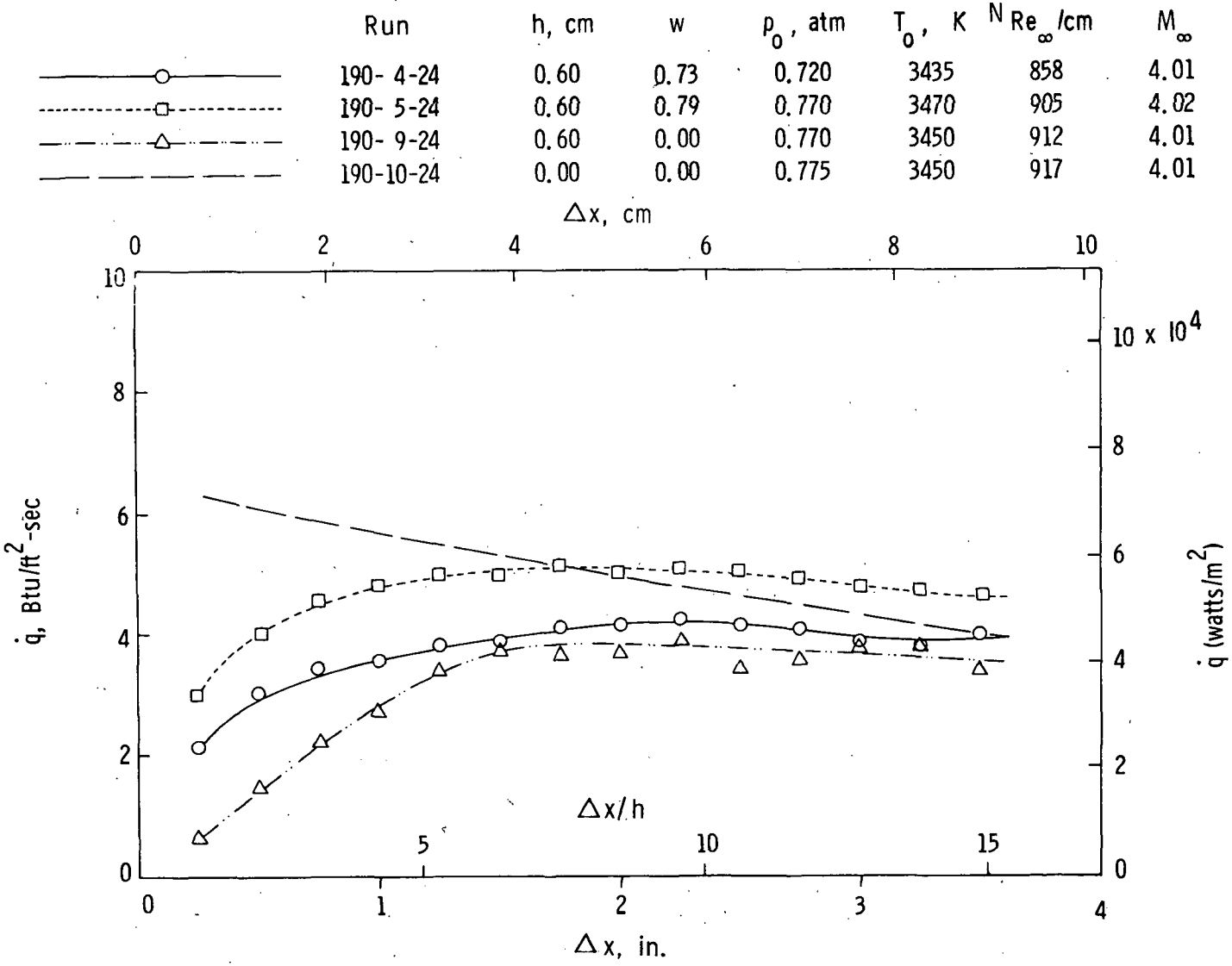

(d) $p_0 \approx 0.77$ atm.

Figure 11.- Concluded.

Run	h, cm	w	p_0, atm	T_0, K	N_{Re_∞}/cm	M_∞
197-1-3	1.02	0.24	0.240	3200	314	4.00
197-4-3	1.02	0.28	0.226	3650	263	4.10
197-3-6	1.02	0.00	0.242	3900	264	4.12
197-5-6	0.00	0.00	0.236	4250	236	4.12

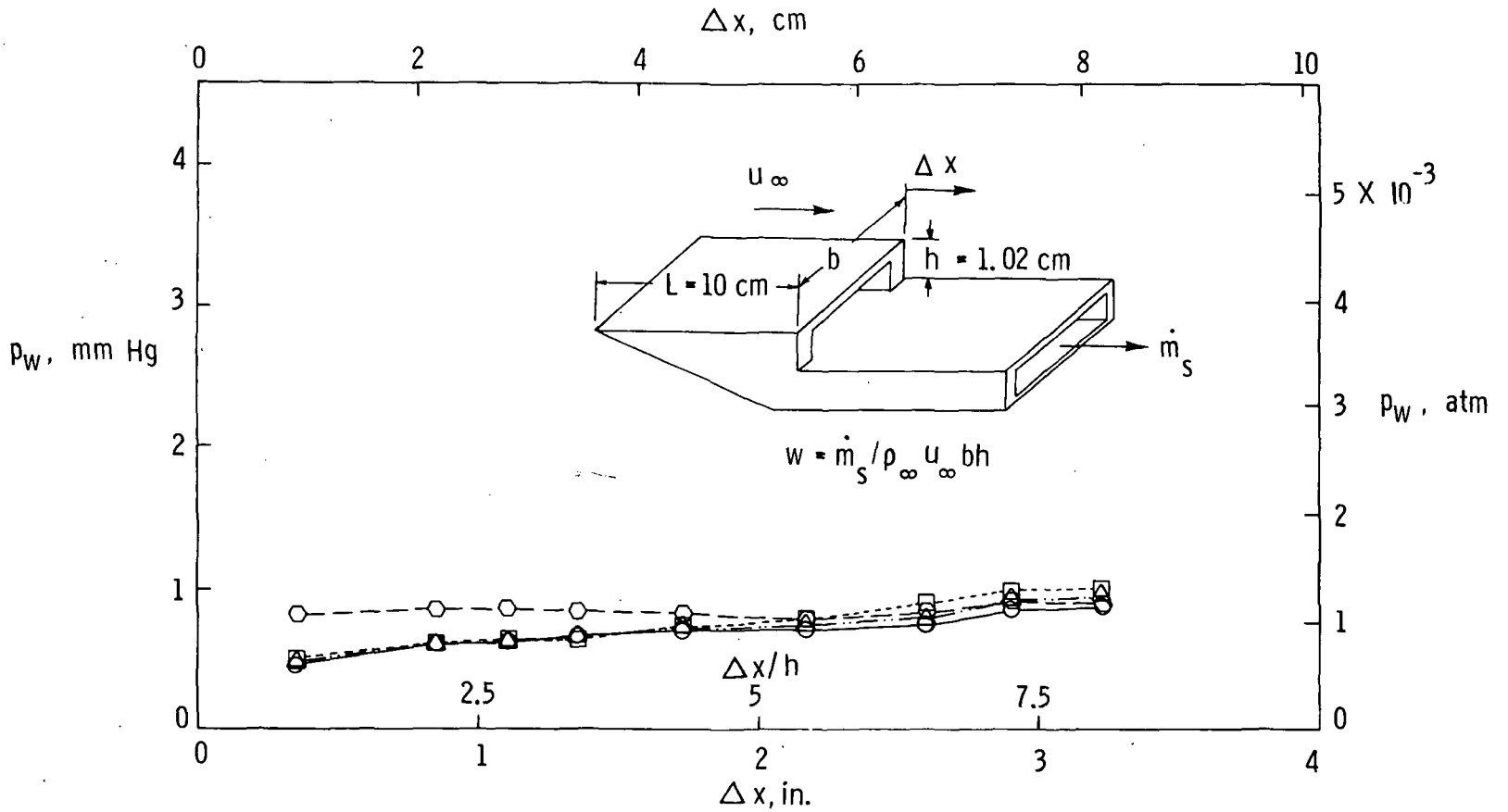

(a) $p_0 \approx 0.24$ atm.

Figure 12.- Effect of mass suction on pressure distribution downstream of a 1.02 cm step.

Run	h, cm	w	p_0, atm	T_0, K	N_{Re_∞}/cm	M_∞
197-1-12	1.02	0.32	0.362	2980	506	3.95
197-4-12	1.02	0.38	0.368	3200	479	3.98
197-3-12	1.02	0.00	0.364	3050	495	3.97
197-5-12	0.00	0.00	0.360	3175	470	3.98

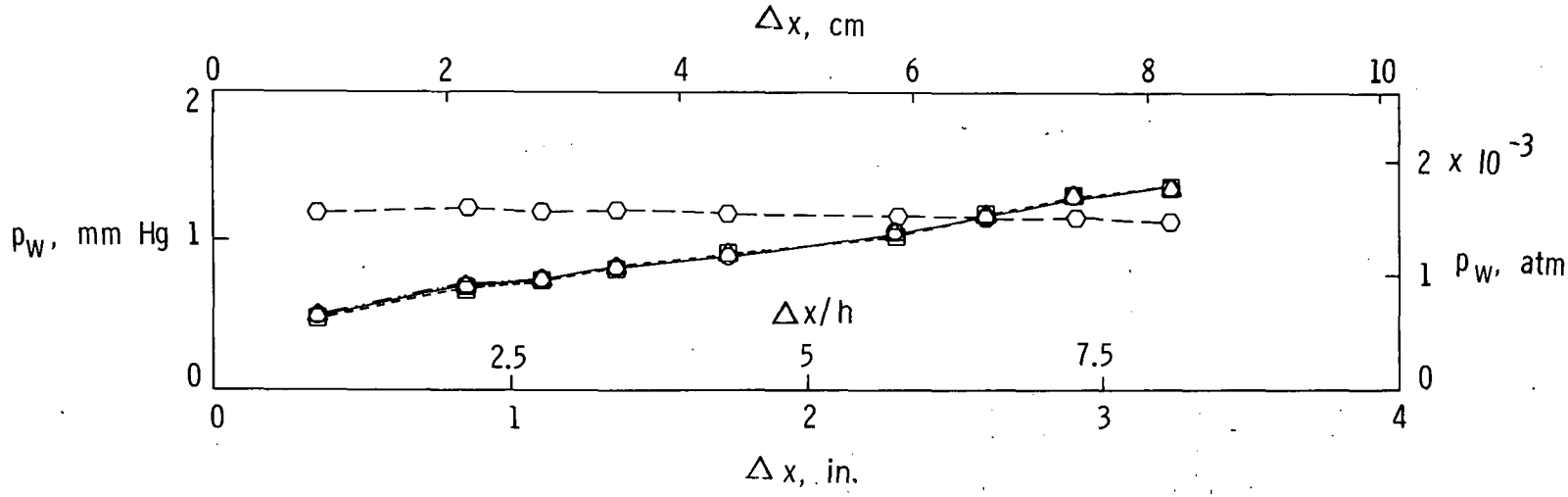

(b) $p_0 \approx 0.36$ atm.

Figure 12.- Continued.

Run	h, cm	w	p_0, atm	T_0, K	N_{Re_∞}/cm	M_∞
197-1-15	1.02	0.39	0.422	3530	491	4.07
197-4-15	1.02	0.43	0.431	3825	471	4.10
197-3-15	1.02	0.00	0.425	3650	486	4.07
197-5-15	0.00	0.00	0.421	3925	449	4.11

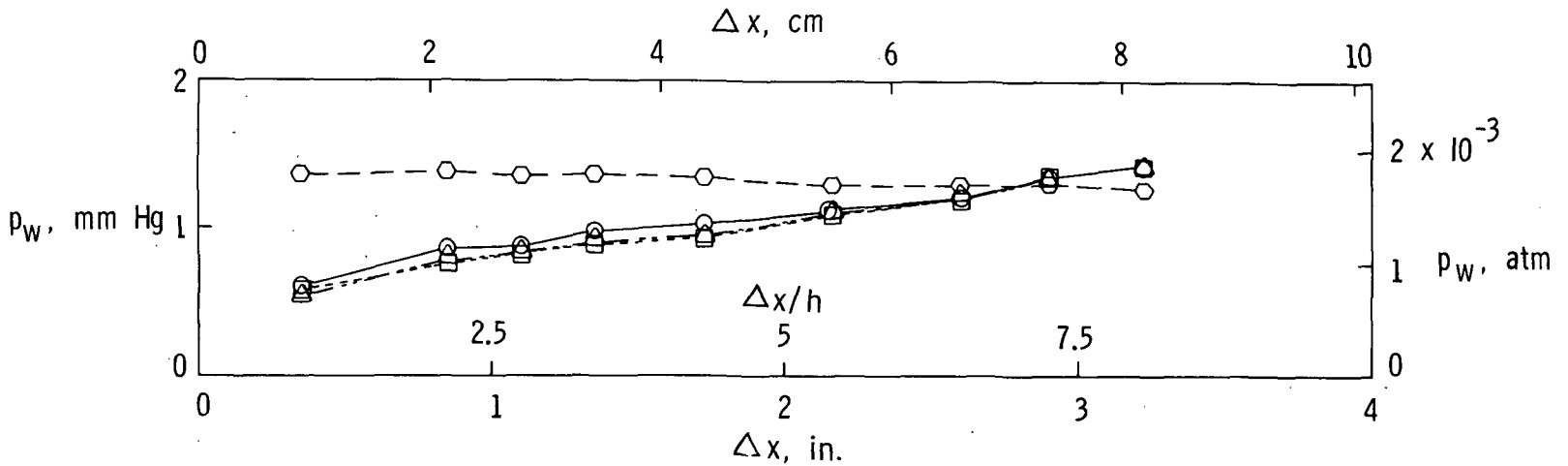

(c) $p_0 \approx 0.43$ atm.

Figure 12.- Continued.

Run	h, cm	w	p_0, atm	T_0, K	N_{Re_∞}/cm	M_∞
197-1-18	1.02	0.46	0.450	4350	429	3.98
197-4-18	1.02	0.47	0.455	4300	438	4.14
197-3-18	1.02	0.00	0.453	4020	471	4.12
197-5-18	0.00	0.00	0.451	4350	430	4.16

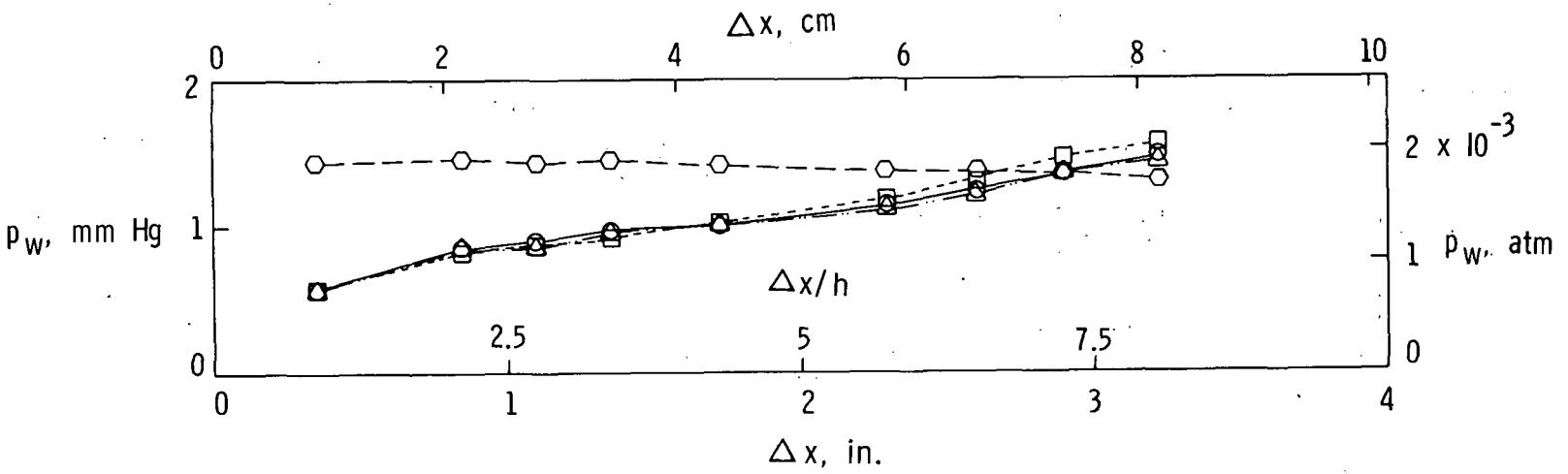

(d) $p_0 \approx 0.45$ atm.

Figure 12.- Continued.

Run	h, cm	w	p_0, atm	T_0, K	N_{Re_∞}/cm	M_∞
197-1-21	1.02	0.39	0.680	2825	987	3.96
197-4-21	1.02	0.38	0.680	2950	937	3.96
197-3-21	1.02	0.00	0.675	2920	948	3.95
197-5-21	0.00	0.00	0.680	2950	937	3.96

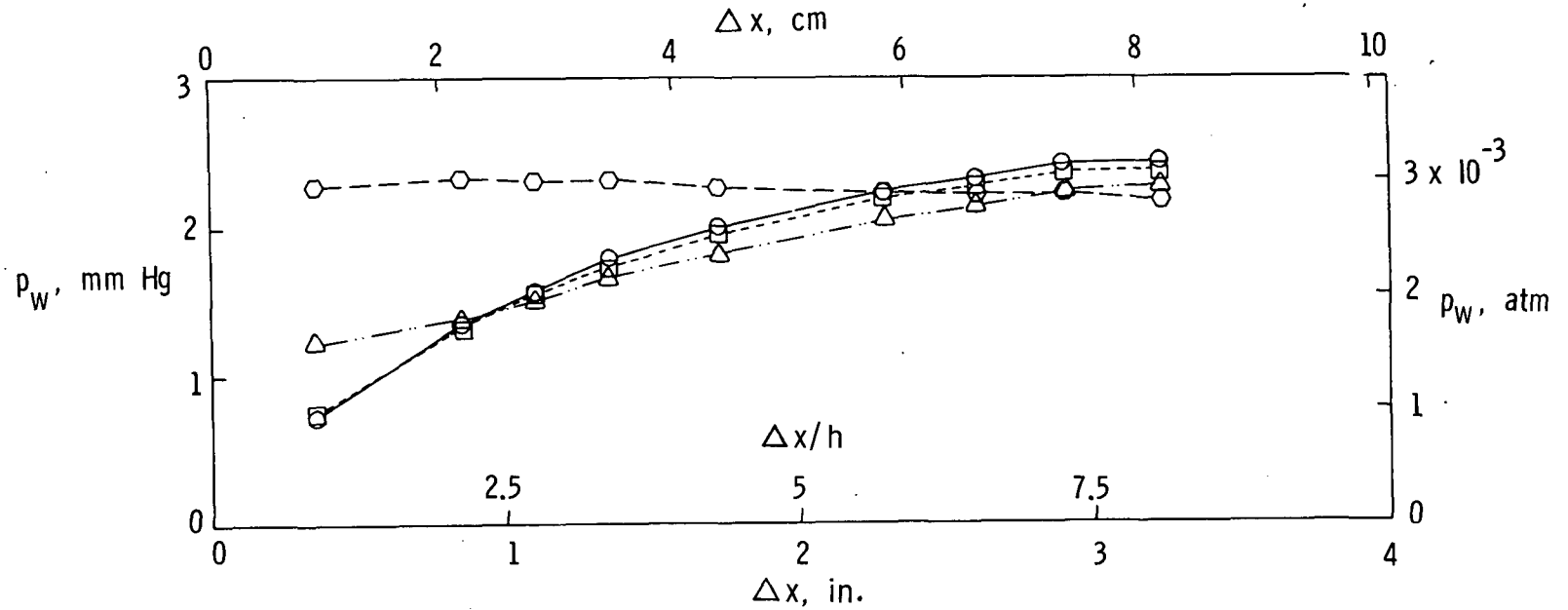

(e) $p_0 \approx 0.68$ atm.

Figure 12.- Continued.

Run	h, cm	w	p_0, atm	T_0, K	N_{Re_∞}/cm	M_∞
197-1-24	1.02	0.39	0.762	3250	951	3.98
197-4-24	1.02	0.38	0.768	3450	909	4.01
197-3-24	1.02	0.00	0.765	3350	911	4.02
197-5-24	0.00	0.00	0.770	3450	912	4.01

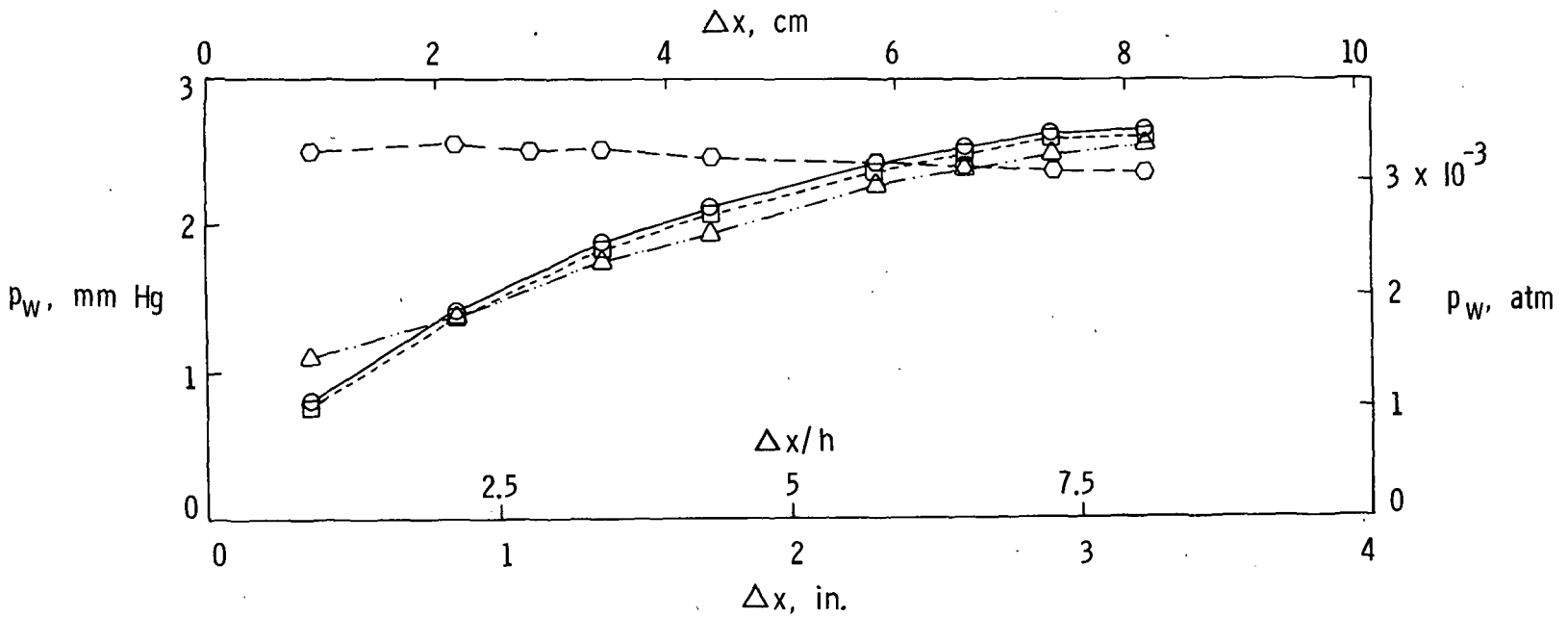

(f) $p_0 \approx 0.77$ atm.

Figure 12.- Continued.

Run	h, cm	w	p_0, atm	T_0, K	N_{Re_∞}/cm	M_∞
197-1-27	1.02	0.42	0.800	3475	937	4.02
197-4-27	1.02	0.38	0.810	3700	896	4.06
197-3-27	1.02	0.00	0.810	3575	928	4.03
197-5-27	0.00	0.00	0.813	3700	899	4.06

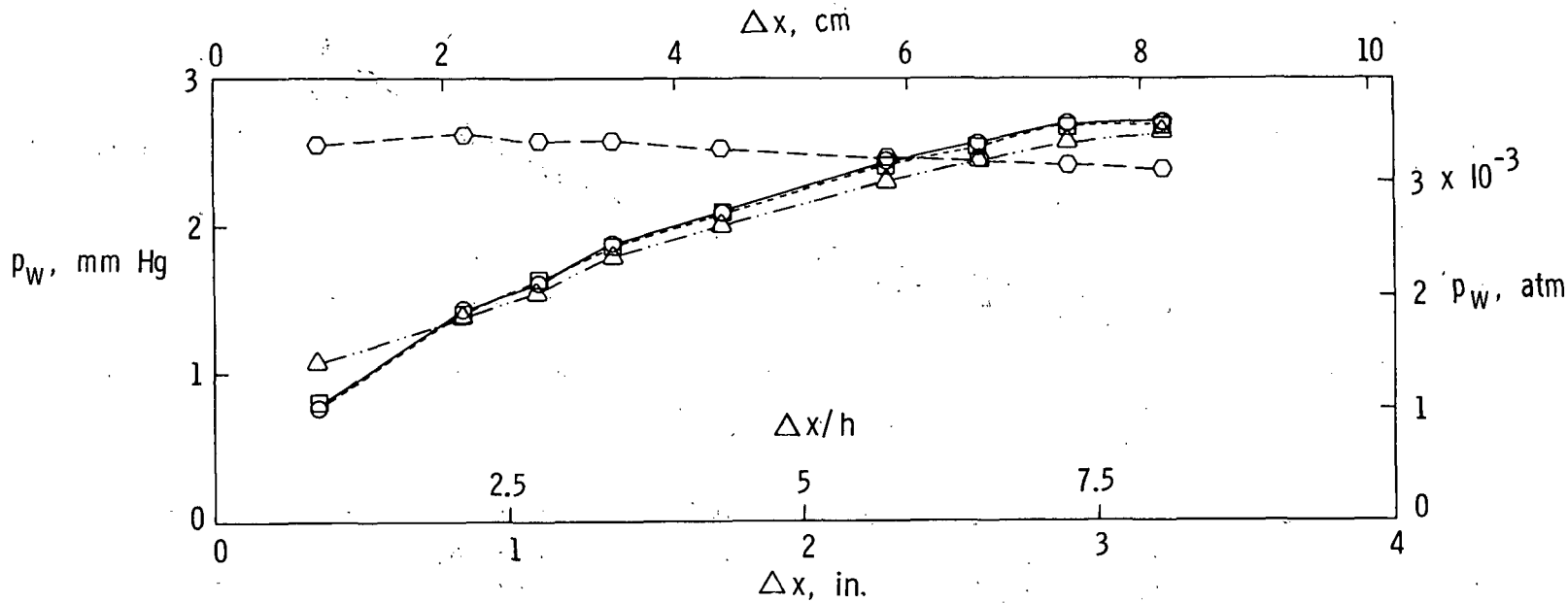

(g) $p_0 \approx 0.81$ atm.

Figure 12.- Continued.

Run	h, cm	w	P_0, atm	T_0, K	N_{Re_∞}/cm	M_∞
197-1-30	1.02	0.42	1.500	3250	1818	3.99
197-4-30	1.02	0.41	1.505	3460	1732	4.00
197-3-30	1.02	0.00	1.495	3350	1761	4.00
197-5-30	0.00	0.00	1.423	3080	1855	3.96

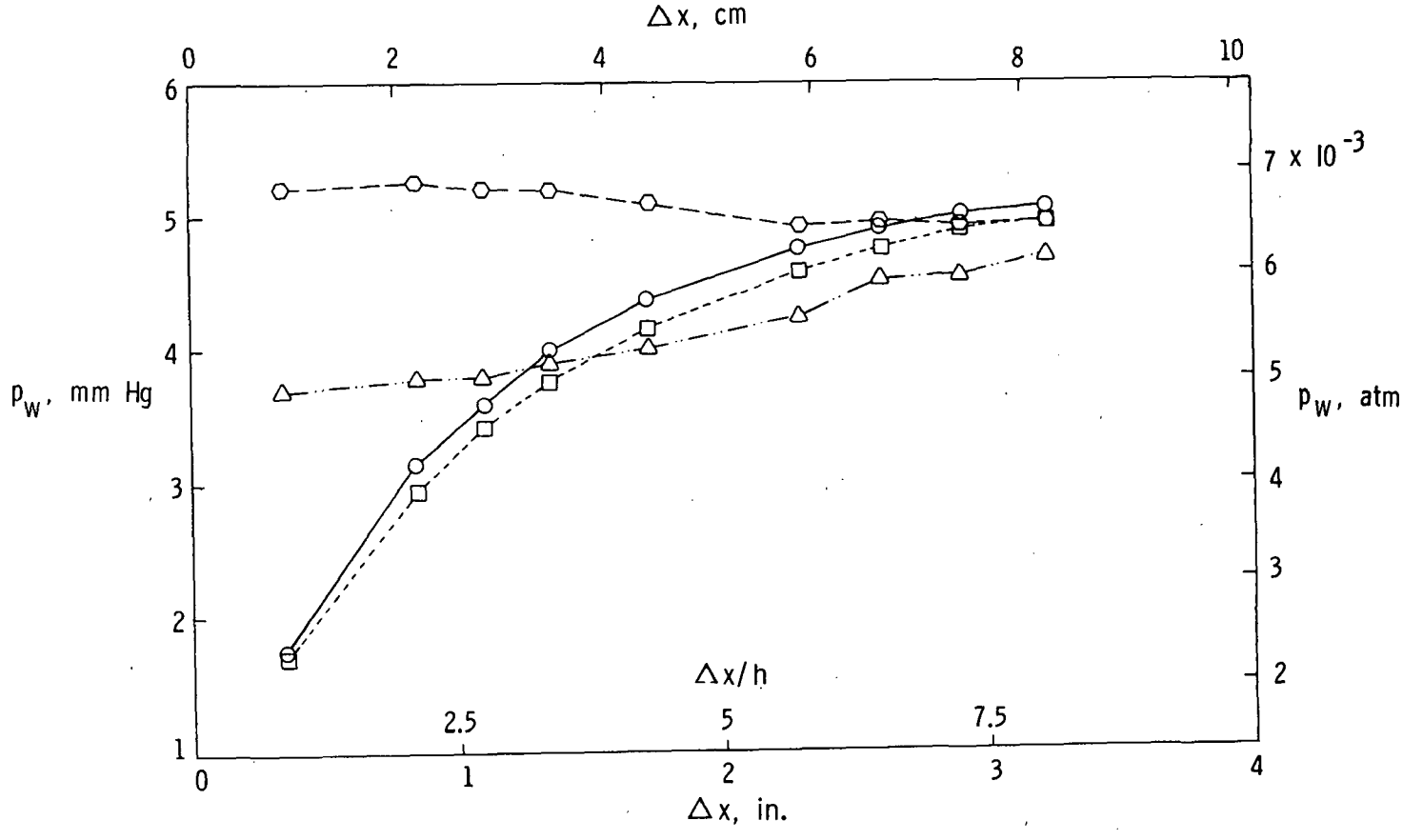

(h) $p_0 \approx 1.5$ atm.

Figure 12.- Continued.

Run	h, cm	w	p_0, atm	T_0, K	N_{Re_∞}/cm	M_∞
197-1-36	1.02	0.48	1.565	3630	1707	4.03
197-4-33	1.02	0.41	1.585	3750	1683	4.05
197-3-33	1.02	0.00	1.595	3630	1736	4.04
197-5-36	0.00	0.00	1.570	3675	1700	4.04

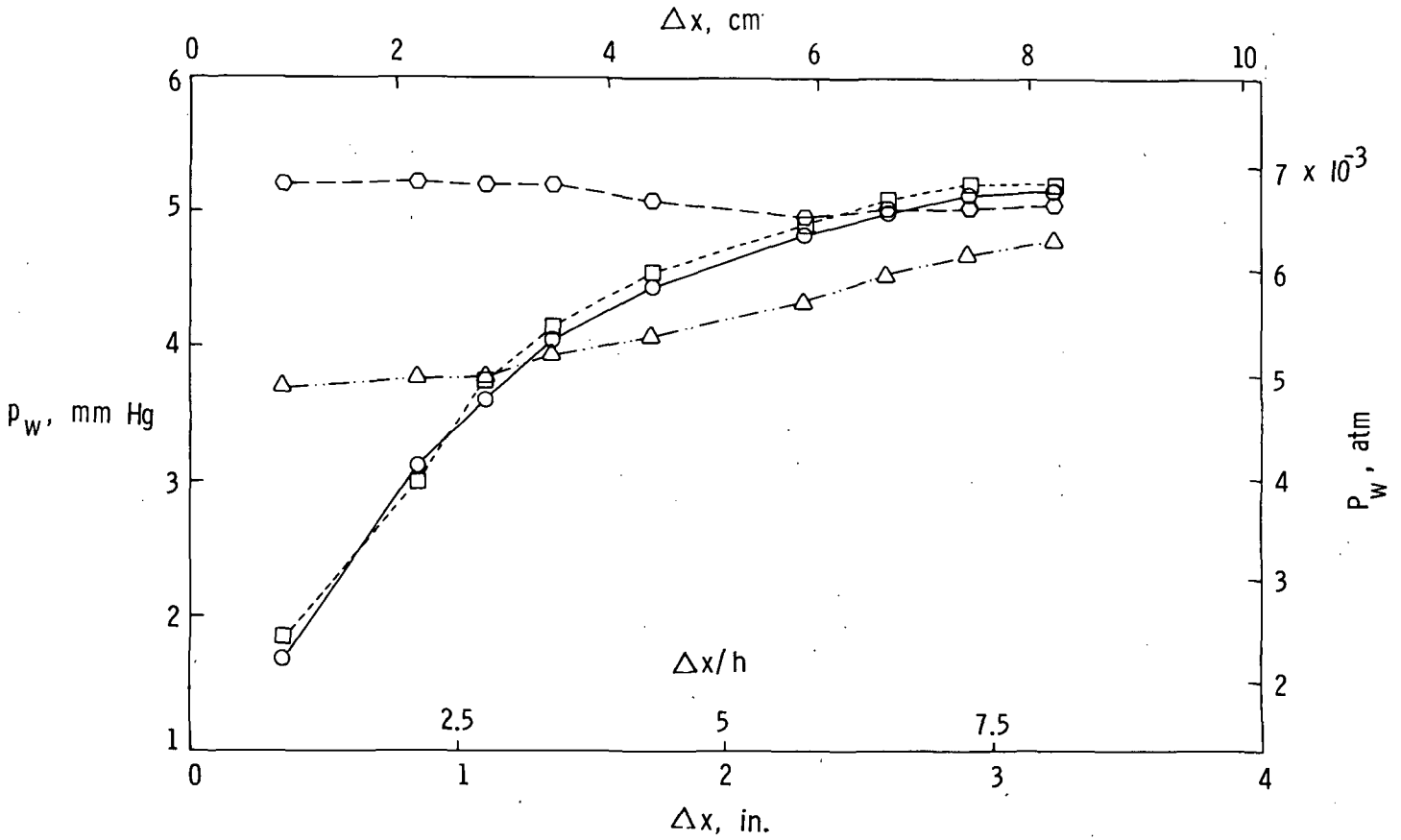

(i) $p_0 \approx 1.58$ atm.

Figure 12.- Continued.

Run	h, cm	w	p_0, atm	T_0, K	N_{Re_∞}/cm	M_∞
197-4-36	1.02	0.36	1.900	3525	2141	4.00
197-3-36	1.02	0.00	1.905	3480	2161	4.00
197-5-39	0.00	0.00	1.895	3550	2077	4.02

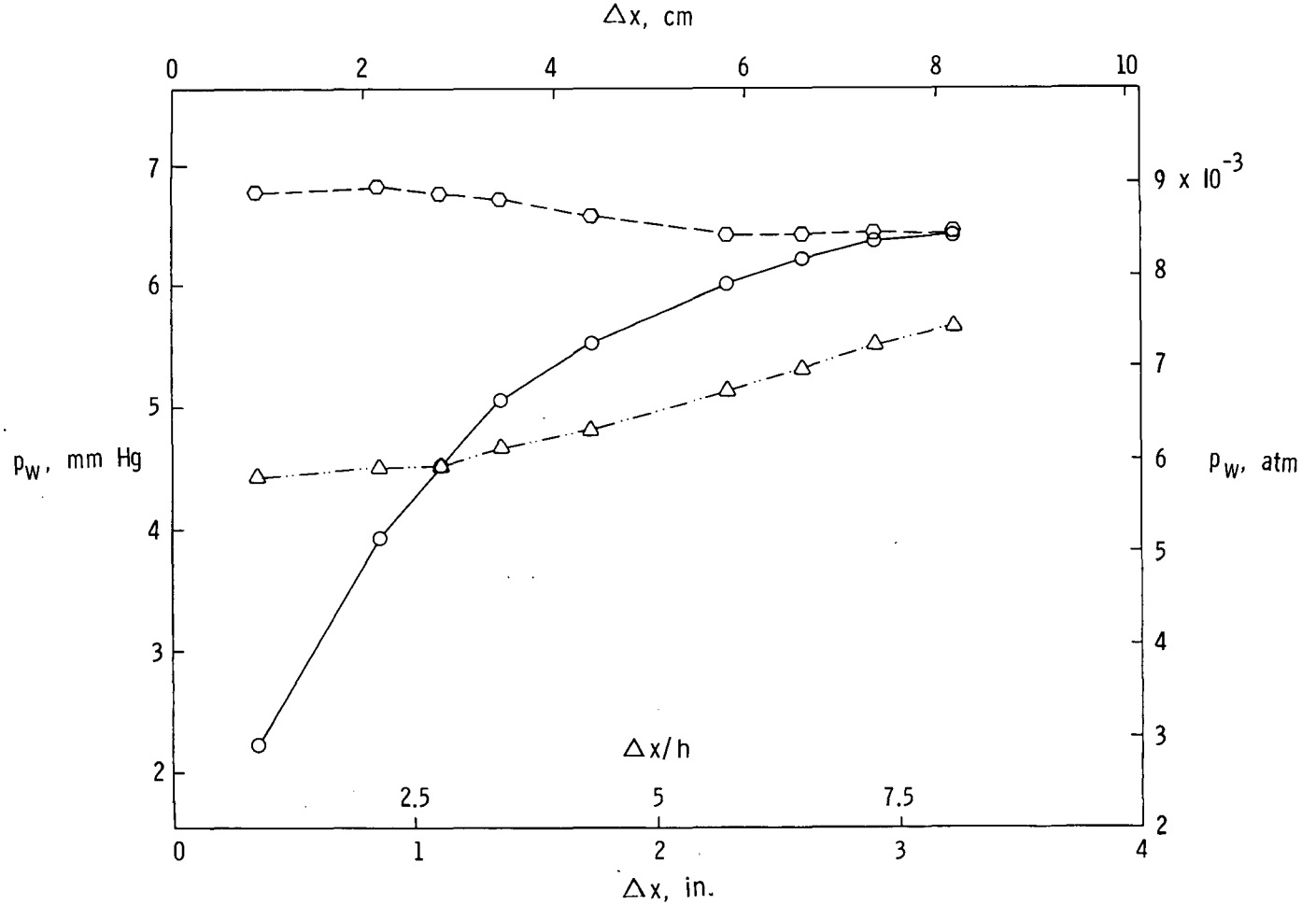

(j) $p_0 \approx 1.90$ atm.

Figure 12.- Concluded.

"The aeronautical and space activities of the United States shall be conducted so as to contribute . . . to the expansion of human knowledge of phenomena in the atmosphere and space. The Administration shall provide for the widest practicable and appropriate dissemination of information concerning its activities and the results thereof."

—NATIONAL AERONAUTICS AND SPACE ACT OF 1958

NASA SCIENTIFIC AND TECHNICAL PUBLICATIONS

TECHNICAL REPORTS: Scientific and technical information considered important, complete, and a lasting contribution to existing knowledge.

TECHNICAL NOTES: Information less broad in scope but nevertheless of importance as a contribution to existing knowledge.

TECHNICAL MEMORANDUMS: Information receiving limited distribution because of preliminary data, security classification, or other reasons. Also includes conference proceedings with either limited or unlimited distribution.

CONTRACTOR REPORTS: Scientific and technical information generated under a NASA contract or grant and considered an important contribution to existing knowledge.

TECHNICAL TRANSLATIONS: Information published in a foreign language considered to merit NASA distribution in English.

SPECIAL PUBLICATIONS: Information derived from or of value to NASA activities. Publications include final reports of major projects, monographs, data compilations, handbooks, sourcebooks, and special bibliographies.

TECHNOLOGY UTILIZATION PUBLICATIONS: Information on technology used by NASA that may be of particular interest in commercial and other non-aerospace applications. Publications include Tech Briefs, Technology Utilization Reports and Technology Surveys.

Details on the availability of these publications may be obtained from:

SCIENTIFIC AND TECHNICAL INFORMATION OFFICE

NATIONAL AERONAUTICS AND SPACE ADMINISTRATION

Washington, D.C. 20546